



*International Energy Agency*

*Energy Conservation in Buildings  
and Community Systems Programme*

*Annex 23: Multizone Air Flow Modelling*

***Evaluation of COMIS***

*Edited by*

*J.-M. Fürbringer*

*C.-A. Roulet*

*R. Borchiellini*

*Swiss Federal Institute of Technology, Lausanne  
LESO.PB, Institute of Building Technology*

*1996*

---

**INTERNATIONAL ENERGY AGENCY**  
**Energy Conservation in Buildings and Community Systems Programme**

---

**Annex 23 : Multizone Air Flow Modelling**

---

**FINAL REPORT**

**EVALUATION OF  
COMIS**

Edited by

J.M. Fürbringer, LESO-PB, EPFL, CH-1015 Lausanne, Switzerland

C.A. Roulet, LESO-PB, EPFL, CH-1015 Lausanne, Switzerland

R. Borchiellini, Politecnico di Torino, Dipartimento di Energetica, Torino, Italy

WITH contributions from

F. Amara, INSA, France

A. Bossaer, BBRI, Belgium

E. Dascalaki, University of Athens, Greece

V. Dorer, EMPA, Switzerland

D. Ducarme, BBRI, Belgium

B. Geerinckx, BBRI, Belgium

F. Haghighat, Concordia University, Canada

F. Huck, EMPA, Switzerland

M. Orme, AIVC, UK

M. Santamouris, University of Athens, Greece

Y. Utsumi, Miyagi National College of Technology, Japan

A. Weber, EMPA, Switzerland

P. Wouters, BBRI, Belgium

H. Yoshino, Tohoku University, Japan

Y. Zhao, Tohoku University, Japan

## TABLE OF CONTENT OF VOLUME 1

<b>Preface</b> .....	<b>IV</b>
<b>IEA Executive committee members</b> .....	<b>V</b>
<b>Authors' Address list</b> .....	<b>VI</b>
<b>Summary</b> .....	<b>VII</b>
<b>How to get A23 documents, programs and data</b> .....	<b>VIII</b>
<b>Selection of some Annex 23 documents</b> .....	<b>IX</b>
<b>Introduction</b> .....	<b>1</b>
<b>1 Strategy, methods and tools</b> .....	<b>3</b>
1.1 Strategy.....	3
1.2 Methods.....	7
1.3 Tools.....	13
1.4 References .....	18
<b>2 Analytical evaluation</b> .....	<b>21</b>
2.1 Introduction .....	21
2.2 A guide through the test cases .....	24
2.3 Conclusions from the analytical evaluation .....	35
2.4 References .....	36
<b>3 Intermodel comparison</b> .....	<b>37</b>
3.1 Introduction .....	37
3.2 Programs used for the comparisons.....	37
3.3 Comparison and results .....	42
3.4 Conclusion from the inter-model comparison.....	64
3.5 Algorithms for some of the air flow models used in 3.2.....	65
3.6 References .....	72
<b>4 Experimental comparison</b> .....	<b>73</b>
4.1 Introduction .....	73
4.2 OPTIBAT facility .....	79
4.3 Japan Solar House .....	83
4.4 Japanese Family House .....	87
4.5 LESO three storey office building.....	91
4.6 Belgian PASSYS cell .....	97
4.7 Belgian Flat .....	101
4.8 PASSYS Cell and large opening experiment in Greece.....	107
4.9 Italgas House .....	109
4.10 Conclusion of the comparison.....	113
4.11 References .....	114
<b>5 User tests</b> .....	<b>115</b>
5.1 Introduction .....	115
5.2 User tests on case 1 .....	115
5.3 User tests on case 2 .....	127
5.4 Conclusions .....	133
5.5 References .....	133
<b>6 Synthesis</b> .....	<b>135</b>
6.1 General results.....	135
6.2 Results from specific evaluation tasks .....	135
6.3 A few hints .....	137
6.4 Conclusion.....	137

## TABLE OF CONTENT OF VOLUME 2

<b>Preface</b> .....	<b>IV</b>
<b>IEA Executive committee members</b> .....	<b>V</b>
<b>Author's address list</b> .....	<b>VI</b>
<b>Summary</b> .....	<b>VII</b>
<b>How to get A23 documents, programs and data</b> .....	<b>VIII</b>
<b>Selection of some Annex 23 documents</b> .....	<b>IX</b>
<b>Introduction</b> .....	<b>1</b>
<b>A 1. LISA (Library for Sensitivity Analyses)</b> .....	<b>3</b>
A 1.1 What is LISA?.....	3
A 1.2 Short description of functions.....	4
<b>A 2. Multirun Interface for Sensitivity Analysis</b> .....	<b>7</b>
A 2.1 Purpose of MISA .....	7
A 2.2 Required files .....	7
A 2.3 File structure .....	8
A 2.4 How to run MISA .....	12
<b>A 3. The EMPA test cases</b> .....	<b>15</b>
A 3.1 Structure of the test case data base.....	15
A 3.2 Content of the test case data base .....	15
<b>A 4. Experimental evaluation</b> .....	<b>25</b>
A 4.1 Introduction.....	25
A 4.2 The OPTIBAT facility .....	25
A 4.3 Japan Solar House.....	35
A 4.4 Japanese Family House .....	49
A 4.5 LESO three storey office building .....	61
A 4.6 Single sided ventilation in a 2-zone test cell.....	71
A 4.7 Namur Flat: Contaminant Spreading .....	93
A 4.8 PASSYS Cell In Greece.....	133
A 4.9 Large opening experiment in Greece .....	137
A 4.10 Italgas House.....	151
<b>A 5. User Tests</b> .....	<b>169</b>
A 5.1 Proposals for changes in the User Manual and COMVEN.....	169
A 5.2 Reference input file for case 2 .....	170

## PREFACE

### *International Energy Agency*

In order to strengthen cooperation in the vital area of energy policy, an Agreement on an International Energy Programme was formulated among a number of industrialised countries in November 1974. The International Energy Agency (IEA) was established as an autonomous body within the Organisation for Economic Cooperation and Development (OECD) to administer that agreement. Twenty-two countries are currently members of the IEA, with the Commission of the European Communities participating under a special arrangement.

As one element of the International Energy Programme, the Participants undertake cooperative activities in energy research, development, and demonstration. A number of new and improved energy technologies which have the potential of making significant contributions to our energy needs were identified for collaborative efforts. The IEA Committee on Energy Research and Development (CRO), assisted by a small Secretariat staff, coordinates the energy research, development, and demonstration programme.

### *Energy Conservation in Buildings and Community Systems*

As one element of the Energy Programme, the IEA encourages research and development in a number of areas related to energy. In one of these areas, energy conservation in buildings, the IEA is encouraging various exercises to predict more accurately the energy use of buildings, including comparison of existing computer programmes, building monitoring, comparison of calculation methods, as well as air quality and inhabitant behaviour studies.

### *The Executive Committee*

Overall control of the R&D programme "Energy Conservation in Buildings and Community Systems" is maintained by an Executive Committee, which not only monitors existing projects but identifies new areas where collaborative effort may be beneficial. The Executive Committee ensures all projects fit into a predetermined strategy without unnecessary overlap or duplication but with effective liaison and communication.

### *Annex XXIII: Multizone Air Flow Modelling*

The prediction and the control of the air flow patterns through the building is necessary to provide an efficient ventilation. Planning methods should allow that prediction from the earliest stage of a project, in order to enhance the comfort and the air quality while saving energy.

The general scope of the Annex XXIII is to provide a validated and user-friendly computer program, based on COMIS, for simulating air flow patterns in multizone buildings. This project has three subtasks:

- Subtask 1: Implementing new features in COMIS, including new models and user-friendly interface
- Subtask 2: Collecting data as well for input as for experimental comparison.
- Subtask 3: Evaluation of the code and its User Guide.

Countries participating to this annex are Belgium, Canada, France, Greece, Italy, Japan, the Netherlands, Switzerland, and USA. Moreover, IEA-ECB Annex V (Air Infiltration and Ventilation Centre) collaborated to this annex.

**IEA EXECUTIVE COMMITTEE MEMBERS**

Belgium	Prof. J. Lebrun
Canada	Dr. S. A. Barakat (chairman)
CEC	Mr. F. Conti
Denmark	Mr. P. Dorph-Petersen / O. Jensen
Germany	Mr. A. Le Marié
Greece	Mr. Malezious
Finland	Prof. R. Kohonen
France	Mr. P. Herant
Italy	Mr. C. Boffa / Mr. D. Malosti
Israel ()	Dr. J. Nowarski
Japan	Dr. Y. Kodama
Netherlands	Mr. P. Heijnen
New Zealand	Mr. P. Graham
Norway	Mr. J. Brunsell
Poland (Associate Member)	Prof. Mierzwinski
Sweden	Mr. J. Lagerstrom
Switzerland	Mr. Zimmermann (vice chairman)
Turkey	Prof. R. Oskay
UK	Dr. E. Perera / Mr. B. Austin / Mr. S. Irving
USA	Mr R. Karney

**Chairman**

Dr. S.A. Barakat, National Research Council of Canada, Building M-24, Ottawa, Ontario, Canada K1A 0R6, Fax: +1 613 954 3733

**IEA Secretariat Liaison**

Ms. Gudrun Maass, International Energy Agency, 2 rue Andre Pascal, 75016 Paris, France

## AUTHORS' ADDRESS LIST

J.-M. Fürbringer, NIST, Building Environment Division, Gaithersburg MD 20899, USA.  
jean-marie.furbringer@nist.gov

C.-A. Roulet, LESO, EPFL, CH-1015 Lausanne, Switzerland, claude.roulet@leso.da.epfl.ch

R. Borchellini, Politecnico di Torino, Dipartimento di Energetica, 24 C.so Duca degli  
Abruzzi, I- 10129 Torino, Italy, borchiel@polito.it

F. Amara, Insa, Rue Albert Einstein, Lyon, France

A. Bossaer, BBRI, 21 Av. Pierre Holoffe, B-3142 Limelette, Belgium

E. Dascalaki, University of Athens, Laboratory of Meteorology, Ippokratous 33, GR-10680  
Athens, Greece

V. Dorer, Empa, CH-8600 Dübendorf, Switzerland, dorer@empa.ch

D. Ducarme, BBRI, 21 Av. Pierre Holoffe, B-3142 Limelette, Belgium

B. Geerinckx, BBRI, 21 Av. Pierre Holoffe, B-3142 Limelette, Belgium

F. Haghghat, Centre for Building Studies, Concordia University, 1455 de Maisonneuve Blvd.  
W., Montreal, Quebec H3G 1M8, Canada

F. Huck, Empa, CH-8600 Dübendorf, Switzerland, huck@empa.ch

M. Orme, AIVC, University of Warwick Science Park, Sir William Lyons Rd., Coventry CV4  
7EZ, UK, msorme@aivc.org

M. Santamouris, University of Athens, Laboratory of Meteorology, Ippokratous 33, GR-10680  
Athens, Greece

Y. Utsumi, Miyagi National College of Technology, Dep. of Architecture, Medeshima Natori,  
Miyagi 981-12, Japan

A. Weber, Empa, CH-8600 Dübendorf, Switzerland, andreasweber@empa.ch

P. Wouters, BBRI, 21 Av. Pierre Holoffe, B-3142 Limelette, Belgium

H. Yoshino, Tohoku University, Sendai, Japan

Y. Zhao, Tohoku University, Sendai, Japan

## SUMMARY

IEA-ECB&CS Annex 23 program intends to provide a validated and user-friendly computer code simulating air and contaminant flows in multizone buildings. When developing such a code, which intends to be a model of the reality, it is essential to check, at each step, its conformity with the model. At the other end, the claimed user-friendliness should also be checked with real users.

This evaluation task took a large part of the efforts and means put into Annex 23 by participating countries. The result is that COMIS was checked very carefully, using up-to-date strategies and tools. This report presents the methods used and the results of this huge validation task. The tools especially developed within this annex include the validation and user test strategy, methods and computer tools for sensitivity analysis of the code.

Simulation results were compared with more than 50 simple **benchmarks** or test cases, for which either an analytical or a numerical solution was obtained using classical tools (such as EXCEL or MATHEMATICA). Each of these test cases was created to check a particular feature of COMIS. This so-called analytical evaluation allowed the correction of several bugs which appeared in the early versions of COMIS.

**Inter-model comparison** with as much as 14 other simulation programs was performed by five different laboratories, using various objects. For each compared program, the objects were adapted or chosen in such a way that they could be modelled by the program. The result of these comparison is that all compared models provided the same results, within a very narrow dispersion band. This comes from the fact that these models all use similar algorithms and simulations were performed with identical input data. However, this also shows that, at least for the checked features, these models do not contain bugs.

The **experimental comparison** task conducted within Annex 23 is very likely the largest ever performed for a computer code. Nine different buildings were monitored for this purpose, each building offering several cases for comparison. For each case, a **sensitivity analysis** was performed, in order to know, not only the uncertainties on the measurements, but also the confidence intervals of the simulations, which result from uncertainties on input data. These were found to be very large. Therefore, the results from simulations and measurements were, in some cases, not significantly different. In other cases, however, important differences were found, showing errors in either the model or in the measurements.

The most significant differences were, however, found in the **user test**. Two cases were submitted to several different users and results were compared. One case was simple and clearly defined, with all essential input data provided. For this case, all users but one (who made a modelling error) provided the same results. The other case, however, was more realistic, since data were provided as usually available in practice: only building plans and some measurement results. The user not only had to design the network model, but also had to choose some essential input data, in particular the pressure coefficients. Very large differences in the results were found in this instance. Most discrepancies can be explained by modelling errors which are partly due to some unclear instructions in the draft User Guide, since corrected, and others from differences in input data.

The limits of applicability of COMIS were not found although they may exist. But other limitations were found by the user: the uncertainty of input data and the way a particular case is modelled have a large effect on the result. This Annex provides an important indication to the user on how the uncertainty of his result is related to the uncertainty of the input data.

## HOW TO GET A23 DOCUMENTS, PROGRAMS AND DATA

- Copies of this report can be obtained from:  
C.-A. Roulet, LESO, EPFL, CH-1015 Lausanne, Switzerland,  
claude.roulet@leso.da.epfl.ch  
as well as the following software:
- MISA (Multirun Interface for Sensitivity Analysis), which is an interface for COMIS working on DOS, UNIX or VMS
- LiSA (library for design of experiment), which runs within MATLAB
- MATLAB which is a mathematical software can be obtained from:  
The Math Works, Inc. 24 prime Park Way, Natick, Mass. 01760-1500, USA  
On Netscape: <http://www.matworks.com>  
E-mail: [info@mathworks.com](mailto:info@mathworks.com)
- COMIS (COMVEN) which is the multizone air flow program evaluated in this report can be obtained from:  
H. Feustel, Lawrence Berkeley Laboratory, Building 90, Room 3074, 1 Cyclotron Road, Berkeley, CA 94720, USA. [hefeustel@lbl.gov](mailto:hefeustel@lbl.gov)  
The availability is submitted to IEA rules and you will probably be directed to your national contact (cf. IEA information at the beginning of this report).
- Annex 23 Papers can be obtained from the authors
- Evaluation data can be obtained from the authors

## SELECTION OF SOME ANNEX 23 DOCUMENTS

The following documents have been selected by the editors to enlarge the view over the annex and especially over subtask 3. There are as well manuals of the Annex as working documents whose interest exceeds their status of internal documents but which have not yet been distributed more widely and whose content has not been reported in this report by care of conciseness. There are also publications which summarise the work. A comprehensive list of the Annex 23 documents and publications can be found in the operating agent report. The listed papers can be ordered to their author.

Borchiellini R.: The inverse problem theory applied to air flow estimation and experiment design in the multizone case. *Paper presented at International Symposium on Air Flow in Multizone Buildings, Technical University of Budapest, Hungary, September 8, 1992. IEA.ECB.A23/92.09.08/RB.*

COMIS: Fundamentals of the Multizone Air Flow Model - COMIS. *Technical Note AIVC 29, May 1990.*

COMIS: COMIS User Guide.

Fürbringer J.-M.: Evaluation procedure using sensitivity analysis of models and measurements. *Paper presented at International Symposium on Air Flow in Multizone Buildings, Technical University of Budapest, Hungary, September 8, 1992. IEA.ECB.A23/92.09.09/JMF*

Fürbringer J.-M., Dorer V.: Air flow simulation of the LESO building including comparison with measurements and sensitivity analysis. *Proc. INDOOR AIR '93, Finland, 1993.*

Fürbringer J.-M., Borchiellini R.: Technique of sensitivity analysis applied to an air infiltration multizone model. *ASHRAE trans. Vol. 100, part 2, pp. 683-691, 1994.*

Fürbringer J.M.: Comparison of the accuracy of detailed and simple models of air infiltration. *Proc. 15th AIVC conf. Buxton, Sept. 1994.*

Fürbringer J.M., Roulet C.-A.: Sensitivity analysis- an unavoidable step in the evaluation of simulation program. *Proc. European conf. on Energy Performance and indoor Climate in Buildings, Lyon, Nov. 1994.*

Fürbringer J.M., Roulet C.-A.: The evaluation of a multizone infiltration Computer Code, 2nd int. Conf. on IAQ and ECB, Montreal, May 10-12, 1995.

Geerinckx B., Wouters P.: Empirical methodology to validate energy related simulation programs. *Paper presented at International Symposium on Air Flow in Multizone Buildings, Technical University of Budapest, Hungary, September 8, 1992. IEA.ECB.A23/92.09.09/BG*

Pelletret R., Feustel H.: A23: General presentation. *Paper presented at The ExCo meeting in Sophia Antipolis, France, 2-4 June 1992, IEA.ECB.A23/92.06.01/RP*

Rao J., Haghghat F.: A procedure for sensitivity analysis of airflow in multizone buildings. *Paper presented at International Symposium on Air Flow in Multizone Buildings, Technical University of Budapest, Hungary, September 8, 1992. IEA.ECB.A23/92.09.09/JR*

Roulet C.-A., Fürbringer J.-M.: The evaluation of a multizone infiltration computer code. *Paper presented at International Symposium on Air Flow in Multizone Buildings, Technical University of Budapest, Hungary, September 8, 1992. IEA.ECB.A23/92.09.09/CAR*

Wouters P.: Validated simulation tools: possibilities and limitations. *Paper distributed at the Tokyo E.M. IEA.ECB.A23/94.09.19/PW.*

## INTRODUCTION

The work undertaken in the frame of Subtask 3 of the IEA-ECB&CS Annex 23 "Multizone air flow modelling" is reported here. This report is the synthesis of the evaluation work made on COMIS within Annex 23, although some previous reports and several publications have been produced by the participants.

COMIS (Conjunction of Multizone Infiltration Specialists) is a multizone air flow and contaminant model which was started in 1989 during a one year international workshop, by specialists coming from China, France, Italy, Japan, The Netherlands, Spain, Sweden, Switzerland and the United States.

The program, consisting of up-to-date models and numerical methods, as well as integrating original works of the group, is aimed at allowing the user to simulate air flow and pollutant pattern in a multizone structure. COMIS is a nodal model based on pressure boundary conditions. Basically, the program includes the following elements: cracks, duct systems, fans, volumes, layers, vertical large openings, source and sink of pollutants, pressure coefficients of facades. It solves a static system of equation using a Newton-Raphson algorithm. It is written in the FORTRAN 77 programming language. More details can be found in related bibliography (cf. p. 10).

Following the impulse of the first year of conjunction and development (which was of course not sufficient to finish all the necessary work), an international research project has been organised within the frame of the IEA-ECB&CS: The Annex 23 Multizone Air Infiltration Modelling. Countries which joined this annex are Belgium, Canada, France, Greece, Italy, Japan, The Netherlands, Switzerland and the United States.

The work has been divided into 3 subtasks. Subtask I which is responsible of the integration of new models (understanding new features available to the user), the user guide and user interfaces. Subtask II was in charge of gathering input data and performing measurements to collect data for the evaluation, and Subtask III involved in the evaluation of COMIS, which is reported in this document.

Validation is a word which is somewhat abused since a model can never be validated, but rather be not yet actually invalidated. The use of simulation in practice requires a warranty of the results and this is only possible by a comprehensive evaluation and generalised sensitivity analysis. For this assessment of the simulation results, several tools have been developed, tested and improved. The whole methodology of 'validation' has been reviewed, re-analysed and adapted to our field.

In conjunction with parallel efforts within other tasks of the IEA (Solar task 12 and ECB & CS Annex 21) and research projects of the European Community (PASSYS) an up-to-date methodology with a robust background and efficient tools is taking form.

This work could be the basis of an exacting treatment of uncertainty in simulation which is an absolute requirement for a confident use of simulation in practice. It is a challenge for modellers to distribute products which can not be misused too easily.

This document is divided into 6 chapters which report on the methodology and the related tools, the analytical comparisons, the inter-model comparisons, the empirical comparisons, the user tests and the conclusions. Taking into account the type of collaboration within the IEA annexes, each author or group of authors, indicated at the bottom of the odd numbered pages, is responsible for the content of his text. However, these texts were first reviewed by external readers and then slightly modified by editors.

# 1 STRATEGY, METHODS AND TOOLS

The result of Annex 23 should be a reliable, practical and user-friendly code for Multizone Air Flow (MAF) modelling. Reliability means that the user should have good reasons to have confidence in the results of the calculations performed with the code on the basis of his input data. User friendliness means not only that the program says "Hello" when started, but also that the program is adapted to the needs of the user, that input data are clearly asked for, easy to introduce, well controlled, and easy to correct. Outputs provided by the program should be useful and understandable. This ambitious goal cannot be reached without a complete evaluation procedure.

The strategy of validation used for COMIS within Annex 23 was decided upon after studying what is done in other fields, especially in the field of heat exchange in building. The theory of experimental design was also widely used to save simulation time.

The validation of a simulation program is part of its development. This procedure should prove that the numerical results are effectively the solution of the problem described in the input files. The validation can also be considered as the quality label of the program. It is a huge, complex and expensive task.

To guarantee a real validation, the output data of the program must be compared with high quality measurement data. The experimental cases included in the validation data set must cover the set of cases which can be simulated by the program.

Another aim of the validation is to allow the evolution of the program towards increasing accuracy. It must be verified whether in fact cutting, adding or changing a routine globally improves the program. There is a risk of decreasing the program quality by adding an element whose input data are difficult to measure accurately. In this process it is most important to consider the possible accuracy of the measurement of the physical quantities which are used as input or verification data.

## 1.1 Strategy

Tools were produced during this project for the evaluation of measurement and simulation accuracy. These tools allow the development of programs towards improving, or at least constant, accuracy. They also allow the user to know the effect of limited accuracy of input data on output data. If it is generally admitted that an experimental result must be provided with a confidence interval, programs computing the confidence interval of output are seldom seen.

### 1.1.1 Knowledge structure

The verification of the output data of a model with corresponding experimental data is equivalent to the scientific process of to-and-fro between model and reality. A maximal redundancy is required between information contained in the program results and the experimental data used for comparisons. But it is not correct to consider experimental data as the reality, the absolute reference. Because of their uncertainty, experiments give only an image of reality and the fidelity of this image is determined by the confidence intervals.

These epistemological concepts are important to define a correct validation procedure. Figure 1.1 presents the knowledge model used in the project. This model is based on the epistemology of Kant [1808]. This theory affirms that we never access directly to the pure reality called *noumen*. Through the measurement, we access the *phenomenon* which is the sensible reality.

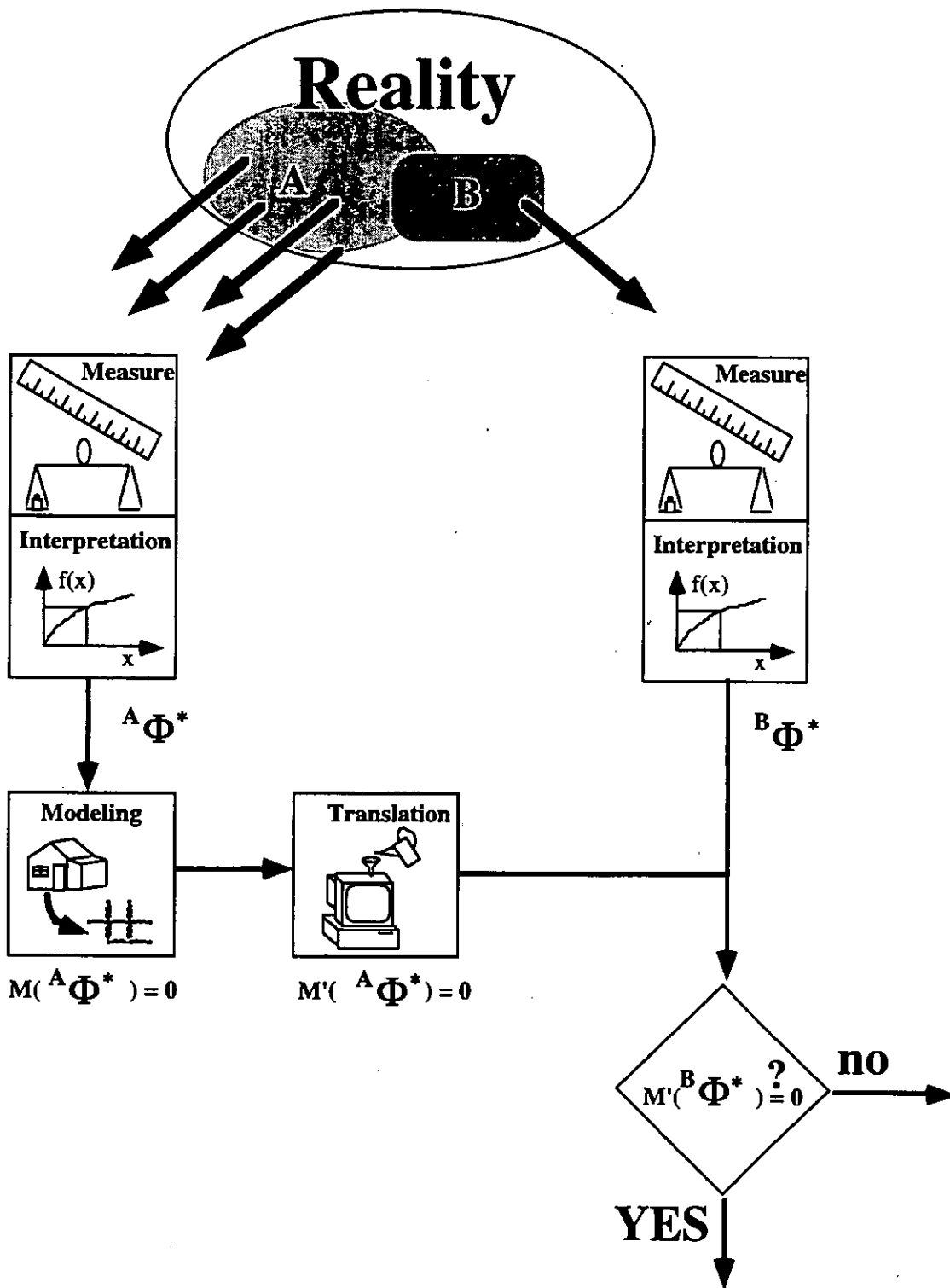


Figure 1.1: Knowledge model used to elaborate the validation process. Squares represent operators acting on the reality or on the output of other operators.

The measurement of some observables on object  $A$ , which is a subset of reality, provides a set  $A\Phi$  of data which gives an image of the reality. The rough results depend on the type of probes which most of the time are electrical signals. These results are interpreted to obtain a set of observables in the usual units of temperature, pressure, flow rates, etc. This interpretation is based on a model of the measuring device. The interpretation of a temperature measurement, for example, implies the modelling of the thermometer. In building physics, the measuring device model is sometime extremely complex.

The modelling of object  $A$  consists of determining the link between some elements of  $A\Phi^*$  to reproduce its behaviour and predict the values of some observables that are functions of the values of some other ones. If  $M$  is the function linking interpreted observables, this can be represented by equation 1.1

$$M(A\Phi^*) = 0 \quad (1.1)$$

The building of a program on the basis of this model  $M$  requires translating it into  $M'$  following the constraints of numerical and computer science. By definition the model is compatible with the data on which it is based.

The interest of a model lies in the possibility of a generalisation, which means the possibility of modelling with the function  $M$ , another object  $B$  similar for some aspect to  $A$ . Typically, in the case of building physics, researchers are elaborating models reproducing thermal and aeraulic behaviour of the highest possible number of buildings in various weather conditions. The validation consists in verifying that whatever the object  $B$  satisfying the validity criteria of the model, relation 1.2 is verified :

$$M(BF^*) = 0 \quad (1.2)$$

When the relation is not verified it is necessary to understand the cause, to know whether it is a limitation of the model or an error. Each operator constituting the measurement, the interpretation, the modelling and the translation are susceptible to errors (cf. fig. 1.1) The validation procedure must take that into account and allow the screening between modelling, measurement and programming errors.

### 1.1.2 Internal and external errors

A distinction is made between internal errors which come from the simulation program and external errors which come from the input data and are principally due to the uncertainty of the experimental data. Table 1.1 adapted from the work of Bowman et Lomas [1985] on the validation of thermal programs, gives a classification of the external errors occurring within the validation procedure [Fürbringer et al, 1990].

The importance of the external error comes from the fact that if they are too large, they make a screen which hinder the detection of possible internal errors. Therefore, in the validation process, the better strategy is not to attempt to measure all the parameters as precisely as possible. It is more judicious to concentrate the effort on parameters whose influence is dominant, the aim being to minimise the external error at a reasonable cost..

Table 1.1: Classification of the external errors during the validation process of a simulation program [Bowman and Lomas, 1985, Scartezzini et al., 1987].

Model input data	Climatic data Site data Building data Occupancy User interface	Data coming from a remote site. Measurement frequency too low (specially for wind). Limited measurement accuracy. Inaccuracy of pressure coefficients Inadequate description of building geometry and construction. Uncertain workmanship. Use of data from literature instead of measured properties. Not modelled adjacent zones are not defined. Limited measurement accuracy. Interference with the building system. Badly defined occupant behaviour. Uncertainty in modelling HVAC. Blunders when entering data. Wrong interpretation of poorly documented input module. Missing data replaced by assumed values. Changing the building so it can be modelled. Program amendments to model a particular building.
Building response data	Data logging Interference	Noisy, missing or spurious data. Measurement frequency too low to define the variable. Limited measurement accuracy. Internal feature of structures altered by monitoring equipment.
Comparison procedure	Data comparison	Errors in transcription from charts or files. Different definitions for measured and predicted parameters. Different locations for measured and predicted parameters.

### 1.1.3 Validation steps

The evaluation procedure can be divided into the following tasks:

1. The **Module Evaluation** controls that each module of the code performs as it should do and determines its own region of validity. Such evaluation is done during the development of each module, and therefore will not be considered below. The evaluation considered here addresses the whole program which comprises an assembly of such modules.
2. The **Sensitivity Study** examines the change in amplitude of some results provided by the code when input data changes from one end of the domain to the other. It provides a selection of the most important input parameters, which are those whose changes result in the greatest variation of the response. The interference effects (e.g. the effect of combined the variation of two or more variables) should also be studied here. Up-to-date statistical methods now make it easily possible. Large domains sometimes result in responses which are difficult to analyse. To avoid such a problem beginning with smaller domain it is recommended, for example 1% or 5% around the centre of the main domain. The studied domain can be enlarged further afterwards.
3. The **Propagation of Error Study** should give the possible error in the result when there are realistic errors in the input data. The Monte-Carlo method was systematically used for that task.

It was first planned to select, from an initial sensitivity analysis, the input parameters having the larger influence on the output, and to perform error analysis only on these ones.

However, the present study showed that, in the COMIS model at least, the effects of the parameters depend on the studied case and on the values of the parameters themselves. Therefore, the strategy was modified in order to be able to perform an error analysis on any input set.

4. **Analytical Evaluation:** as some simple cases have an analytical solution, it is possible to compare them with their simulation by the program. It is possible to compare COMVEN with commercial mathematical software to test if the mathematical treatment within COMVEN is as correct as the mathematical software, which can be assumed to be up-to-date in its field. A comparison between COMVEN and pieces of mathematical software has been included in chapter 2 "Analytical Evaluation".
5. **Numerical Comparison:** the result of different programs for the same case are compared in chapter 3 "Inter model comparison". There are different perspectives depending on whether the compared programs are equivalent or not. COMVEN can be compared with a simple model or a more complex one to evaluate the influence of the level of complexity on the solution. COMVEN can also be compared with another equivalent program to assess that equivalence. It would appear that if two programs give the same response, it is not conclusive proof that they are right. If they do not agree, one or both are wrong.
6. **Comparison with experiments:** knowing the accuracy of the experimental data gathered for evaluation and the propagation of errors through the computer code, the results of the calculation based on measured input data on some selected cases can effectively be compared with the measured output data. The simple comparison with a two-axes graph, where one axis is dedicated to the experimental data and the other to the numerical one, is not sufficient. The validation should allow the identification of the causes of discrepancies between measured and simulated data so that it could be possible to adapt the program if necessary. Only minimal confidence intervals and a precise experimental report can warrant that.
7. **Performance of Program and User feedback:** Important limits of the application domain come from the interaction between the user and the code. In order to evaluate these limits and to enlarge the application domain by improving the user-friendliness, the program was distributed to interested users, together with test cases. The users treated the cases with the program and noted the problems encountered together with comments on the user-friendliness. These comments were collected together with the input files and the results obtained by the users. All this information was used to improve the man-code interface.
8. In the next chapter, the way in which some of these points are treated within Annex 23 is presented with more detail

## 1.2 Methods

### 1.2.1 Module test

All the routines included in the code must be checked to verify their physical and numerical behaviour. This is the responsibility of the author. This essential work belongs to Subtask 1 (program development) and is not reported but simply highlighted here.

### 1.2.2 Analytical evaluation

The analytical evaluation consists in comparing the results of the programs with cases which have an analytical solution. The aim of this task can be either the evaluation of the numerical or the physical behaviour of the code. 44 tests provided were used within this project.

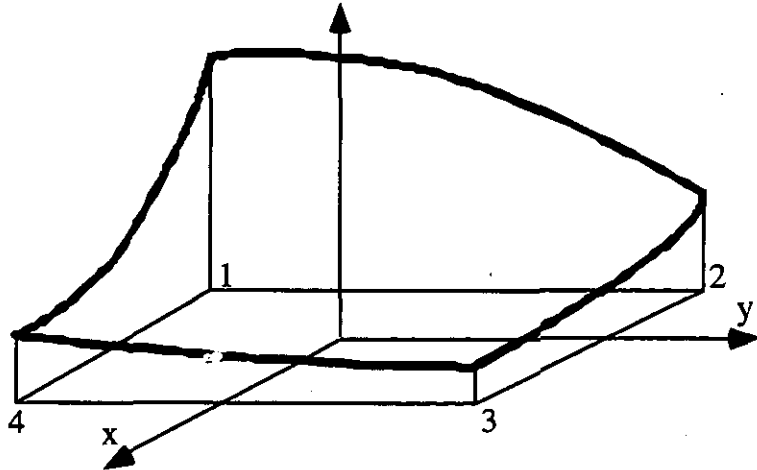
### 1.2.3 Inter-model comparison

The inter-model comparison is the comparison of the results of COMIS with other pieces of software. Comparisons have been made with 14 models classified as single zone and multi-zone network models, simplified models or specific models.

### 1.2.4 Sensitivity analysis

This very important task is a base for any subsequent work. Since the input parameters are numerous, it is important to know those which have the largest effect on the results.

*Figure 1.2: Principle of the sensitivity analysis with two input parameters (x and y) and one output. In this case, calculations at points 1 to 4 will show that the output depends more on the value of x than on y, but there is a strong interference effect.*



The various steps of this study are:

1. Definition of the **application space**, which results in a list of input parameters together with their possible range of variation (minimum and maximum values). The region of validity determined for each module is input information for this step.
2. Choice of **significant results**. The computer code provides several results (for example all air flow rates between each pair of zones), which cannot be fully inspected, therefore only some of them, or a combination of these (for example, the total air infiltration rate, or the global mean age of the air), should be chosen before the analysis.
3. For the **sensitivity analysis**, many runs of the computer code are performed, each with a different input file, in order to see the effect of large variations of the input parameters on the results. In order to minimise the number of runs and to get significant results, the use of a good experimental design is of great help here. Several designs were proposed for such a task, such as differential sensitivity analysis (DSA) [Judkoff, Wortman, O'Doherty and Burch, 1983], Monte-Carlo analysis (MCA) [Lomas, Bloomfield, Parand and Piney, 1989] or stochastic sensitivity analysis (SSA) [Irving, 1987]. These possible designs are better described below.
4. Perform the runs with the selected input data. This task is greatly simplified if done automatically by a purpose developed code, like MISA.

In DSA, the code is run twice for two extreme values of each parameter, all the other parameters being maintained at their most likely value. This provides the pure effect of each parameter, but does not give any indication of the cross interferences, and requires nevertheless  $2N+1$  runs,  $N$  being the number of input parameters.

For the MCA, all the parameters are changed at random for each run, according to their probability distribution. After enough runs, the probability distribution of the chosen result is obtained. This technique provides only the global variation of the result without any informa-

tion on the effect of each parameter, but requires generally less than 100 runs [Lomas and Eppel, 1992].

In SSA, all the input parameters are varied at random and at every time step of the time-dependant simulation. The sensitivity of the result on each parameter is obtained from the correlation function between input and output variations and from auto correlation function of the changes of input parameters.

These plans look attractive and may be, in some cases, the only practical ones. It is shown however that more information could be obtained with less effort (smaller number of runs) when several parameters are changed at each run (in contrast to DSA) and when they are changed in a properly chosen, systematic way (not at random) [e.g. Silvey, 1980 or Box, Hunter and Hunter, 1978]. A good experimental design for that purpose is a partial two-level factorial design (e.g. a Plackett-Burman or a half factorial experimental design), having selected points at several corners of the N-dimensional parallelepiped limited by the maximum and minimum values of each input variable. Such designs are used for the sensitivity study of COMIS [Fürbringer, 1992]. Non linearity can be detected by adding the central point (average co-ordinates) and "star" points (points on the ends of the axes) to the previous experimental design.

The sensitivity analysis allows one to select the most important input parameters, which are those which present the greatest absolute or relative variation of the response. The interference effects (e.g. the effect of combined variation of two or more variables) of several variables are automatically obtained when using MCA or partial factorial designs. Such effects may be important in infiltration models, which are non linear.

Nevertheless, the critical point resides in the number of important parameters and the magnitude of the variation range. For small variation (<10% of the mean value) linear effects on responses have been observed making it possible to use the Hadamard matrixes available for up to 200 factors and hugely minimising the number of simulations. When variations are larger, it is imperative to use fractional factorial design. But this design implies a larger number of simulations, and because of that the parameters should be divided into sub-groups.

### 1.2.5 Experimental comparison

In a workshop on validation, Lomas [1992] has proposed the following strategy:

*Most frequently, validation is undertaken using an approach in which predictions are compared with measurement data and, if mismatches are found, the input data is changed, within the bounds of plausibility, to improve the fit; this circle may be repeated a number of time. This will be termed a Class B approach. It has been shown that it is easy to fit the predictions of programs to measured data and that the Class B approach is extremely unlikely to reveal the existence of internal errors. Thus, programs may be accepted as valid even when they contain serious errors. It is much more valuable to adopt a Class A approach which involves firstly modelling the structure as accurately as possible, and preferably 'blind': that is, without any knowledge of the measurements. Then, the predictions must be compared with the measurements without making refinements or repeating simulations. These are termed the 'base Case Prediction', and they remain fixed throughout the remainder of the validation process. The difference between the measurements and predictions is then a true measure of the accuracy possible under conditions approaching those in which the program will be used in practice.*

*The uncertainties in the base case predictions are then accounted for, in a logical and systematic way, by quantifying the magnitude of all the errors in both the measurements and the*

*predictions. The measurements and predictions are then compared statistically taking these errors into account. This approach leads to a three tier empirical validation methodology.*

*Level 1: A base case prediction is obtained without regard to the measured performance. These predictions, and corresponding measurements, are then compared and if they differ by less than the errors in the measurements alone, the model is deemed to be satisfactory at level 1 for the particular situation examined; if not, it is advisable to progress to level 2.*

*Level 2: The total uncertainty in the predictions due to external errors in the model input data, is quantified. If the base case predictions for the parameters of interest differ from the measurements by less than the total uncertainty, the model is deemed to be satisfactory at level 2 for the particular situation studied, if not it is useful to progress to level 3.*

*Level 3: The internal errors which cause the divergent predictions are detected, either by comparing the predictions of individual algorithms with detailed mechanism level data, or by using some other validation techniques (...).*

*Having completed Level 3, it will be possible to rectify the internal errors and repeat the validation process.*

*If a program is deemed to be satisfactory at either Level 1 or Level 2, this does not mean there are no internal errors. Rather, any errors which exist are either small (and not detectable by the data set) or larger but they are either compensated for by other internal errors (which have an equal but opposite effect) or they lie in parts of the program which are not stressed by the data set chosen or the parameters compared.*

For the 10 cases analysed and reported in detail in appendix, the above methodology has been used.

### 1.2.6 Data specifications

To be useful for an experimental validation, the data should fulfil the following specifications:

- **compatibility:** the data shall be measured on a building or a case which can be modelled with COMIS,
- **completeness:** all the data necessary to run the code for the specified case and to compare results should be provided,
- **known accuracy:** all the data shall be provided with their correct confidence intervals
- **good accuracy:** the confidence intervals should be small, according to the state of the art,
- **synchronism:** all variable parameters should be measured at the same time,

Usually, these specifications are met only in data sets measured on purpose of validation. These specifications are developed more in detail below.

#### *Compatibility*

This is an obvious specification. Data measured on a case which cannot be modelled with COMIS cannot be used within Annex 23. For this reason and with that meaning, any Annex 23 participant, and in particular those providing data, should understand COMIS.

Another aspect is that the data should be presented in a way they are useful with COMIS. The ideal way is to provide an input file filled with the measured data provided as input data (together with information on their accuracy). Moreover, the measured data to be compared with predicted ones shall have the same physical definition as in COMIS.

It is planned that the experimental validation tasks will be performed by teams, including specialists of measurements and of COMIS, each team being in charge of one case. In order to ensure the compatibility of data, this team should work together from the very beginning.

Ideally, the computer specialists should also work for the measurements and the measuring people should also use COMIS.

### ***Completeness***

The data provided should contain all the input data necessary to compute, with the COMIS code, the output data which should be compared with the provided, measured data. For a typical infiltration problem, the input parameters set should include the following measured data [Scartezzini, Fürbringer, Roulet, 1987]:

- permeability distribution of the envelope,
- permeability distribution of the partition between zones,
- wind pressure coefficients (with standard deviation when available),
- internal temperatures and temperature gradients,
- mechanical ventilation data,
- meteorological conditions,

and the output parameters are air flow rates.

To validate special parts of the program such as the large openings, the inhabitant behaviour, the contaminants transportation, etc., the corresponding data should be provided.

An important point is the meteorological data. At least wind and temperature data should be measured on site. In particular, wind speed and direction could be completely different in locations which could be quite close to each other, and data provided by a nearby weather station could be inappropriate.

The AIVC technical note 32 should be used as reporting guideline. However, it is not necessary to report data which will not be used in the validation task for which the data set is planned.

### ***Accuracy***

It is essential that the data be provided together with realistic error bars or better with confidence intervals, that is intervals in which the data is contained with a given probability P (e.g. 95%). These intervals shall be realistic, hence neither under- or over-estimated.

High accuracy may not be essential, but is useful anyway. A comparison between accurate data provide more information than a comparison between data with large confidence intervals, since if these intervals are large enough, data will always fit.

The sensitivity analysis and the error analysis will provide the accuracy required for a given purpose, in particular for obtaining results with prescribed accuracy. However, it is not possible to wait until the completion of these tasks to begin with the collection of validation data, which is a huge work. Therefore, it makes sense to perform the measurements with the best possible accuracy, according today's knowledge in measurement techniques. For that reason, laboratory measurements are of great value, since the parameters are much better controlled than for on site measurements.

### ***Synchronism***

The typical time constants in ventilation are quite short, and the flow rates generally follow the variations of the acting forces. This simplifies the model, which generally does not have to take account of storage, but requires fast and quasi-synchronous measurements of every variable parameters. The synchronism specification is fulfilled if:

- a) measurement of all variable parameters are performed at short time intervals, their time average being recorded at longer time intervals,
- b) the measurement schedule is known.

Data should be recorded several times per hour (typical interval is 5 to 15 minutes). It is better to provide data sets recorded at short time intervals during a relatively short period (from an hour up to a day) than to record during a whole year daily averages.

Special care should be taken in averaging the wind parameters [Fürbringer, Compagnon, Roulet, 1989]. The measurements of the wind should be taken with fast reacting anemometers at short intervals (ideally at 10 Hz, but 1 Hz may be sufficient). Basically, the time average of the three (or at least the two horizontal) components of the wind should be provided together with their corresponding standard deviation, which are used to estimate the turbulence intensity.

In most cases, data loggers are used, which scan the various channels one after the other. The resulting data are also provided one after the other, together with the date and hour of the first measurement or of the recording time. The schedule of the measurements of the various channels, that is their scanning order and the time between two channels, shall be provided together with the data, in such a way that the influence of the asynchronism can be evaluated. The exact measurement time of each channel can also be recalculated if required.

### *Selection of cases*

Below are listed some criteria to select validation cases, that is buildings or part of buildings on which measurement should be performed for purpose of validation. It is obviously not possible to perform experimental validation on any type of building submitted to any external conditions.

Three main classes of parameters can be mentioned:

- Structure of the building, modelled by a nodal network with a number of nodes and links.
- Climatic conditions and surroundings, resulting in various forces acting on ventilation:
  - wind dominated ventilation
  - stack dominated ventilation
  - mixed conditions
- typology of the zones, e.g. with or without internal thermal gradients, large openings, etc.
- type of ventilation, natural or mechanical or combined
- steady (or quasi-steady) or non steady (or dynamic) state.

Within the present work, the measured buildings were not actually selected according to such ideal criteria. Practical criteria such as existing instrumentation, cost of the measurements, availability of data, were of prime importance. In measured buildings however, data were compatible, complete, synchronous, and provided with confidence intervals.

## 1.3 Tools

### 1.3.1 Design of experiments

#### *Theoretical basis*

When the experimental conditions can be controlled, they should be defined before performing the experiment to familiarise oneself with the work to be done. In the case of simulations, the definition of "experimental" conditions consists of giving a numerical value to each input variable. The way these values are given for a set of successive experiments is experimental planning design.

The aim of a good design of experiments is to determine the experimental condition in order to obtain the required information with a minimum of work and the highest possible confidence. One argument which supports the claim for optimal design is that, in any case, there is always a design of experiments, and if it is not optimised by a suitable analysis procedure before the experiment phase, the researcher is constrained to use sophisticated statistic tools to analyse his data, with a considerable risk that the interesting information is not in the obtained data.

The 'star' design, which is varying one parameter at a time, is not a satisfactory design at all because no interaction effects can be estimated that way and the distribution of information within the experimental space is not at all uniform. This design requires, nevertheless, a larger number of experiments.

#### *Factorial design*

Factorial design is a classical experiment design method which allows the determination of the coefficients  $\alpha_i$ ,  $\alpha_{ij}$ , etc., of a linear model with interactions, as in Equation (1.3), with a minimum number of experiments.

$$Y = \alpha_0 + \sum_i \alpha_i X_i + \sum_{i \neq j} \alpha_{ij} X_i X_j + \dots \quad (1.3)$$

The matrix of experiments  $E$  includes the elements  $e_{ij}$  which are the values of the input parameters  $X_j$  for the experiment  $i$ . In factorial design, measurements or simulations are done only at the minimum and maximum values of each of the  $N$  parameters. As all the combinations are used, this provides  $2^N$  points in the experimental space corresponding to the vertex of a  $N$ - dimensional parallelepiped.

If the input parameters are centred and normalised, the matrix of experiments contain only -1 and +1 values. That gives, in the case of three dimensions, the matrix presented in Equation 1.4 and illustrated in Figure 1.3.

The factorial design allows the identification of the  $2^N$  coefficients of a saturated model such as that of Equation 1.4. If all the coefficients are not of interest, for example if only the first order interaction are required, it is possible to use a fraction of the full factorial matrix. The fractional matrix is built from one or more relations called generators, which define which coefficients are aliased.

Without going into too many detail (interested people will find them in [Box et al, 1978]), it can be said that fractional factorial designs are sorted of functions of their resolution,  $R$ . The resolution index indicates which kind of coefficients are confounded as explained in Table 1.2.

For the moment, there are no straightforward algorithms to build the suitable fractional factorial design from the desired coefficients. It is necessary to use tables [Box et al, 1978] or a trial and error method to obtain satisfactory matrices.

$$E = \begin{pmatrix} -1 & -1 & -1 \\ -1 & -1 & 1 \\ -1 & 1 & -1 \\ -1 & 1 & 1 \\ 1 & -1 & -1 \\ 1 & -1 & 1 \\ 1 & 1 & -1 \\ 1 & 1 & -1 \end{pmatrix} \quad (1.4)$$

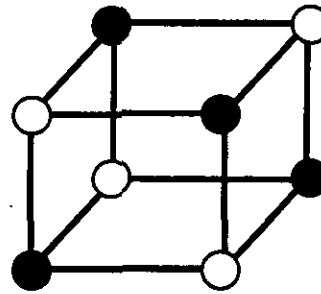


Figure 1.3: Space position of a factorial design of dimension 3.

Table 1.2: Resolution of fractional factorial matrices

Resolution	Definition
R=III	does not confound main effects with one another but does confound main effects with two-factor interactions.
R=IV	does not confound main effects and two-factor interactions but does confound two-factor interactions with other two-factor interactions.
R=V	does not confound main effects and two-factor interactions with each other, but does confound two-factor interactions with three-factor interactions.

### Plackett & Burman design

The Plackett & Burman [1946] designs are a sub-group of the factorial designs. They allow estimation of the main effects of the factors of a process but not the interaction effects. Because of a very complicated structure of aliases, these designs can not be de-aliased.

For the estimation of the main effects of  $N$  factors, a Plackett and Burman design needs  $N+1$  experiments. Up to 200 such designs exist.

### Monte Carlo design

In the Monte Carlo experimental plan, simulation points in the experimental space are chosen at random [Rubinstein, 1991]. A probability distribution is associated with each input parameter representing the quality of the information available to the modeller. The random choice of the simulation points is done with respect to these distributions. The output data, obtained after each run, are stored and then analysed to extract statistical information, allowing the qualification of the statistical behaviour of the output parameters  $Y_i$ . One is usually interested in the probability distribution of the  $Y_i$ , their mean values  $m(Y_i)$  and standard deviations  $s(Y_i)$ .

Estimates of the mean and the standard deviation of the output parameters' population can be calculated after any simulation number ( $>2$ ). However, it is the only information available using this method: a mean answer and its standard deviation related to the (input) experimen-

tal domain. This space is determined by the combination of the definition set of input probability distributions.

For a large number of input parameters, whatever their probability distributions, one expects answers more or less normally distributed if the simulation process is continuous. The estimates of the confidence intervals of the mean  $m(Y_i)$  and the standard deviation  $s(Y_i)$  are based on the hypothesis that the output distributions are gaussian.

The confidence interval of the real mean  $\mu_j$  of the output  $Y_i$  follows a Student distribution  $T$  with  $N-1$  degree of freedom. That means that if  $\gamma$  is the confidence level of a two-sided test, usually 95% or 99%, the real mean  $\mu_j$  verifies the probability Equation 1.5:

$$\text{Prob}[(T: N-1) \leq \mu_j] = \frac{1}{2}(1+\gamma) \quad (1.5)$$

From the tabulated values  $t_{1-\gamma/2}[N-1]$ , the confidence interval of  $\mu_j$  is then given by Equation 1.6:

$$m(Y_j) - \frac{s(Y_j) t_{1-\gamma/2}[N-1]}{\sqrt{N}} \leq (\mu_j) \leq m(Y_j) + \frac{s(Y_j) t_{1-\gamma/2}[N-1]}{\sqrt{N}} \quad (1.6)$$

The true confidence interval of the standard deviation  $\sigma_j^2$  follows a  $\chi^2$  law with  $N-1$  degrees of freedom. That means that if  $\gamma$  is the confidence level of a two-sided test, the real standard deviation  $\sigma_j^2$  verifies the probability Equations 1.7 and 1.8:

$$\text{Prob}[(\chi^2: N-1) < (\sigma_j)^2] = \frac{1}{2}(1+\gamma) \quad (1.7)$$

$$\text{Prob}[(\chi^2: N-1) > (\sigma_j)^2] = \frac{1}{2}(1-\gamma) \quad (1.8)$$

From the tabulated values  $\chi^2_{\gamma/2}[N-1]$  and  $\chi^2_{1-\gamma/2}[N-1]$ , the confidence interval of  $\sigma_j$  is then given by Equation 1.9:

$$(N-1) \frac{s(Y_j)^2}{\chi^2_{\gamma/2}[N-1]} \leq (\sigma_j)^2 \leq (N-1) \frac{s(Y_j)^2}{\chi^2_{1-\gamma/2}[N-1]} \quad (1.9)$$

Figure 1.4 shows the relation between the number of runs and these confidence intervals normalised by the standard deviation  $s(Y_i)$ . The boundaries of the confidence interval of the standard deviation tend towards 1. However, after 60-80 runs the improvement in accuracy is very small. This behaviour is independent of the number of input parameters. This characteristic of the Monte-Carlo method makes its accuracy entirely dependent on the number of runs.

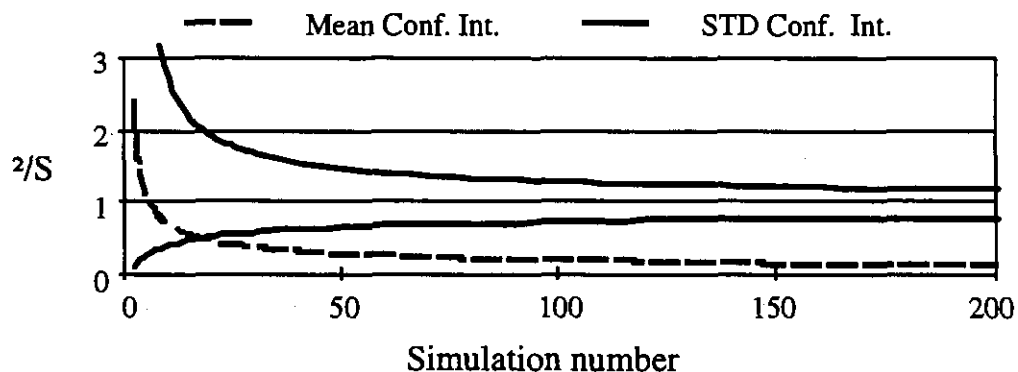


Figure 1.4: Relation between the number of runs and these confidence intervals at 95% normalised by the standard deviation  $s(Y_i)$

Factorial and Monte-Carlo designs may be (and were) combined in sensitivity analysis [Fürbringer and Roulet, 1995].

### 1.3.2 LISA (Library for Sensitivity Analyses)

A library called LiSA (Library for Sensitivity Analyses) was devised within the mathematical software MATLAB for the design of simulations and their analyses. The list of the main functions is given below. The library is available for PC, UNIX or MACINTOSH from the LESO group.

The functions of the LiSA library can be linked through script files or used on-line one after the other. A short description of the main functions is given in appendix A. A minimum of knowledge of experimental planning theory is required to use them. For that we recommend reading one of the following references: [Box et al. 1978, Gunter 1993, Goupy 1988 or Fürbringer 1994].

### 1.3.3 MISA

MISA, which means Multirun Interface for Sensitivity Analysis, is the software used for the sensitivity analysis of COMVEN. At that stage of development no user friendly program is available to design the planning of the simulation nor to process the result files. These features should be available only with SAM (Sensitivity Analysis Module) to be included in COMIS 3.0.

MISA prepares a series of input files for COMVEN, according to proper experimental planning. It then runs COMVEN as many times as necessary and collects the resulting outputs.

A user guide for MISA, which is available for PC, VMS and UNIX, is provided in Appendix B.

### 1.3.4 SAM (Sensitivity Analysis Module)

At the beginning of the project, a month or more was necessary to make a sensitivity analysis. With MISA, a building can be investigated in one week, but with SAM, this work will take no more than one day. This progress is possible by integrating the sensitivity analysis in the simulation environment and taking advantage of the graphical interface provided with COMIS 3 [Soubra, 1992].

Below are presented the proposed steps for a sensitivity analysis session:

Action	Example
 - The user chooses a COMIS input file (or an internal model at the ISE level) corresponding to the building he intends to analyse.	- The file LESO.CIF is chosen
 - SAM provides the list of the parameters which can be chosen as variables.	- The list contains air tightness coefficients $C_i$ , related exponents $n_i$ , crack high $h_i$ and length $l_i$ , pressure coefficients $C_{pj}$ , zone temperature $T_k$ , volumes $V_k$ , wind velocity, direction etc....

- 
  - The user chooses the number of groups and the parameters whose effects should be analysed.
  - The user chooses 4 parameters:
    - $X_1 = C(\text{front door}),$
    - $X_2 = n(\text{front door}),$
    - $X_3 = C_p(\text{front door})$
    - $X_4 = T(\text{zone 1}).$
- He chooses the level of interactions to consider and the metrics in which the selected parameters have to be varied.
  - He chooses also a factorial fractional design.
- He chooses the type of design: Plackett-Burman, fractional factorial or Monte Carlo.
- 
  - SAM can provide a preferred number of groups and level of interaction.
  - SAM advises the user that with 1 parameter more, he would have a better design for the same number of simulations.
- It provides the number of simulations, the alias set and the list of estimable coefficients.
  - The design proposed has 8 simulations and has the following alias list:  $a_{12} = \hat{E}a_{34}, a_{13} = \hat{E}a_{24}, a_{14} = \hat{E}a_{23}.$  Then the estimable coefficients are  $a_0, a_1, a_2, a_3, a_4, a_{12}, a_{13}, a_{14}.$
- 
  - The user can adapt his requirements to the SAM advice's.
  - The user decides that this design is satisfactory. He has sufficient information on wind effect.
- He chooses the variation ranges of the selected parameters either group by group or uniformly, either relatively or absolutely
  - He chooses to fix the variation range to  $\pm 10\%.$
- 
  - SAM provides a list of output parameters and offers the possibility of building combinations with them.
  - The list of output parameters is : the pressures  $P_i$  in all the zone of the building and the volume and mass transfer between the zones, the global incoming air flow, the thermal loss, etc.
- 
  - The user chooses the output parameters to be analysed and gives the definition of the possible synthetic output parameters.
  - The user chooses the global incoming air flow and the sum of the air incoming in zone 1 from outside and from zone 2.
- 
  - SAM manages the runs, collects the output data and provides selected effects on tables and charts with some basic interactive possibilities.
  - SAM provides tables and bar charts with some interactive tools, of the effects  $a_j$  and  $a_{ij}$  of the variation of the selected input parameters on the global incoming air flow.

### Data flow when coupling SAM with ISE

The scheme in Figure 1.5 explains the data flow between MISA and its graphical front end in more detail. SAM works as an interface dedicated exclusively to the sensitivity analysis between the program and the user. The requirements of the user are stored, pre-processed and sent to MISA. The ISE also provides the RANGE file and the REFERENCE file (cf. § 1.3.2). In MISA, the user requirements are analysed and if necessary, a proposal to change the requirement is sent back to SAM. If not, the design file is produced and the multirun simulation begins. At the end of the simulations, MISA hands control back to SAM which has some tools to select the interesting results.

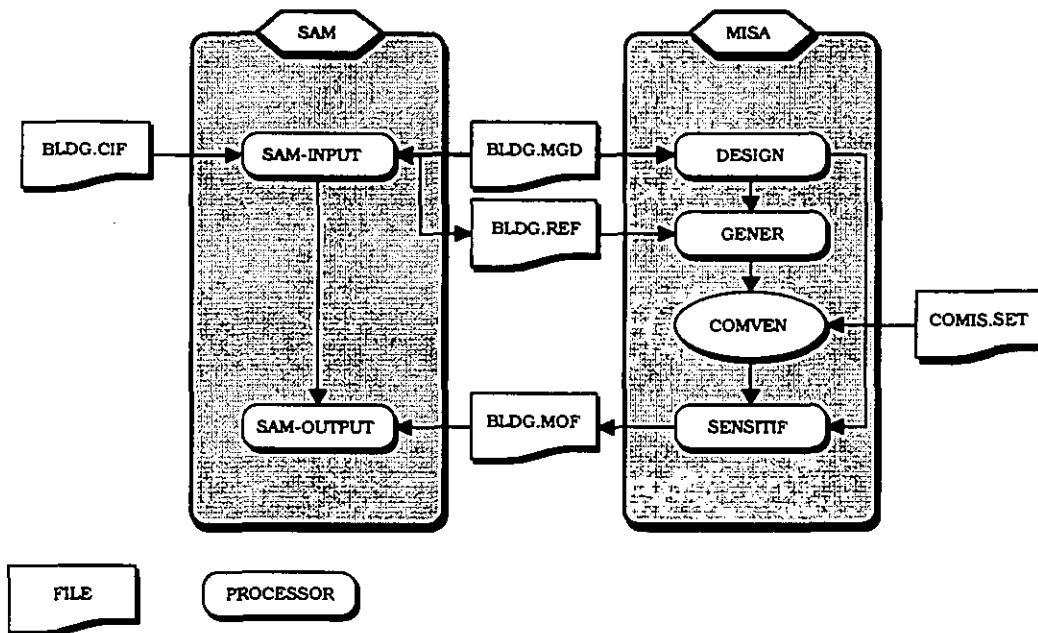


Figure 1.5: Scheme of data flow between ISE, SAM and MISA. SAM is a process developed within AIDA with the language LELISP from ILOG. The processors DESIGN et SENSITIF are part of LiSA developed within the mathematical software MATLAB. GENER is written in standard FORTRAN.

## 1.4 References

- Bowman N. T. and Lomas K. J.: Empirical validation of Dynamic Thermal Programs of Buildings. *Building Services Engineering Research and Technology* 6 (4) 153-162 (1985)
- Box G. E. P., Hunter W. G., Hunter J. S.: Statistics for Experimenters, an Introduction to Design, Data Analysis and Model Building. *John Wiley, New York, 1978.*
- Dorer V., Fürbringer J.M., Huck F., Roulet C.A.: Evaluation of COMERL with the LESO Dataset, *Final report BEW, EMPA, Dübendorf, CH, 1992.*
- Feustel H.G., Allard F., Dorer V., Rodrigez Garcia E., Grosso M., Herlin M., Mingsheng L., Phaff H.C., Utsumi Y., Yoshino H.: Fundamentals of the Multizone Air flow Model - COMIS. *AIVC TN 29, Coventry, UK, 1990.*
- Feustel H.G., Allard F., Dorer V., Rodrigez Garcia E., Grosso M., Herlin M., Mingsheng L., Phaff H.C., Utsumi Y., Yoshino H.: COMIS 1.2 - user guide. *Lawrence Berkeley Laboratory, Berkeley, USA, 1993.*

- Fürbringer J.M., Compagnon R., Roulet C.A.: 1989: Wind and Pressure Requirements for the Validation of a Multizone Air Infiltration Program. *10th AIVC Conference, Espoo, Finland, 1989. Published by AIVC, Coventry, UK.*
- Fürbringer J.M., and Roulet C.A.: 1995: Comparison and combination of factorial and Monte-Carlo designs in sensitivity analysis. *Building and Environment 30 (1995) No 4 pp 505-519.*
- Fürbringer J.M.: Evaluation procedure using sensitivity analysis of model and measurement, *Int. Symposium on Air Flow in Multizone Structures, Budapest, Sept 9-10, 1992.*
- Fürbringer J.-M.: Sensibilité de modèles et de mesures en aéraulique du bâtiment à l'aide de plans d'expériences. *Thesis No 1217, EPFL, Lausanne, 1994.*
- Goupy J.: La méthode des plan d'expériences, optimisation du choix des essais & de l'interprétation des résultats. *Dunod, Paris, 1988.*
- Gunter B. H.: How experimental design concepts can improve experimentation in the physical sciences. *Computer in physics, vol. 7, n° 3 May/Jun 1993.*
- Irving, A. D.: An Investigation into Analytical and Empirical Validation Techniques for Dynamic Thermal Models of Buildings. *Final Report to SERC, Vol. 5, Grant GR/C/62871, BRE, Garston, Watford, UK, 1987.*
- Judkoff, R., Wortman, D., O'Doherty, B., and Burch, J.: A Methodology for Validating Building Energy Analysis Simulations. *Report TR-254-1508, SERI, Goldend CO, USA, 1983*
- Lomas, K. J., Bloomfield, D. and Martin, C.: Three-Level Method for Empirical Validation of Dynamic Thermal Simulation Programs, 1992. *Workshop on Validation of Building Energy Models, Centre EDF des Renardières, France, June 9 and 10, 1992.*
- Lomas, K., J., and Bowman, N. T.: An Investigation into Analytical and Empirical Validation Techniques for Dynamic Thermal Programs of Buildings. *Final Report to SERC, Vol. 4, Grant GR/C/62871, BRE, Garston, Watford, UK, 1987.*
- Lomas, K. J., Bloomfield, D. P., Parand F. and Piney, A.: Applicability Study 1: a UK Initiative to Determine the Error Characteristics of Detailed Thermal Simulation Models. *Proc. 2nd European Conference on Architecture, Paris, 1989*
- Lomas K. J., Eppel H.: Sensitivity analysis techniques for building thermal simulation programs, *Energy and buildings, vol. 19, 1992*
- Plackett R.L. and Burman J.P.: The design of optimum multifactorial experiments, *Biometrika, n°33,1946*
- Rubinstein R.Y.: Simulation and the Monte Carlo method. *John Wiley and Sons, New York, 1981.*
- Scartezzini J.L., Fürbringer J.M., Roulet C.A.: Data Needs for Purpose of Air Infiltration Computer Code Validation. *8th AIVC Conference, Überlingen, Germany, 1987. Published by AIVC, Coventry, UK.*
- Silvey, S. D.: Optimal Design. *Chapman & Hall, London, 1980.*
- Soubra, S: Concepts et méthodes pour le développement d'environnements de simulation intelligents - Application au bâtiment. *PhD Thesis presented at ENPC, Paris, 1992.*



## 2 ANALYTICAL EVALUATION

### 2.1 Introduction

A mathematical model of a physical phenomenon (a set of equations) is defined by means of mathematical knowledge of the physical law and empirical knowledge of the phenomenon. When a computer program is used to solve the model, many different tests can be performed to evaluate its behaviour (Figure 2.1), e.g. the program results may be compared with an analytical solution or with the solution of another program or with measured values.

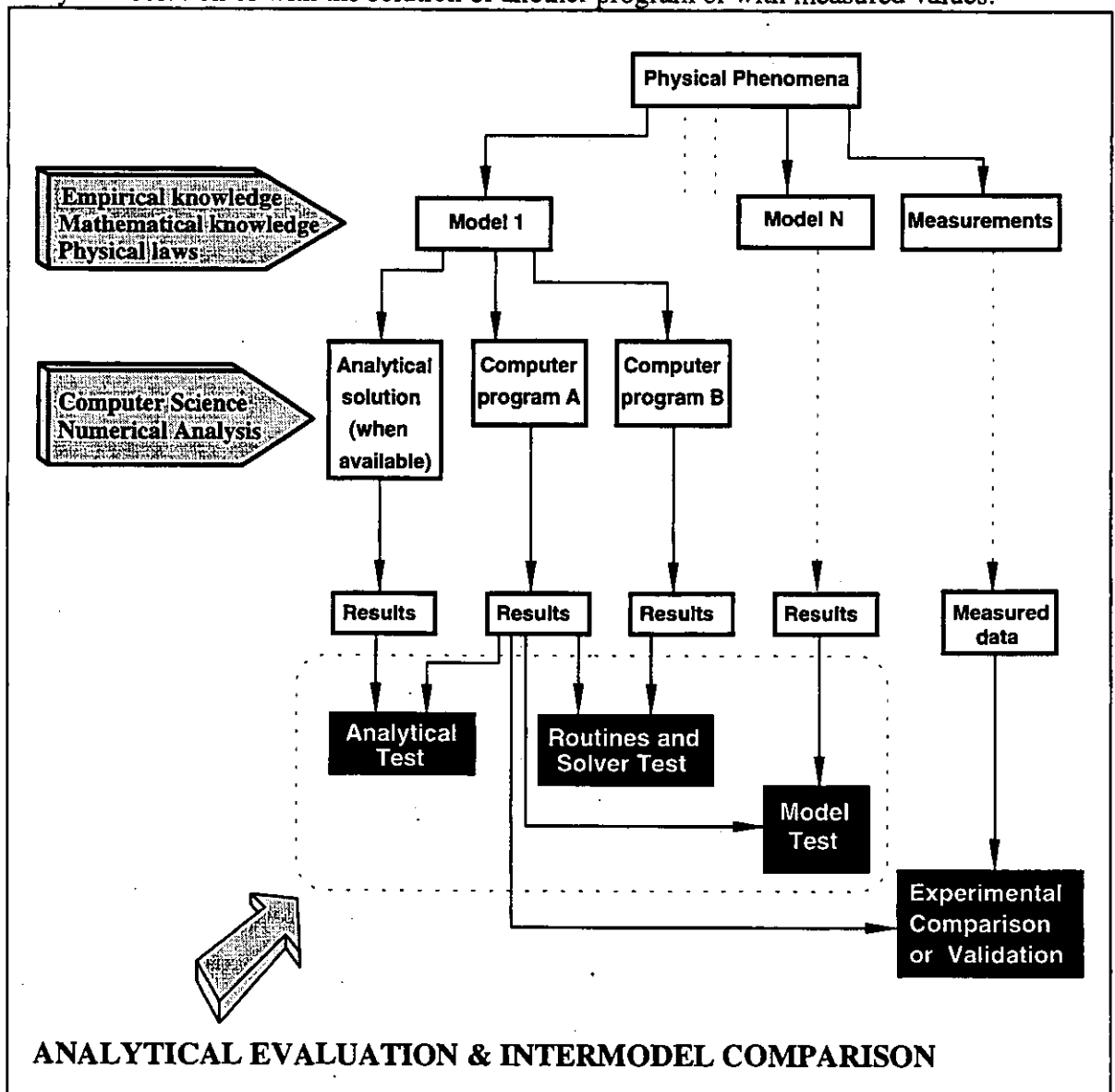


Figure 2.1 - Scheme of different kinds of tests

Within the framework of the Annex 23 evaluation task, many different tests for evaluating COMIS have been produced by the annex participants. This chapter refers to those tests in which COMIS results are compared with the analytical solution of single problems. These are sometimes obtained using a specialised mathematical package.

**General comment:** In chapter 0 and the corresponding appendix, the reader will find much information about analytical cases prepared and documented in the frame of the COMIS code development work and in the frame of the evaluation task of Annex 23. It is obvious that

given the huge amount of cases and information involved, any subsequent data gathering and studying of these cases will require considerable time and effort.

### 2.1.1 Classification of the test cases

Some of the cases are more dedicated to check the modelling of the physical effects and the respective algorithms in the code, while others are set up to check the proper functioning of the program in respect to input data processing, error handling etc. In this report, emphasis is put on the first type of cases, since those are the ones which can be backed up by an independent analytical solution. Nevertheless, the reasons for deviations from these analytical solutions may be related to not only the modelling, but also to other errors in the program, and therefore both aspects have to be covered in the frame of the program testing.

Most cases are set up to test one specific topic, e.g. the correct interpolation between the given pressure coefficients for any wind direction. Despite covering only one topic, the case itself can either cover one specific situation only or the full application range for the code. Cases covering several topics are, in general, more complex and the interpretation of the results more difficult.

Figure 2.2 tries to visualise this fact. In this Figure, the presently available stock of test cases is represented by the grey shaded volume. From this it is clear that the cases still missing are the complex ones which cover several topics.

In Table 2.1 an attempt is made to very roughly summarise the available test cases by defining some topics related to the individual elements of the modelling and the calculation steps implemented in COMIS and to classify the cases accordingly.

Table 2.1 - Input and calculation related topics covered by the available test cases

Topic related to input	Topic related to calculation							
	Meteo	Wind pressure	Stack pressure	Flow crack	Window	HVAC	Pollutant transport	Schedules
Meteorological data	X	X	X				X	X
Building orientation		X						
One zone		X	X	X	X	X	X	
Several zones		X	X	X	X	X	X	X
Zone layers			X	X	X	X	X	
Crack			X	X				
Window				X	X		X	
HVAC						X		
Pollutants, sources, sink, filters			X	X	X		X	X
Schedules								X
Occupants								

The rows represent the part of the case related to the input data, and the columns refer to the topic to be checked by the test. The Table is not complete and shows only the most important topics. Also more complex cases cannot be shown since the matrix is only two-dimensional.

**Comparison of analytical results and COMIS results:** Tables where the analytical results are directly compared to the COMIS output are given in several test case data sets, namely the one

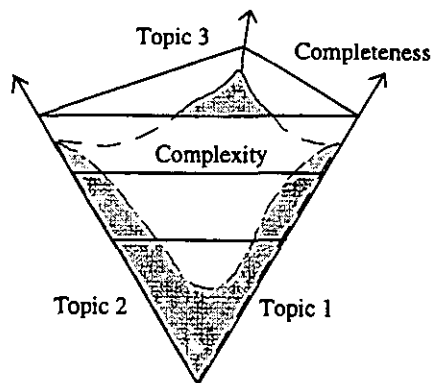


Figure 2.2 - Distribution of the available test cases versus complexity.

from EMPA. With the release of new COMIS versions, the test cases should be run with this new release and the Tables be updated accordingly.

### 2.1.2 Internet Server

As the amount of numerical values obtained from these tests is very extensive, a computer service, AIS (Annex23 Information Server) at LBL (Lawrence Berkeley Laboratory), has been used to collect the input and output files related to the evaluation work.

The main features of the developed tests will be described in the following sections. The directory of the AIS in which the files are located will be specified for each test. Also available in this directory is a text file (ASCII format) that corresponds to the "Paper Building Data Set".

The "Paper Building Data Set" is a form in which the main features of the test are summarised by the following items:

- **REFERENCE NUMBER:** chosen by the authors of the test; it will be used in the test file name;
- **RELEASE NUMBER:** the authors have to upgrade this number for each test change;
- **DATE:** day-month-year;
- **GENERIC NAME:** any name chosen by the author, usually the LBL-AIS name;
- **LBL-AIS NAME:** the name of the file contained in the sub directory level 1;
- **GENERALITY:** an abstract of the problem analysed;
- **AUTHOR:** personal name of the authors, institution and nationality;
- **DATA INCLUDED IN THE ORIGINAL FILE:** a list of the main keywords that are included in the COMIS file which the author must mark;
- **TEST CLASSIFICATION:** the kind of test;
- **COMIS INPUT PARAMETERS ANALYSED:** the parameters that the authors change for testing the COMIS results;
- **NUMERICAL TOOLS OR ANALYTICAL SOLUTIONS THAT THE AUTHORS HAVE USED BESIDES COMIS:** this section is useful to understand which are tools used to analyse COMIS;
- **ANALYTICAL RESULTS AVAILABLE FOR COMPARISON WITH COMIS RESULTS:** the data that are possible to compare;
- **REFERENCES:** where it is possible to find more information about the test;
- **COMPARISON:** the comparison results;
- **COMMENTS:** description of the problems found using the program, describing the test, etc.
- **CONCLUSION:** few words to summarise test results.

## 2.2 A guide through the test cases

### 2.2.1 EMPA test cases

#### *Introduction*

Within the framework of the development of the COMIS simulation code COMVEN, a data base of test cases has been established at EMPA<sup>1</sup>. The cases range from simple cases for testing specific physical models or routines in the code, up to complex problems combining different physical effects and topics.

These test cases can be sorted into a category of tests for checking the functionality of the code and for the evaluation of algorithms and thus for checking the numerical results.

These second category cases are systematically sorted according to the underlying physical phenomena, e.g. air flow through a large opening, and are solved independently using analytical methods or other means such as using a mathematical software package like MATHEMATICA.

This section first outlines how these cases are documented, then describes both the and the content of the data base, also making reference to where the analytical solutions are documented.

#### *Description of the test case data base*

The test cases are built up systematically according to different subjects. In the final state, they include a wide spectrum of subjects relevant to the coverage of the options available within COMIS.

The analytical test cases developed at EMPA are documented in three parts:

1. The introduction to the data base is formed by this section.
2. The second part of the data base is set up in ASCII files and is available at EMPA and at the A23 Information server at the LBL. This section of the data base is described in more detail in Appendix 3. These files are easily accessible by electronic means (file transfer, e-mail).

There are three types of files available:

- A. A global summary file (Named 'testfiles.res') containing a list with a short description of the different subjects, a list of the respective input/output, and the subject summary file names.
  - B. A result file (\*.RES) per subject which contains the subject description, a short description of the analytical calculation procedure and the parameter varied in the input file versions. Also included in these files are the comparison of results between analytical solution and the simulation results (one column for each COMVEN version), and the conclusions concerning this comparison.
  - C. Per subject the individual COMIS input (\*.CIF) and output (\*.COF) files.
3. Analytical results for the individual topics are documented in separate technical reports.

For each test case numerical results have been calculated analytically, or by other means. In many cases the MATHEMATICA package has been used. In these cases, the analytical solution is documented in the technical report only with a printout for one input version.

In parallel, a COMIS input file has been created and has been run by COMVEN.

---

<sup>1</sup> Swiss Federal Institute for Materials Testing and Research, 8600 Dübendorf, Switzerland

Both the analytical and COMIS results are listed in a file, which contains a summary of the main input parameters, the calculation procedure used for the COMIS-independent analytical calculation and the conclusions.

When a new version of COMVEN has been issued, the test runs have been repeated and the various results added to the respective result files.

The data base is structured into subjects which are defined according to the different groups of parameters influencing the air flow modelling, the input file items (top to bottom) and also according to the complexity of the problem.

Test cases are available for the following subjects:

- Input data processing
  - Barometric pressure, air densities
  - Extrapolation of wind pressure coefficient data
  - Wind speed at reference height
- Single or two zone models with cracks
  - Wind effects
  - Stack effects
  - Non horizontal cracks
- Two zone models with different types of air flow components:
  - Large vertical openings including test for the updated routines [*Schauwecker, 1994*]
  - HVAC components
- Cases for contaminant spreading
  - Pollutant
  - Humidity
- Cases for checking the zone layers
  - In combination with large vertical openings
  - In combination with LVO's and pollutant transport
- Cases for checking the schedule processing routines

These test cases are presented in Appendix 3. Main conclusions are as follows:

Many bugs were detected in Comven by the use of the benchmarks. These bugs were of course fixed.

When calculating variation in concentration of a contaminant, the final results of the concentrations depend significantly on the time step length chosen by the user. For those cases where the mass flows depend on the time dependent concentrations it is very important to choose a short enough time step (about 0.1 to 0.2 of the zone time constant) to avoid incorrect results.

The COMVEN results for the mass flow through a large opening between two zones can show significant deviations (up to 25%) from the analytical solution, if there are layers in one or both zones.

### 2.2.2 LESO test cases

The 4 test cases provided by the LESO<sup>1</sup> consist of crack networks in very simple situations with few indoor nodes.

#### **ROOM4**

ROOM4, has 4 indoor zones arranged in a square (Figure 2.3). The network has a 90° rotational symmetry. The aim is to check whether COMVEN correctly manages the rotation be-

<sup>1</sup> LESO-PB, EPFL, 1015 Lausanne, Switzerland

tween pressure coefficients, the wind direction and the building direction. The results show this symmetry (Figure 2.4).

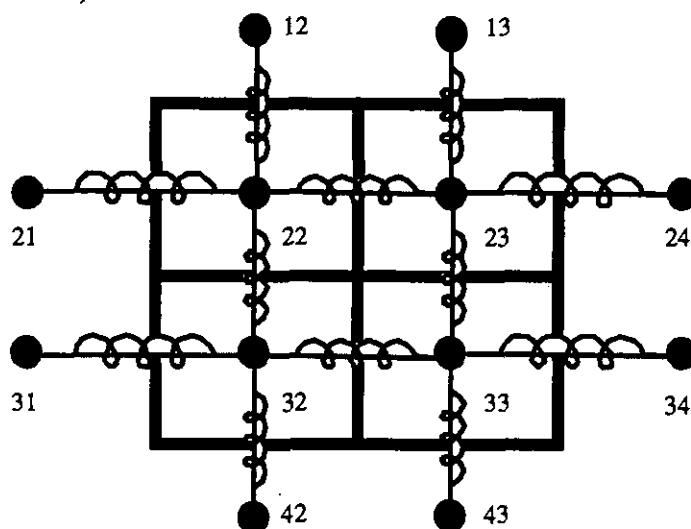


Figure 2.3: Conductance network of ROOM4. The numbers indicates the nodes.

In *room\_4.cif* the pressure coefficient distribution does not depend on the wind direction and has been defined for eight wind sectors only.

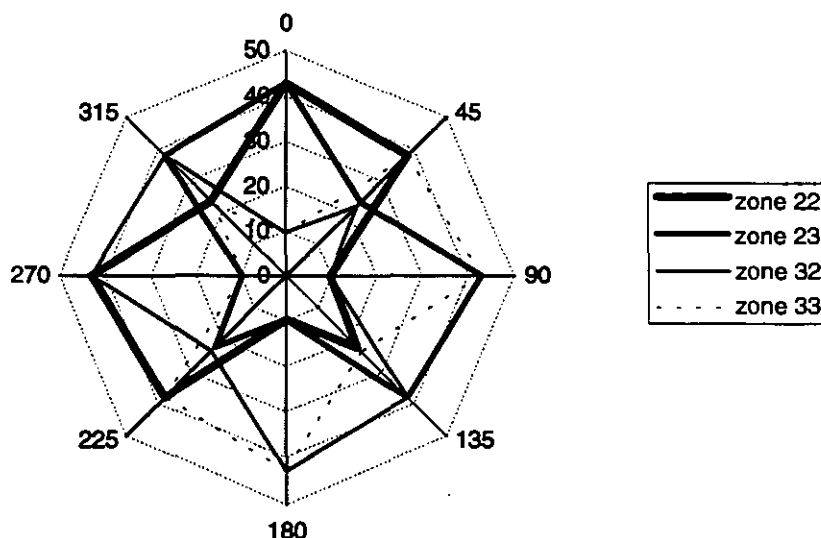


Figure 2.4 -  
Results for test ROOM4

The files describing this case (*/sample/room4.cif* and */sample/room4.txt*) can be found in AIS.

### MONOWIND

This consists of one zone with 4 cracks (

Figure 2.5). This structure which has an analytical solution, is used to check wind consequences [Fürbringer et al, 1989]. In *monowind.cif* the pressure coefficient distribution does not depend on the wind direction and has been defined for 4 wind sectors only. There are no stack effect.

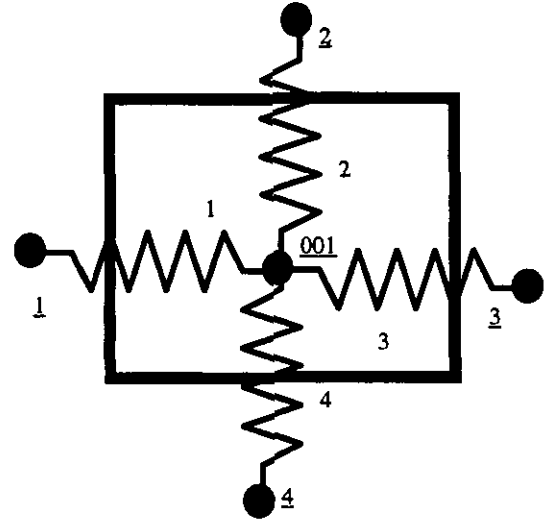
The parameters are defined as follows:

$C_w$	windward air tightness coeff., [ $\text{m}^3 \text{h}^{-1} \text{Pa}^{-n}$ ]	$P_w$	windward pressure, [Pa]
$C_L$	leeward air tightness coeff., [ $\text{m}^3 \text{h}^{-1} \text{Pa}^{-n}$ ]	$P_L$	leeward pressure, [Pa]

$C_{pW}$  windward pressure coefficient, [-]  
 $C_{pL}$  leeward pressure coefficient, [-]  
 $n$  exponent, [-]  
 $V$  wind speed, [m s<sup>-1</sup>]

$P_I$  indoor pressure, [Pa]  
 $\rho$  air density, [kg m<sup>-3</sup>]  
 $Q_W$  windward exfiltration, [m<sup>3</sup> h<sup>-1</sup>]  
 $Q_L$  leeward infiltration, [m<sup>3</sup> h<sup>-1</sup>]

Figure 2.5: Conductance network. The underlined numbers indicate the nodes while the other indicates the cracks.



The wind induced infiltration is modelled by the following equations:

$$\text{Flow equation } Q_W = C_W(P_W - P_I)^n \quad \text{with } 0.5 < n < 1 \quad (0.1)$$

$$Q_L = C_L(P_L - P_I)^n \quad (2.2)$$

Wind induced pressure:  $P_W = C_{pW} P_{stat} \quad (2.3)$

$$P_L = C_{pL} P_{stat} \quad (2.4)$$

Static pressure:  $P_{stat} = 0.5 \rho V^2 \quad (2.5)$

Mass conservation:  $\rho Q_W = \rho Q_L \quad (2.6)$

Solving this system, one gets the following output parameters:

$$P_I = P_{stat} (C_{pW} (C_W)^{1/n} + C_{pL} (C_L)^{1/n}) / ((C_W)^{1/n} + (C_L)^{1/n}) \quad (0.7)$$

$$Q_W = Q_L = C_W C_L (P_W - P_L)^n / ((C_W)^{1/n} + (C_L)^{1/n})^n = C_{eq} (P_W - P_L)^n \quad (0.8)$$

The files describing this case (/sample/monowind .cif and /sample/monowind .txt) can be found in AIS:

Numerical application example

Input	Intermediary Output
$C_W = 20 \text{ [m}^3 \text{ h}^{-1} \text{ Pa}^{-n}\text{]}$	$P_W = 40 \text{ [Pa]}$
$C_L = 40 \text{ [m}^3 \text{ h}^{-1} \text{ Pa}^{-n}\text{]}$	$P_L = -10 \text{ [Pa]}$
$n = 0.65$	$P_I = 50 (0.8 (20)^{1/0.65} - 0.2 (40)^{1/0.65} / (20)^{1/0.65} - (40)^{1/0.65}) = 2.8 \text{ [Pa]}$
$C_{pW} = 0.8$	<b>Final output</b>
$C_{pL} = -0.2$	
$V = 8.8 \text{ [m s}^{-1}\text{]}$	
$\rho = 1.2929 \text{ [kg m}^{-3}\text{]}$	
	$Q_W = 20 (40 - 2.8)^{0.65} = 209.83 \text{ [m}^3 \text{ h}^{-1}\text{]}$
	$Q_L = 40 (2.8 + 10)^{0.65} = 209.83 \text{ [m}^3 \text{ h}^{-1}\text{]}$

**MONOSTACK**

This consists of a monozone building (Figure 2.6) with 2 cracks. This structure, which has an analytical solution, is used for checking stack effect. Pressure coefficients have been defined for 4 wind sectors only. This test cell has been described by Allard et al. [1989].

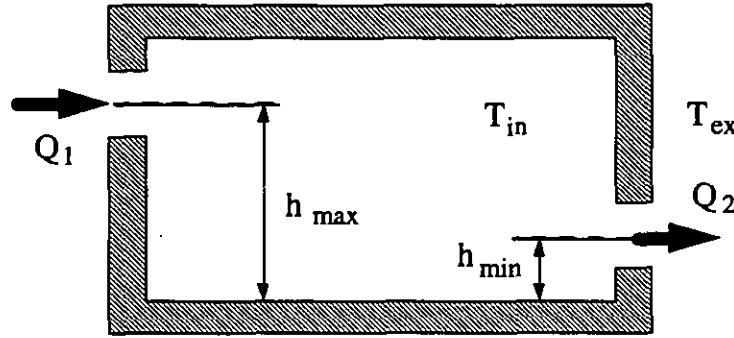


Figure 2.6 : Section of the cells

The significance of the symbols is as follows:

$\Delta P_i$  pressure difference through the opening  $i$ , [Pa]

$P_{ex-ref}$  pressure at the outdoor reference point, [Pa]

$P_{in-ref}$  pressure at the indoor reference point, [Pa]

$h_i$  height of the opening  $i$ , [m]

$\rho_{ex}$  outdoor air density, [kg m<sup>-3</sup>]

$\rho_{in}$  indoor air density, [kg m<sup>-3</sup>]

The flow and the pressure difference across the crack are defined as negative when the air goes out. The analytical solution is obtained through the following steps:

$$\Delta P_1 = (P_{ex-ref} - h_1 g \rho_{ex}) - (P_{in-ref} - h_1 g \rho_{in}) \quad (2.9)$$

$$\text{if } P_{ex-ref} = 0 \text{ then } \Delta P_1 = h_1 g (\rho_{ex} - \rho_{in}) - P_{in-ref} \quad (2.10)$$

$$\text{if } C_1 = C_2 \text{ and } n_1 = n_2 = 1 \text{ then}$$

$$\Delta P_1 + \Delta P_2 = h_1 g (\rho_{ex} - \rho_{in}) + h_2 g (\rho_{ex} - \rho_{in}) - 2 P_{in-ref} = 0 \quad (2.11)$$

Finally one gets:

$$P_{in-ref} = (h_1 + h_2)/2 g (\rho_{ex} - \rho_{in}) \quad (2.12)$$

$$\Delta P_1 = -\Delta P_2 = (h_2 - h_1)/2 g (\rho_{ex} - \rho_{in}) \quad (2.13)$$

The corresponding files are /sample/monos .cif and /sample/monos .txt.

**MONOWS**

This has the same structure as the previous case, but now wind and stack effects are both taken into consideration. This structure, which has an analytical solution, is used for checking wind and stack effect interaction. In the case of equilibrium between both forces, if the windward crack is higher than the leeward one, the flow is stopped. The modelled situations have been specifically chosen to have the building in the two kinds of flow directions. Modifying the previous case, the analytical solution is obtained this way:

$$\Delta P_i = P_{stat} C_{p_i} - P_{in} - (\rho_{ex} - \rho_{in}) g h_i, \quad i = 1, 2 \quad (2.14)$$

if  $C_1 = C_2$ ,  $n_1 = n_2 = 1$  and because  $Q_1 + Q_2 = 0$  we get :

$$\Delta P_1 + \Delta P_2 = P_{stat} C_{p_1} - P_{in} - (\rho_{ex} - \rho_{in}) g h_1 + P_{stat} C_{p_2} - P_{in} - (\rho_{ex} - \rho_{in}) g h_2 = 0 \quad (2.15)$$

Finally one gets:

$$P_{in-ref} = P_{stat} (C_{p_1} + C_{p_2})/2 - (h_1 + h_2) g (\rho_{ex} - \rho_{in})/2 \quad (2.16)$$

$$\Delta P_1 = P_{stat} (Cp_1 - Cp_2)/2 - (h_2 - h_1)g (\rho_{ex} - \rho_{in})/2 \quad (2.17)$$

The equilibrium is obtained when (2.17) is null.

The good agreement between the COMIS and analytical results for these tests is shown in Table 2.1.

*Table 2.1 - Comparison results test monostack, monows and monowind*

TEST NAME	PRESSURE AND FLOW	COMIS RESULTS	ANALYTICAL RESULTS
monostack	$\Delta p$ [Pa]	0.040	0.040
	Mass flow link 1 [kg/s]	-0.06185	-0.06183
	Mass flow link 2 [kg/s]	+0.06185	+0.06183
monows	$\Delta p$ [Pa]	1.990	1.993
	Mass flow link 1 [kg/s]	+0.9974	+0.9972
	Mass flow link 2 [kg/s]	-0.9974	-0.9972
monowind	$\Delta p$ [Pa]	2.824	2.804
	Mass flow link 1 [kg/s]	-0.07563	-0.07536
	Mass flow link 2 [kg/s]	+0.07563	+0.07536

The corresponding AIS files are: /sample/monows.cif, and /sample/monows.txt

### 2.2.3 POLITECNICO test cases

#### *Effect of link height*

The first set of tests to be developed at the Politecnico<sup>2</sup> involve simple networks and are used for studying the effects of the link height in COMVEN. For all tests, inside and outside conditions are chosen in order to have stack effects and wind pressure equal to zero; therefore, zero air flow should be found by COMVEN and for this reason the tests are named "zero-cases".

The meteorological conditions in all tests are:

- wind speed = 0
- internal nodes temperature = external temperature
- internal humidity = external humidity
- fan not present

The "zero-cases" can be divided into three groups:

- A links-tests to check the influence of the number and the height of the link;
- B zone tests to check the influence of the vertical and horizontal nodes;
- C height-tests to check the influence of the reference height.

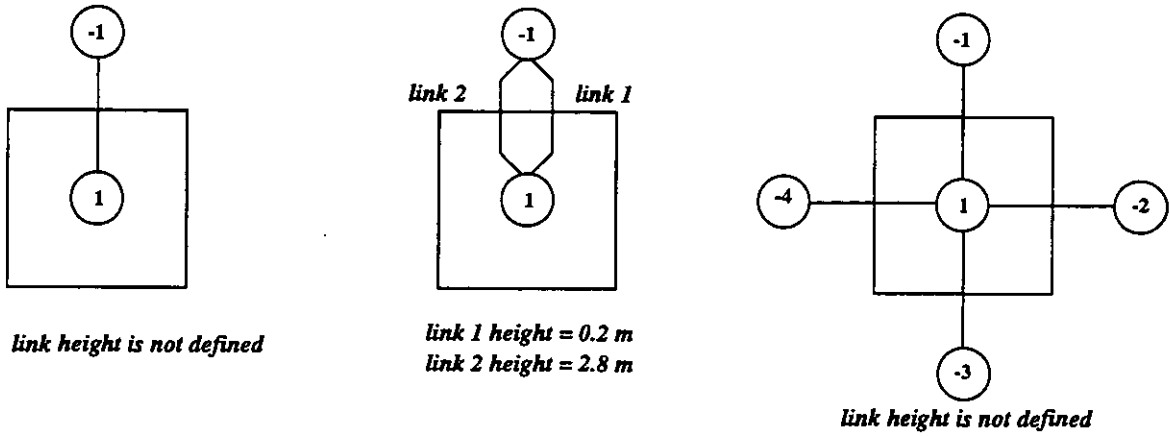
Figure 2.1, Figure 2.2 and Figure 2.3 show the networks corresponding to each test, and

Table 2.2 summarises the results obtained using COMVEN 1.2. As the analytic mass flows are zero, the results of tests A and B are correct, but some problems are found for test C. In fact, the flow is not zero when the reference height is different from 0, 1.5 or 3 metres. These problems have been solved in later COMVEN releases.

The files describing this case can be found in AIS as follows:

ANALYTIC.EVA\POLITECZERO\_CASE\\*.cif and \*.cof

<sup>2</sup> Dipartimento di Energetica, Politecnico di Torino, 10129 Torino, ITALY



**A1-t0v0**

**A2-t0v0**

**A3-t0v0**

Figure 2.1 - Tests group A: link tests (the picture show the plan of the test cells and the COMVEN networks)

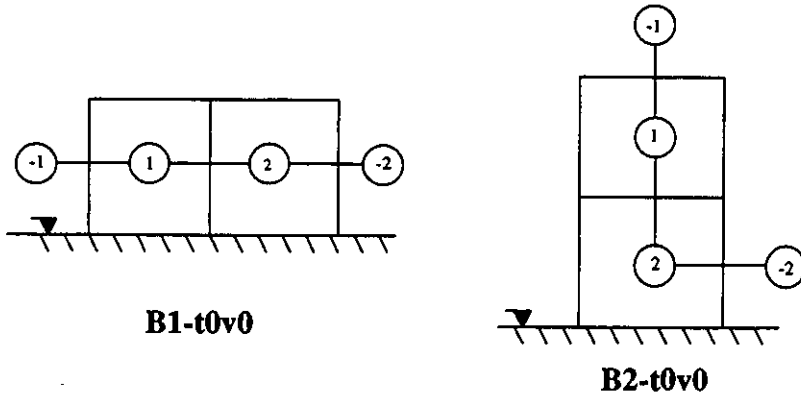


Figure 2.2 - Tests group B: zone tests (the picture show the section of the test cells and the COMVEN networks)

Table 2.2 - Results for group A, B and C. Theoretical results are all zero.

TEST NAME	Pressure [Pa]	Mass flow [kg/s]
A1-t0v0	0	0
A2-t0v0	0	0
A3-t0v0	0	0
B1-t0v0	0	0
B2-t0v0	0	0
C1-t0v0	0	0
C2-t0v0	$9.54 \cdot 10^{-7}$	0.04639
C3-t0v0	0	0
C4-t0v0	$9.54 \cdot 10^{-7}$	0.04639
C5-t0v0	0	0
C6-t0v0	$1.91 \cdot 10^{-6}$	0.06698
C7-t0v0	$-7.63 \cdot 10^{-6}$	0.1397

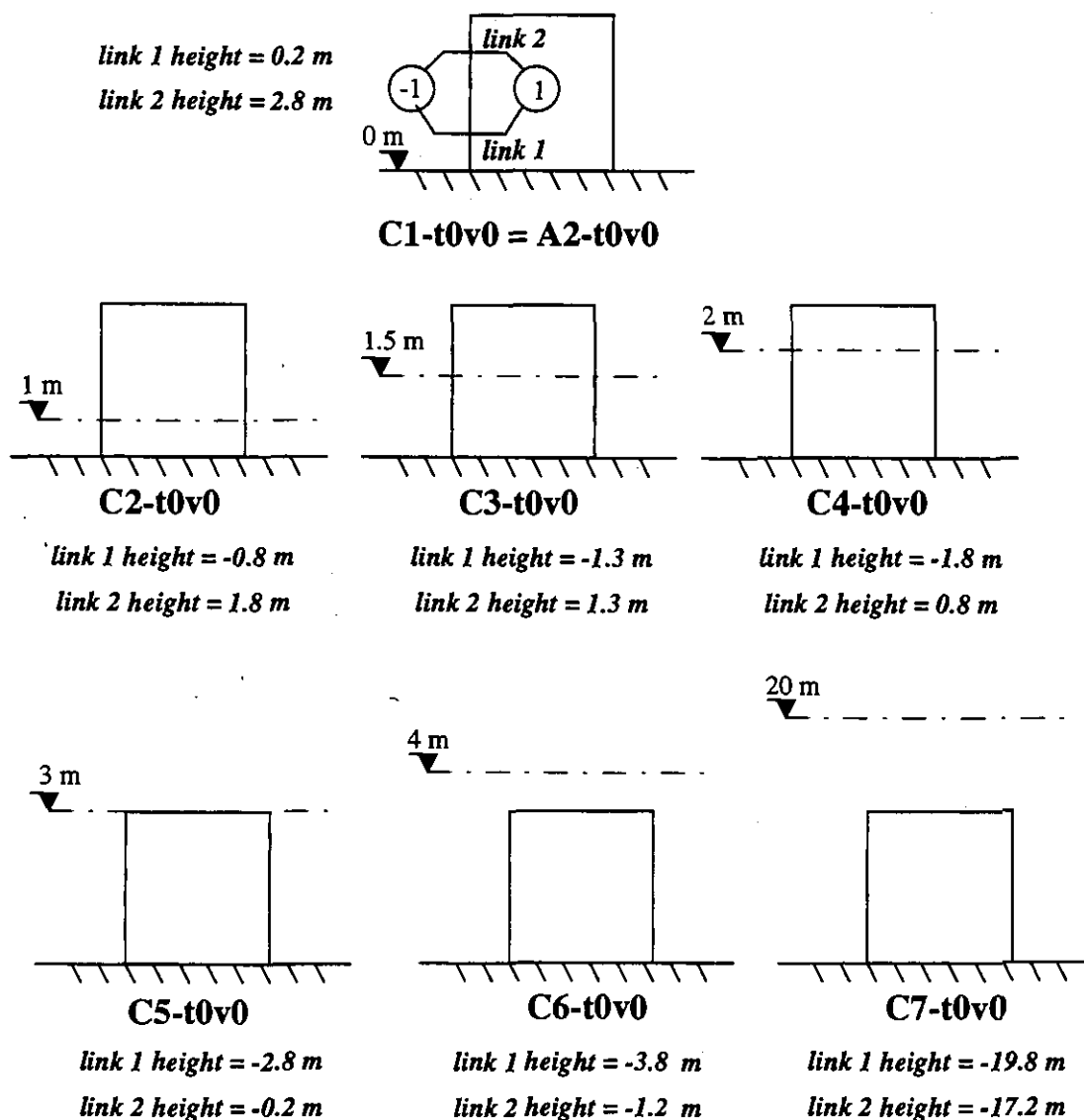


Figure 2.3 - Tests group C: reference height tests (the picture show the section of the test cells and the COMVEN networks, the ref. height in every link has been changed)

### Thermal gradients and wind influence

In the second set of tests the results of COMVEN are compared with the solution obtained using the MATHCAD software package. These tests were developed in the frame of the inter-model comparison between COMIS and ASCOS (see next chapter) and address thermal gradients and wind influence (e.g. wind velocity and wind exponent). The MATHCAD solutions are numerical solutions, since the MATHCAD solver was used on a non-linear equation set.

For every case two different evaluations have been made:

- I) Changing the thermal gradient between outside and inside with no wind;
- II) Changing the wind velocity (from 1 to 9 m/s) and the wind exponent (from 0.16 to 0.40) with no thermal gradient.

The evaluation of the COMIS results with respect to the MATHCAD results is made by calculating the relative deviation  $\delta$ :

$$\delta = \frac{G_{Mathcad} - G_{COMIS}}{G_{COMIS}} \cdot 100.$$

that estimates the difference in percent between the flows  $G$ .

### CASE A: single zone

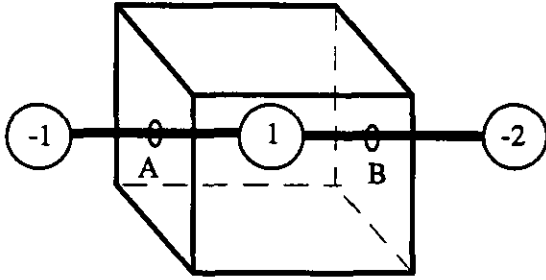


Figure 2.4 - COMIS network for case A

The structure of the name of the files is: 1AC-CTTT.EXT. Where TTT is the temperature difference between inside and outside and EXT is equal to CIF, COF or MCD respectively for COMIS input, COMIS output and MATHCAD files.

**A-II** in this sub-set of test cases the change of the wind velocity (from 1 to 9 m/s) and of the wind profile exponent (from 0.16 to 0.40) was taken into account and no thermal gradient was considered. The main data used in this sub-set are illustrated in Table 2.3.

The files referring to these test can be found in AIS directory :

ANALYTIC.EVA\POLITEC\SMOKE\CASE\_A\WIND.

The structure of the name of the files is: 1AC-CVEE.EXT. Where VEE is: V the wind velocity and EE represents the wind exponent at the meteo station; EXT is equal to CIF, COF or MCD respectively for the COMIS input, COMIS output and MATHCAD files.

The results obtained for case A-II are given in Table 2.4. Note that relative deviations are very small, but nevertheless larger than the limit adopted for convergence criterion. In fact, there is no relation between  $\delta$  and the convergence criteria in COMIS. The convergence limit of the results (both for COMIS and MATHCAD) was set to a very high level (i.e.  $10^{-7}$ ) so the comparison between the results is not affected by the numerical approximation.

Table 2.3 - Main data used for tests A-II

network	internal node 1: $T_{int} = 21^{\circ}\text{C}$ . link A and link B: $C_s = 0.0072062 \text{ kg/s}@1\text{Pa}$ ; $n = 0.5$ ; length = 1 m; height link A = height link B = 1.5 m; wall properties: thickness = 0.1 m and $U$ -value = $5.174 \text{ W/m}^2 \text{ K}$ ;
external data	Test = $21^{\circ}\text{C}$ ; Relative humidity = 0 %
Cp value	$C_p$ link A = 0.7; $C_p$ link B = -0.7; ( $C_p$ value is calculated with the formula in Table 3.18)
ref. height for $C_p$ :	10 m
wind velocity at ref. height:	1 - 3 - 5 - 7 - 9 m/s
ref. height for wind speed:	10 m
wind profile exp. at meteorological station:	0.16 - 0.22 - 0.28 - 0.34 - 0.40
wind velocity profile exponent:	0.16 - 0.22 - 0.28 - 0.34 - 0.40
wind direction:	0 degree.
altitude meteorological station:	0 m
barometer absolute pressure:	101325 Pa.

Table 2.4 - Results for case A-II

Wind Velocity [m/s]	$\delta$ [%]				
	Wind exponent 0.16	Wind exponent 0.22	Wind exponent 0.28	Wind exponent 0.34	Wind exponent 0.40
1	0.19	0.17	0.20	0.19	0.20
3	0.2	0.2	0.21	0.19	0.18
5	0.2	0.21	0.19	0.19	0.20
7	0.2	0.2	0.2	0.2	0.19
9	0.21	0.2	0.19	0.2	0.19

**CASE B: two connected zones on different levels to consider the stack-effect**

**B-I)** in this sub-set of test cases the thermal gradient between outside and inside was changed and no wind was considered. The main data used in this sub-set are illustrated in Table 2.5. The test was passed and correct mass flows were found.

Table 2.5 - Main data used for tests B-I

network	internal node 1: $T_{int} = 30 - 70 - 100 - 120 - 150 - 180 - 220^{\circ}\text{C}$ ; internal node 2: $T_{int} = 30 - 70 - 100 - 120 - 150 - 180 - 220^{\circ}\text{C}$ ; link A. link B and link C: $C_s = 0.0072062 \text{ kg/s}@1\text{Pa}$ ; $n = 0.5$ ; length = 1 m; height link A = 1.5 m; height link B = 3 m; height link C = 4.5 m; wall properties: thickness = 0.1 m; and $U$ -value = $5.174 \text{ W/m}^2 \text{ K}$ ;
external data	$T_{ext} = 20^{\circ}\text{C}$ ; Rel. humidity = 0 %
Cp value:	$C_p$ link A = 0.7; $C_p$ link C = -0.7; ( $C_p$ value is calculated with the formula in table 3.18)
ref. height for $C_p$ :	10 m
wind velocity. at ref. height:	0 m/s
ref. height for wind speed:	10 m
wind direction:	0 degree.
altitude meteorological station:	0 m
barometer absolute. pressure:	101325 Pa.

The files referring to these test can be found in AIS directory: ANALYTIC.EVA\POLITEC\SMOKE\CASE\_B\TEMP.

The structure of the name of the files is: 2AC-CITT.EXT. Where TTT is the temperature difference between inside and outside and EXT is equal to CIF, COF or MCD respectively for COMIS input, COMIS output and MATHCAD files.

The results obtained for case B-I are given in Table 2.6.

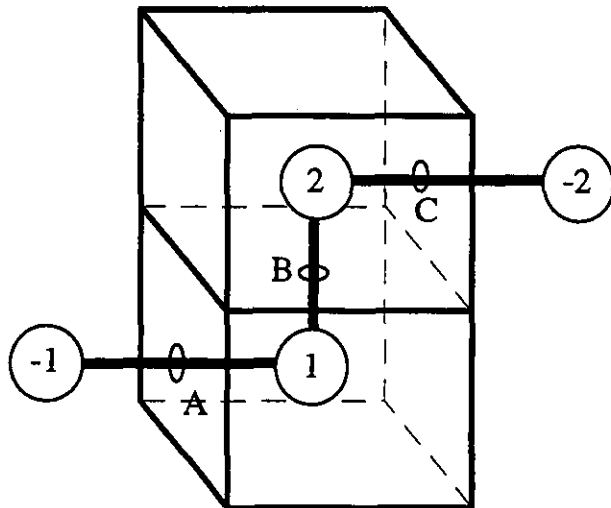


Figure 2.5 - COMIS network for case B

Table 2.6 - Results for case B-I

Temperature difference	d [%]
10	0.19
50	0.14
80	0.13
100	0.12
130	0.09
160	0.09
200	0.07

**B-II** in this sub-set of test cases the change of the wind velocity (from 1 to 9 m/s) and of the wind exponent (from 0.16 to 0.40) was taken into account and no thermal gradient was considered. The main data used in this sub-set are illustrated in Table 2.8.

The files referring to these test can be found in AIS directory :  
ANALYTIC.EVA\POLITEC\SMOKE\CASE\_B\WIND.

The structure of the name of the files is: 1AC-CVEE.EXT. Where VEE is: V the wind velocity and EE represents the wind exponent at the Meteorological Station; EXT is equal to CIF, COF or MCD respectively for the COMIS input, COMIS output and MATHCAD files.

Table 2.7 - Main data used for tests B-II

network	internal node 1 and 2: $T = 21\text{ }^{\circ}\text{C}$ link A, link B and link C: $C_s = 0.0072062\text{ kg/s}@1\text{Pa}$ ; $n = 0.5$ ; length = 1 m; height link A = 1.5 m; height link B = 3 m; height link C = 4.5 m; wall properties: thickness = 0.1 m and $U\text{-value} = 5.174\text{ W/m}^2\text{ K}$ ;
external data	Test = $21\text{ }^{\circ}\text{C}$ ; Rel. humidity = 0 %
Cp value	$C_p$ link A = 0.7; $C_p$ link C = -0.7 ( $C_p$ value is calculated with the formula in Table 3.18)
ref. height for Cp:	10 m
wind velocity, at ref. height:	1 - 3 - 5 - 7 - 9 m/s
ref. height for wind speed	10 m
wind profile exp. at meteo station	0.16 - 0.22 - 0.28 - 0.34 - 0.40
wind velocity, profile exponent	0.16 - 0.22 - 0.28 - 0.34 - 0.40
wind direction	0 degree.
altitude meteorological station	0 m
barometer absolute, pressure	101325 Pa

The results obtained for case B-II are given in Table 2.8.

Table 2.8- Results for case B-II

Wind Velocity	$\delta$ [%]				
	Wind exponent 0.16	Wind exponent 0.22	Wind exponent 0.28	Wind exponent 0.34	Wind exponent 0.40
1	0.21	0.16	0.20	0.20	0.20
3	0.21	0.19	0.21	0.20	0.19
5	0.21	0.20	0.20	0.21	0.20
7	0.20	0.21	0.21	0.20	0.20
9	0.18	0.21	0.20	0.21	0.21

### 2.3 Conclusions from the analytical evaluation

In this section an attempt is made to summarise the results of the comparative tests performed by giving some general conclusions in relation to the previously defined topics defined in the foregoing paragraph.

**Meteorological data:** The physical properties of the air and the temperature and pressure boundary conditions are checked by several tests, and found to be correctly calculated by COMVEN.

**Wind pressures:** Tests were performed to verify the correct interpolation between given pressure coefficient data according to the actual wind direction and building axis. Wind speed corrections due to the different wind profiles at meteorological station and at site are also performed correctly.

**Stack effects:** These are checked for the links in a zone and also when density gradient are defined. Gradients per layer are averaged over the room height in COMIS, which may lead to discrepancies with analytical results. Convergence problems with non-horizontal links have been solved.

**Air flow components:** Flows through cracks are correctly determined in most test cases. The air flow and the contaminant spread through a large opening are compared with independently derived analytical results, also in presence of gradients modelled by layers.

Cases with HVAC systems were created and run for single and multizone networks. Convergence problems may arise when T-junctions are connected to short ducts with small flow resistance.

**Density gradients:** The individual gradients defined per zone layers are averaged over the zone height in COMIS. For cases with layers having different gradients this may lead to quite substantial deviations from analytical solutions, especially for large opening flows.

**Pollutant transport:** Pollutant transport cases are available for single and multizone networks including combined cases of zones with layers and large openings. Especially for stack driven flow (and thus also flow through large openings) the final concentration values depend significantly on the time step length chosen. A short enough time step should be used in such cases.

**Schedules:** Schedules are defined in many cases and the proper processing of the schedule input has been verified.

## 2.4 References

- Allard F. et al : Wind induced ventilation, *ASHRAE trans.* (1989)
- Fürbringer J.-M., Compagnon R., Roulet C.-A.: Wind and pressure requirements for the validation of a multizone air infiltration program. *Proc. 10th AIVC Conf., Espoo, Finland, (1989).*
- Schauwecker R.: COMVEN test cases: Problem description and analytical results. Subject: Zone, layer and link input; cracks. *EMPA 175 Dübendorf, Switzerland, IEA-ECB.A23/93-05-01/RS (1993 a)*
- Schauwecker R.: COMVEN test cases: Problem description and analytical results. Subject: Non-horizontal cracks. *EMPA 175 Dübendorf, Switzerland, IEA-ECB.A23/93-09-01/RS (1993 b)*
- Schauwecker R.: COMVEN test cases: Problem description and analytical results. Subject: Large openings. *EMPA 175 Dübendorf, Switzerland, IEA-ECB.A23/93-12-01/RS (1993 c)*
- Schauwecker R.: COMVEN test cases: Problem description and analytical results. Subject: Mass Flow through Large Openings. *EMPA 175 Dübendorf, Switzerland, IEA-ECB.A23/94-11-01/RS (1994)*

## 3 INTERMODEL COMPARISON

### 3.1 Introduction

In the previous chapter the COMIS/COMVEN results have been compared with the analytical solution or with the results obtained solving the equation using a mathematical software package. Referring to Figure 2.1 another important task in the evaluation procedure is the relative comparison of different models.

This chapter refers to this relative comparison. The test developed by the Annex 23 participants in the frame of the work on evaluation is illustrated; the COMIS results are compared here with those of 14 different models: AIDA, AIRNET, ASCOS, BREEZE, BREVENT, CBSAIR, CONTAM93/CONTAM94, ESP, LBL model, MZAP, NORMA, PASSPORT AIR, TURBUL and VENCON.

For each of these models a brief presentation is given in the next section to allow the reader an overview of the main features of the models used; at the end of each model presentation a reference for further information is also given.

Each contribution to this task of the evaluation work corresponds to a comparison work focused on a defined topic: comparison of the results using the same sets of input data for AIVC, large opening for Athens University, User Test 1 for BBRI, mass flow equation for Concordia University, sensitivity to uncertainty in input data for LESO, smoke control for Politecnico of Torino.

The results of each comparison are illustrated by means of tables and diagrams. The files are available in the AIS (in the same way as the analytical evaluation) for only a few contributions. For the remaining cases more information can be requested directly from the Annex 23 participants.

### 3.2 Programs used for the comparisons

In this chapter the different computer programs used for intermodel comparison are listed. The most important features of the programs are described and a reference and/or the supplier address is given.

#### 3.2.1 Single zone and multizone network models

Network models calculate the air flows between the zone(s) of a building and the outside environment. The flow system is represented by the nodes (the zones) and the air flow resistances (named 'links' in COMIS) connecting the zones to the outside or to adjacent zones. A zone represents a completely mixed building volume. Related to each zone node is a set of state variables of the air (pressure, temperature, concentrations). The flow resistances can be of various types ('air flow components') such as cracks, windows, ducts or fans. Boundary conditions are the inside and outside temperatures (and concentrations) and the pressures due to wind and mechanical systems.

Flows in the links are non-linear functions of pressure differences across the link. The mass balance equation per zone is formulated and the system is solved by iterations for the unknown zone pressure. Pollutant concentrations are then calculated on the basis of the resulting room air flows.

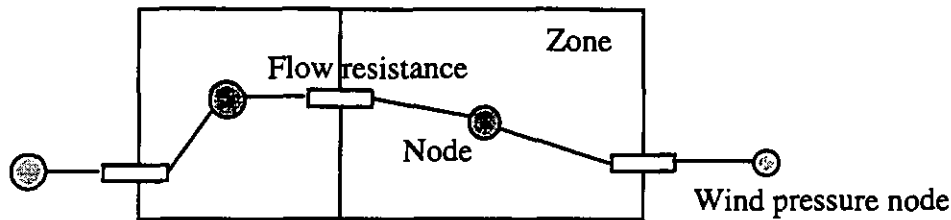


Figure 3.1 - The elements of a flow network

### **AIDA**

AIDA is a single zone network model designed only for cracks flow and developed by M. Liddament (1989).

Reference: Liddament M: AIDA - an Air Infiltration Development Algorithm, Air Infiltration Review, Vol 11, Dec. 1989

### **AIRNET**

This network multizone air flow model treating cracks and large openings, was developed by G. Walton at the NIST, USA, for the interactive use on a PC. The basis of this model is the code AIRMOVE, which also forms a part of the thermal building research analysis code, TARP.

Reference: AIRNET - A computer Program for Building Airflow Network Modelling, NISTIR 89-4072, 1989

### **ASCOS**

ASCOS (Analysis of Smoke Control Systems) is a program for steady air flow analysis of smoke control systems. This program can analyse any smoke control system that produces pressure differences with the intent of limiting smoke movement in building fire situations. The input consists of the outside and building temperatures, a description of the building flow network and the flows produced by the ventilation or smoke control system. The output consists of the steady state pressures and flows throughout the building. ASCOS was written in FORTRAN by J.H. Klote (NIST, USA).

Some changes have been made by the Politecnico of Torino to the original program to permit the use of the program on personal computers, however the basic structure of the program and of the data files remains as described in the ASHRAE Smoke Control Manual. Modifications and amendments to the original code concern the unit conversion to SI units, the proper initialisation of the variables, increased temperature profile options and additional output format options.

References: ASHRAE Smoke Control Manual by Klote, J.H., Milke, J.A.: "Design of Smoke Management Systems" published by the American Society of Heating, Refrigerating and Air-Conditioning Engineers (ASHRAE), Atlanta, Georgia

### **BREEZE**

BREEZE is a PC based interactive computer program for estimating the ventilation and inter-zonal air flows in both simple and complex multizone buildings. The definition of the zones and the air flow path is on a floor based graphical representation and the resulting air flows are superimposed on these floor plans on the screen.

Supplier: BRE, Garston, Watford, WD2 7JR, UK

References: BREEZE 6.0f User Manual. Building Research Establishment, UK, 1994.

## **CBSAIR**

CBSAIR is a research program developed to verify theoretical multi-zone air flow models. The derivation and solution of the model uses matrix representations. Like other models, CBSAIR considers a building as nodes connected by openings. Only power law flow relationship is implemented at the present, although any arbitrary flow equations are included in the theoretical model.

The computer implementation is done in MATLAB, a software package that directly uses matrices as basic variables in expressions. The input file is in MATLAB programming code. The data is entered as vectors or zonal connections, zone reference heights and temperatures, opening location, power law coefficients and exponents, wind and exponents, wind-pressure coefficients and reference wind speed.

The modelling and solution parts is a one-to-one implementation of the theoretical model in the matrix form. Zonal pressure updates use the built-in matrix inversion function, with an accelerated solution scheme similar to that of AIRNET. Due to MATLAB's interactive environment (in addition to programming capability) data and results can be displayed and manipulated easily. Modification of the program is also very easy and fast. This program is best suitable for in-house use. A sensitivity analysis procedure for air flow in buildings is also included in CBSAIR.

References: F. Haghghat and J. Rao, Computer-Aided Building Ventilation System Design - A System theoretic approach, Energy and Buildings Vol. 1, pp. 147-155, 1991

J. Rao and F. Haghghat, A procedure for sensitivity analysis of airflow in multi-zone buildings, Building Environment, Vol. 28, pp. 53-62, 1993

## **COMIS/COMVEN**

This is the multizone air flow model used and further developed within this annex. The code has been originally developed at the Lawrence Berkeley Lab, USA, in the frame of the COMIS one year workshop.

User interfaces for input and output processing are available for PC. The simulation program in the COMIS package is named COMVEN and is programmed in FORTRAN 77. This program allows for sophisticated multizone air flow and contaminant transport simulations. Air flow components for natural as well as mechanical ventilation can be modelled.

Various schedules can be defined for the outdoor climate, indoor room temperatures, pollutant sources and sinks, and air flow component operation schedules, e.g. for window opening or for fan operation. The time evolution of flows and concentrations as well as integrated and mean values for the whole simulation time period can be determined.

Reference: COMIS User Guide, Lawrence Berkeley Laboratory, USA

## **CONTAM**

The CONTAM model performs inter-zonal air movement and contaminant dispersal analyses for buildings. The program is quite user friendly, in that the user can define the airflow network in terms of a simplified floor plan of the building. In CONTAM94 the input processing, simulation, and graphic review of the results are merged into a single program. This program can access all available memory if needed for very large simulations.

CONTAM94 includes several types of flow elements: openings allowing only one-way flow (e.g. cracks), openings allowing two-way flow (e.g. doorways), and elements which force air flow (e.g. fans). Interactive menus are provided for entering data for these elements based on

direct entry of equation coefficients for various physical descriptions. CONTAM uses exactly the same solution of the airflow network as AIRNET.

Reference: CONTAM93 User Manual. Walton, G.N. United States Department of Commerce, Technology Administration, National Institute of Standards and Technology. NISTIR 5385, 1994.

Walton, G.N. et al. - Application of a multizone airflow and contaminant dispersal model to indoor air quality control in residential buildings, 15<sup>th</sup> AIVC Conference, Buxton, Great Britain, 1994..

### **ESP**

ESP (Environmental Systems Performance) is a transient building and systems simulation tool comparable to DOE-2, TRNSYS and others. It has been used in the frame of the PASSYS project and some considerable validation work has been done with this program. The program package consist of several parts, including modules for the graphical representation of the building. Recent development work concentrated on the integral formulation of fluid flow [Hensen, 1991]. In the simulation and analysis tools package, the module *mfs* allows for building air flow simulation, either independently or in tandem, with the heat balance module *bps*.

The ESP package is distributed by ABACUS Simulations Ltd, Glasgow, UK

References: Hensen J L M: On the thermal interaction of building structure and heating and ventilating system, Thesis Eindhoven, 1991

Clarke J A: Energy Simulation in Building Design, Adam Hilger Ltd, Bristol and Boston, 1985

### **MZAP**

MZAP (Multi-Zone Airflow Programme) - Developed at the AIVC, this is an unpublished multi-zone model, based on a modified version of Walton's 1983 algorithm. It was included in this study because it was possible to modify the source code, thus enabling customisation to suit this application. Input data are entered into the model by means of a 'spread-sheet' style editor.

References: Walton G.N.: A Computer Algorithm for Estimating Infiltration and Inter-Room Air Flows. United States Department of Commerce, Technology Administration, National Institute of Standards and Technology. NBSIR 83-2635, 1983.

### **NORMA**

NORMA is a single zone design tool which enables the designer to examine how altering different aspects of the design can influence the natural cooling characteristics of a building, considering solar control, thermal mass, natural ventilation, night ventilation and buried pipes. The program was developed by M. Santamouris in the framework of the Zephyr Architectural Competition of EEC.

Reference: NORMA manual, CEC Directorate General XII for Science, Research and Development, University of Athens, Greece.

***Passport-air***

This program is developed in the framework of the PASCOOL research project of the Commission of the European Union, Directorate General XII for science, research and development, sub task ventilation and thermal inertia.

Reference: PASSPORT-AIR manual, E. Descalaki and M. Santamouris (Editors), PASCOOL Research Program, CEC DGRD, 1994.

***VenCon***

VENCON (Ventilation and Concentration program) is a TNO-Delft (Netherlands) made HP-BASIC program for steady state multizone ventilation simulations. It dates from 1978-1989.

It can work conveniently with about 50 zones, and some 100 links, which are TNO-ELA including a flow exponent or polynomial approximated Fans. All cracks are handled as large openings if the velocity in the openings is low. The temperature of all links is made equal to the temperature of the incoming flow. VENCON stores all flows for one building variant in a database with the meteo conditions as index. Flows can be plotted in floor plans or cross sections of the building. A blower door program can trim the link-network to a demanded blower door value. From an interpolation of this database the concentration model runs a dynamic concentration simulation and calculates doses per occupant and histograms of effective ventilation flow rates.

**3.2.2 Simplified models**

In these types of models, the modelling of the underlying physical phenomena is simplified and flow equations are established on an empirical or semi-empirical basis in such a way that the flow equation system is explicit and does not require an iterative solution. Also, simplifying assumptions are made, for example in regard to the distribution of the leakages in the building.

***BREvent***

The program BREVENT is available at the Building Research Establishment. The model has been developed by P.R. Warren et B.C. Webb [1980] for row houses, as commonly encountered in Great Britain.

***The LBL model***

The so called LBL model (Lawrence Berkeley Laboratory) is a single zone model calculating the wind and stack induced infiltration flows separately. This model is based on similar hypothesis as BREVENT in regard to the indoor zone and the distribution of air tightness. The total infiltration is calculated by a quadrature. The air tightness is represented by an equivalent leakage area  $A_0$  which corresponds to the surface of an orifice debiting the same flow rate for a reference pressure arbitrarily fixed to 4 Pa [Sherman et al., 1980].

**3.2.3 Specific models**

These type of models are used to study specific air flow topics, such as the effects of the compressibility of the air.

## TURBUL

The model TURBUL has been developed at the LESO-PB [Fürbringer, 1995]. It simulates the non-linear resistance-capacity model (Figure 3.2), with the aim of modelling a permeable zone taking into account the effects of the air compressibility and the wind turbulence.

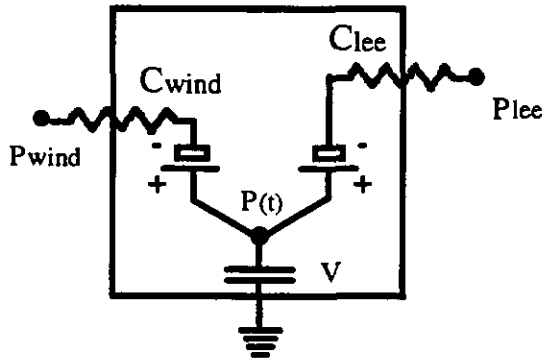


Figure 3.2 - Non-linear RC model used in TURBUL for simulating the indoor pressure  $P(t)$  of a permeable room. The subscript 'wind' refers to the windward side and, 'lee' to the leeward side.

## 3.3 Comparison and results

### 3.3.1 Comparison of the results using the same sets of input data

The purpose of this section is to report on a comparison of the results of several multi-zone air flow models which have been configured using the same sets of input data. The results are presented below, in the form of mass flow rates through every leakage path, for each of the models. It was not intended to test the full capabilities of each model, and therefore only a straightforward configuration was devised for the test. This is similar to User Test 1 which was developed jointly by Annex 23 and the AIVC.

The main emphasis of this study was to ensure that identical input data was used in all of the models, and only then to check how they responded. Four multi-zone air flow models have been configured in order to simulate the same building in the same meteorological conditions: COMIS 1.3, CONTAM93, MZAP and BREEZE 6.0f.

#### Configuring the Models

There are many factors which can influence the results found using multi-zone models. Limitations of the models themselves, due to physical approximations, are difficult to correct. On the other hand, lack of clarity or misunderstanding of the instructions can also give rise to incorrect results. This type of problem is easier to rectify, once it has been identified. Configuration errors may be avoided with graphical user interfaces, which allow floor plans to be drawn and leakage openings positioned correctly. Both BREEZE and CONTAM93 have this facility. The accuracy of the results given by a model is not governed by its solver, but by the accuracy of the input data.

Multi-zone models may require an initial familiarisation period of up to several days. However, once this has been completed, users can often set up a simulation in substantially less time (perhaps in a matter of hours). The time taken for a model to converge to a solution is generally insignificant compared to that needed for correct configuration. (In this particular case less than one minute in each instance).

The four codes had varying methods for dealing with flow through horizontal openings. For instance, MZAP handled them as direct links, with a pressure differential determined by the zone pressure above and below. In BREEZE, horizontal openings between floors were defined with stacks which penetrate more than one floor and by appropriately assigning vertical openings to these stacks. It was assumed for BREEZE that two openings in series (with appropriate flow characteristics) and with a temperature inside the stack equal to the average of the two zone temperatures would approximate a single horizontal opening.

### General Information About the Building

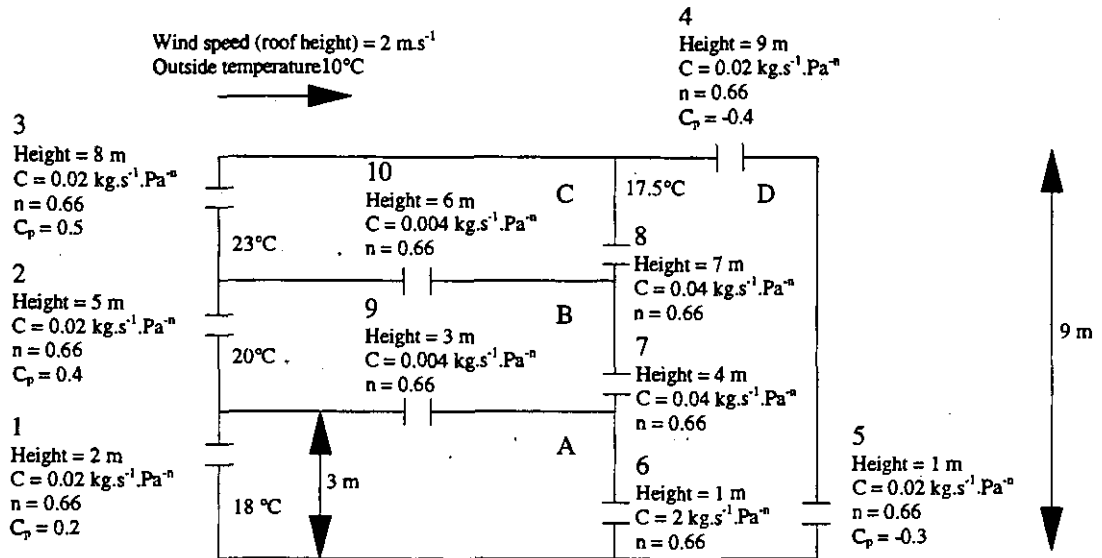


Figure 3.3: Cross-section of the building simulation

The building has 3 storeys together with a connecting enclosed stairwell. A section is shown in Figure 3.3. Each floor has a volume of  $150 \text{ m}^3$  (zones A, B, and C in Figure 3.3) and the stairwell itself has a volume of  $135 \text{ m}^3$  (zone D in Figure 3.3). The total building volume is therefore  $585 \text{ m}^3$ . Flow characteristics of the leakage paths have been represented using power law expressions (with the flow coefficients,  $C$ , and flow exponents,  $n$ ). Wind pressure coefficients,  $C_p$ , have been given for external openings.

Atmospheric pressure is taken to equal  $101.325 \text{ kPa}$ , with an outdoor air temperature of  $10^\circ\text{C}$ . The wind speed at the roof height of the building ( $9 \text{ m}$ ) is  $2 \text{ m.s}^{-1}$ .

Both the indoor and outdoor humidity ratios were assumed to equal  $0.0 \text{ g.kg}^{-1}$  (completely dry air). The reason for this was in order to use identical air density profiles in all of the models, although such a situation would be very unlikely to occur in reality. The physical arrangement of leakage paths in the building structure is shown in Figure 3.3.

### Results

The results found using COMIS, CONTAM93, MZAP, and BREEZE are shown in Figure 3.4. In this Figure, mass flow rates are listed for each leakage opening in the order COMIS, CONTAM93, MZAP, and then BREEZE. The distribution of these flow rates is analysed in Table 3.1: The variation of the mass flow rates predicted by the models, for each leakage path. Table 3.2: Predicted outgoing mass flow rates lists both the flow rates of air calculated to leave every zone, and the total flow rate of air leaving the building for all of the models. The author of CONTAM93 has discovered that the slight differences observed between it and the

other models are mainly caused by the different modelling approaches used. When a power law model was included in CONTAM93, even better agreement was obtained

In addition to the results shown in Figure 3.4, it was determined using MZAP that, by removing all internal floors and walls from the model configuration and assuming a uniform internal temperature of 18 °C, the mass flow rate of air leaving the building was 158.0 kg.h<sup>-1</sup>. Similarly a uniform internal temperature of 20 °C gave an outgoing flow of 188.6 kg.h<sup>-1</sup>. The flow rate of air leaving the building with the internal partitioning present was 154.2 kg.h<sup>-1</sup>, for the conditions as previously described. (The values for all the models are shown in Table 3.2.).

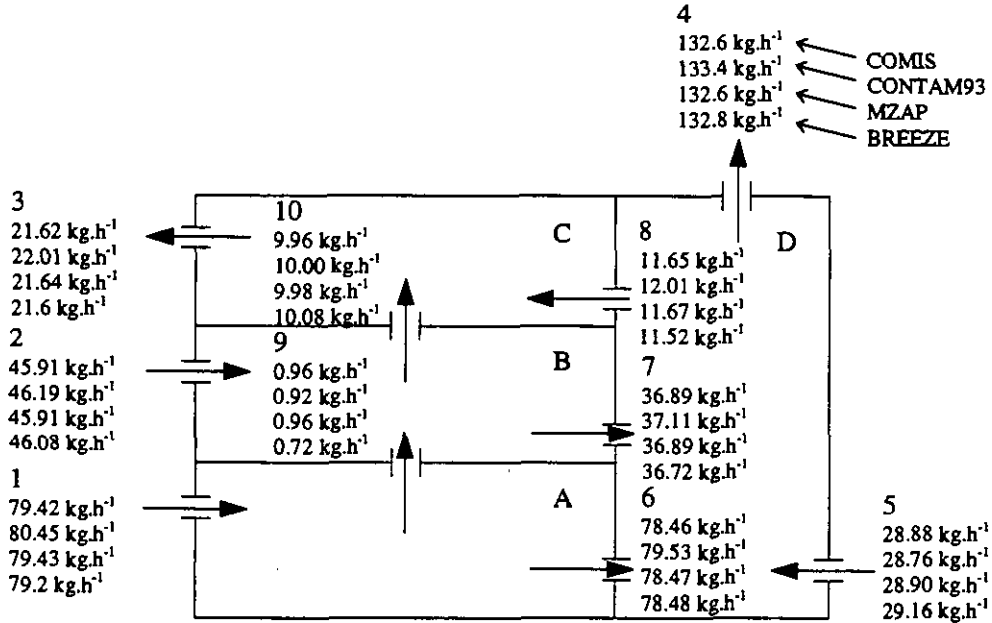


Figure 3.4 - Results of the simulations - Mass of air flow rates through the leakage paths

The lower overall flow rate with the partitioning compared to the overall flow rates without it, can be accounted for by a combination of the stack effect and increased flow resistance due to the partitioning. (Removing the internal partitioning reduces the problem to a single zone building.)

Table 3.1: The variation of the mass flow rates predicted by the models

Leakage path	Number of samples	Mean flow rate kg.h <sup>-1</sup>	Standard deviation of flow rates/ kg.h <sup>-1</sup>	100*(standard deviation)/(mean)
1	4	79.6	0.56	0.70
2	4	46.0	0.14	0.30
3	4	21.7	0.20	0.90
4	4	132.9	0.38	0.28
5	4	28.9	0.17	0.58
6	4	78.7	0.53	0.67
7	4	36.9	0.16	0.43
8	4	11.7	0.21	1.8
9	4	0.89	0.12	13
10	4	10.0	0.053	0.53
Total outgoing	4	154.6	0.57	0.37

In absolute terms, the standard deviation of the results for each opening was low in magnitude and reasonably constant (ranging from  $0.053 \text{ kg.h}^{-1}$  to  $0.56 \text{ kg.h}^{-1}$  - see 4<sup>th</sup> column in Table 3.1). On the other hand, the relative spread of values around the mean value was high for some openings (see 5<sup>th</sup> column in Table 3.2). In particular, this applies to path 9, which flow rate is very low. For this path only, BREEZE gives an air flow significantly lower than that given by the other codes.

Table 3.2: Predicted outgoing mass flow rates

Model	Zone A outgoing flow rate/kg.h <sup>-1</sup>	Zone B outgoing flow rate/kg.h <sup>-1</sup>	Zone C outgoing flow rate/kg.h <sup>-1</sup>	Zone D outgoing flow rate/kg.h <sup>-1</sup>	Total Building outgoing flow rate/kg.h <sup>-1</sup>
COMIS	79.42	46.85	21.62	144.25	154.2
CONTAM93	80.45	47.11	22.01	145.41	155.4
MZAP	79.43	46.87	21.64	144.27	154.2
BREEZE	79.20	46.80	21.6	144.32	154.4

### Conclusion

It was found that when identical data are applied to each model, the variations between the total outgoing air flow rates predicted by the models were low, shown in Table 3.2 as were the variations for the individual zones.

### 3.3.2 Large openings

This section deals with the results of a study aiming to compare the predictions of COMIS for single side natural ventilation configurations, regarding the predictions of Passport Air, AIRNET, BREEZE, ESP and NORMA, for the same configurations.

All studied cases refer to single side ventilation experiments performed in the PASSYS single-zone test cells, (4 Experiments), and in the NOA building, (19 Experiments). Tracer gas techniques have been used while all indoor and outdoor climatic and meteorological parameters have been measured on the site. In the following section the main characteristics of the experiments are given.

### PASSYS Test Cell Experiments

The surface and the volume of the single zone is  $8.6 \text{ m}^2$  and  $28.3 \text{ m}^3$  respectively. The surface of the single opening is  $2.24 \text{ m}^2$ , and the height 2.2 m. The mean climatic data during the experiments is given in Table 3.3

Table 3.3 - Characteristics of the Test Cell experiments

Experiment	Mean Ambient Temperature	Mean Indoor Temperature	Mean Wind Speed, (m/s)
Experiment 1	24.1	23.4	3.35
Experiment 2	24.7	24.3	2.51
Experiment 3	25.7	26.2	3.82
Experiment 4	25.6	26.6	3.56

### NOA Experiments

The surface of the zone is  $13.6 \text{ m}^2$ , the volume  $61.1 \text{ m}^3$  and the total surface of the window is  $2.41 \text{ m}^2$ . The window is divided into 5 parts as shown in Figure 3.5.

The area of each window part is as follows:  $A1 = 0.26 \text{ m}^2$ ,  $A2 = 0.286 \text{ m}^2$ ,  $B1=0.576 \text{ m}^2$ ,  $B2 = 0.62 \text{ m}^2$ ,  $C = 0.66 \text{ m}^2$ .

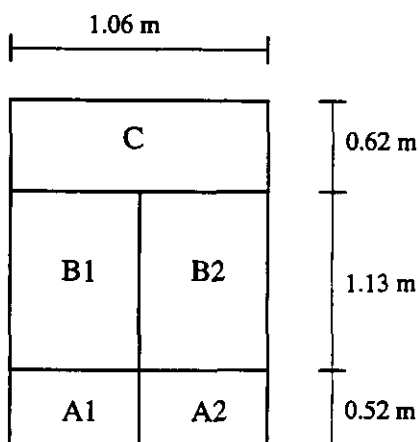


Figure 3.5 - Dimensions of the window of the NOA building.

The mean climatic data set used for the 19 experiments performed in NOA building are given in

Table 3.11

Table 3.4 - Mean climatic values in NOA building.

Experiment	Openings	Ambient Temperature	Indoor Temperature	Wind Speed @ 10 m height. [m/s]
Experiment 5	A1+A2	31.3	31.4	6.8
Experiment 6	B1+B2	32.6	31.8	3.0
Experiment 7	C	30.6	32.1	5.0
Experiment 8	A2+B2	32.5	31.8	6.7
Experiment 9	A1+A2+B1+B2	30.5	31.5	1.7
Experiment 10	B1+B2+C	28.8	29.2	1.6
Experiment 11	ALL	30.2	31.0	3.6
Experiment 12	A1+A2+B1+C	29.6	31.0	3.1
Experiment 13	A1+A2+B2+C	28.2	31.0	3.4
Experiment 14	A2+C	31.2	31.7	5.4
Experiment 15	B2+C	30.7	31.8	4.9
Experiment 16	A1+A2+C	30.8	31.0	4.2
Experiment 17	A1+B1+C	27.6	28.8	2.0
Experiment 18	A2+B2+C	30.1	31.6	5.0
Experiment 19	A2+B1+B2+C	29.4	31.2	4.7
Experiment 20	ALL	27.0	31.7	3.7
Experiment 21	B1+B2+C	31.2	31.8	4.1
Experiment 22	ALL	30.8	31.4	4.0
Experiment 23	ALL	30.8	31.3	3.6

### Prediction of the air flow

COMIS, and all the other tools previously referred to, have been used to predict the air flow for all the 23 single sided configurations. The calculated values, in cubic meters per hour, for all the tools are given in

Table 3.11. Based on the above values, the correlation coefficients between the six tools are given in Table 3.12. As shown, all tools except NORMA, which is a simplified tool, present correlation coefficients which are very close to unity.

Table 3.5 - Calculated air flow rates for all tools

Experiment	PASSPORT	COMIS	AIRNET	BREEZE	NORMA	ESP
1	631	606.9	620.2	626.8	584.0	608.1
2	466	455.5	458.6	437.2	344.0	454.0
3	538.7	528.9	525.9	421.9	459.0	535.2
4	761.6	746.5	746.1	687.9	732.0	731.7
5	28.1	33.63	33.6	34.5	21.2	29.9
6	192.8	229.3	229.3	242.4	163.5	240.0
7	115.0	134.5	134.5	135.9	98.3	138.1
8	171.0	210.9	204.8	210.0	178.0	204.4
9	413.0	498.3	498.3	506.9	470.0	498.7
10	296.0	357.7	357.7	362.7	243	354
11	560.0	663.0	663.0	674.1	635.0	657.2
12	656.0	755.1	755.0	634	726	596.9
13	872.0	1060.8	804.0	1093.2	1015	841.7
14	181.9	220.1	168.1	182.0	211.0	220.1
15	323.5	320.9	269.1	376.3	375.0	390.7
16	223.4	269.0	189.5	224.4	257.0	193.4
17	451.5	437.1	400.5	541.1	510.0	533.5
18	516.0	507.5	440.0	631.7	612.0	607.0
19	901.0	941.5	822.3	879.0	889.0	946.8
20	1351.7	1595.8	1595.7	1610.0	1619.0	1621.0
21	343.3	412.6	412.5	422.0	349.0	428.6
22	507.0	596.1	596.1	601.1	544.0	594.6
23	471.9	556.4	553.0	564.3	483.0	578.0

Table 3.6 - Correlation Coefficients

Tool	PASSPORT	AIRNET	COMIS	NORMA	BREEZE	ESP
<b>PASSPORT</b>	1	0.96	0.97	0.65	0.96	0.96
<b>AIRNET</b>	0.96	1	0.98	0.69	0.97	0.98
<b>COMIS</b>	0.97	0.98	1	0.69	0.99	0.98
<b>NORMA</b>	0.65	0.69	0.69	1	0.70	0.69
<b>BREEZE</b>	0.96	0.97	0.99	0.70	1	0.98
<b>ESP</b>	0.96	0.98	0.98	0.69	0.98	1

### Conclusion

The predictions of COMIS for the case of single sided natural ventilation in 23 tests is very close to the predictions of other network models. Only with respect to NORMA, which is a monozone tool, is the correlation coefficient (0.69) less than 0.95. The best agreement is found with BREEZE: with a correlation coefficient equal to 0.99; this was expected because the same algorithms are used to simulate large opening.

### 3.3.3 User Test 1

At the beginning of 1993, a user test was distributed among the IEA Annex 23 participants (see chapter 5). The purpose of the user test was to monitor the results of a multizone air flow simulation obtained by different users employing different simulation tools. The total user test consisted of two exercises.

This section only compares the results obtained by using three different simulation codes on the first exercise. The three simulation codes used are:

COMIS 1.1, LBL, USA

VENCON, TNO, The Netherlands

ESP 6.28, University of Strathclyde, Scotland

#### *Description of the building*

The modelled building is illustrated in Figure 3.3, and also in Figures 5.1 and Table 5.1. The crack characteristics are given in Tables 5.2 and 5.3. As one can see, the air leakage distribution is simple and the boundary conditions are well known. The temperature gradient in the staircase is neglected because only COMIS has a routine incorporated to model this phenomena in one zone. During the exercise the air temperature in the staircase is kept at a constant value: 17.5 °C.

#### *Results*

The results obtained with the different simulation codes are given in Table 3.14 and Figure 3.6. Figure 3.7 illustrates the air flow directions through the different components.

*Table 3.7 - Comparison of the results obtained by VENCON, COMIS and ESP-r (no temperature gradient).*

From	To	Crack	VENCON air flow (g/s)	COMIS air flow (g/s)	ESP-r air flow (g/s)
ext.	z1	1	22.36	21.94	21.87
ext.	z2	2	12.03	12.37	12.64
ext.	z3	3	-6.14	-6.72	-5.97
ext.	z4	4	8.81	8.78	7.97
ext.	z4	5	-37.07	-36.38	-36.51
z1	z4	6	22.10	21.64	21.61
z2	z4	7	10.31	9.93	10.16
z3	z4	8	-3.36	-3.94	-3.22
z1	z2	9	0.26	0.33	0.27
z2	z3	10	2.78	2.78	2.75

One can remark that the performances of the three different models are similar. These results could be expected because the air flow components used in this exercise are modelled in the same way by the three different programs.

#### *Conclusion*

For a paper building, COMIS results are very close to those obtained using VENCON and ESP. This result was expected because the air flow component used in this test are modelled in the same way by these three programs. Some of the differences are caused by different ways the programs calculate the temperature in the cracks. VENCON assumes the crack has the tem-

perature of the incoming flow, while COMIS has a more realistic temperature calculation taking into account the flow rate and heat conduction through the wall.

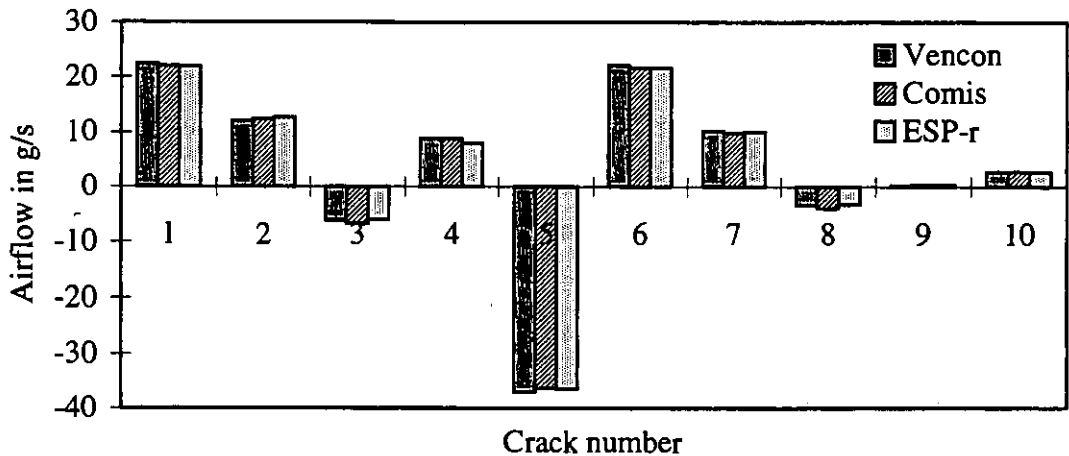


Figure 3.6 - Graphical comparison of the results.

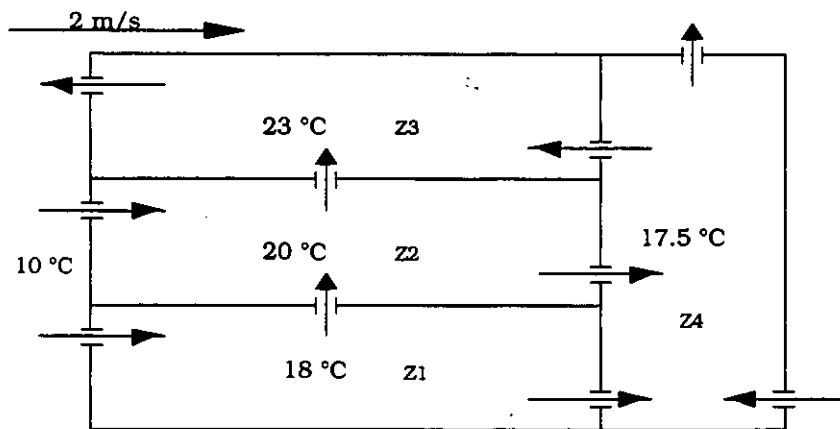


Figure 3.7 - Flow direction for each path and numbers of zones.

### 3.3.4 Comparison of mass flow equations

The estimated air flow rates and pressures in a four zone building predicted by COMIS are compared here with those predicted by CBSAIR, AIRNET and CONTAM94.

The test case for air infiltration is similar to that used by Haghghat and Rao (1991). It consists of a four zone building with eight air flow paths. The building and room dimensions, opening characteristics, temperature distribution and wind induced pressures are shown in Figure 3.8. Power law flow elements are selected, and the values of the parameters for each element are presented in Table 3.15.

The coefficients used in the flow equations depend on the exact form of the equation used in the simulation program. COMIS Fundamentals [Feustel et al., 1990] identifies three possible flow equations:

$$W = \rho \cdot Q = K_a C_a \rho (\Delta P)^n \tag{3.1}$$

$$K_a = \left( \frac{\rho_0}{\rho} \right)^n \left( \frac{v_0}{v} \right)^{2n-1}$$

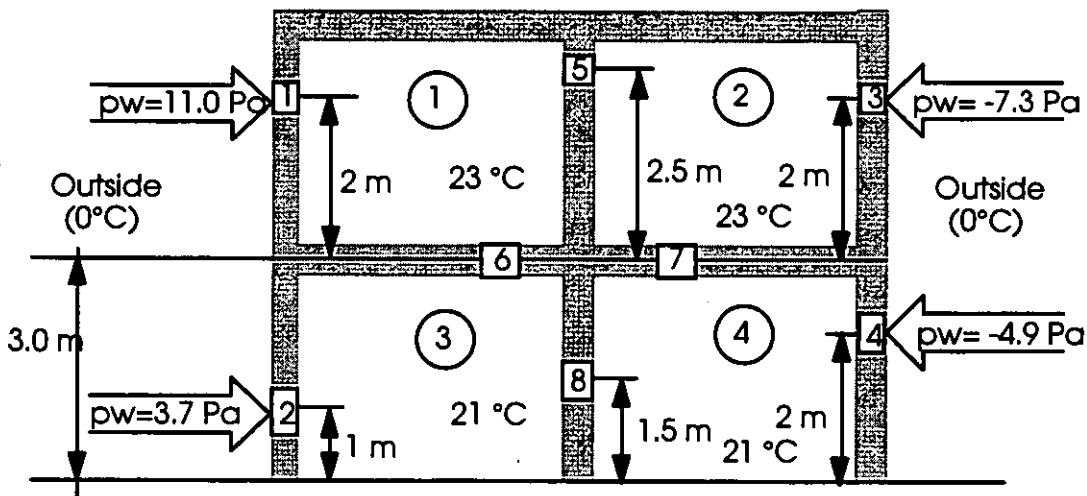


Figure 3.8 - Paper building

Table 3.8 - Flow element parameters for the test case

Flow element number	C [m <sup>3</sup> s <sup>-1</sup> Pa <sup>-n</sup> ]	n
1	0.005	0.65
2	0.008	0.65
3	0.007	0.65
4	0.009	0.65
5	0.015	0.5
6	0.020	0.5
7	0.020	0.5
8	0.015	0.5

$$W = K_b C_b \rho^{1/2} (\Delta P)^n \quad (3.2)$$

$$K_b = \left( \frac{\rho_0}{\rho} \right)^{n-1/2} \left( \frac{v_0}{v} \right)^{2n-1}$$

$$W = K_c C_c (\Delta P)^n \quad (3.3)$$

$$K_c = \left( \frac{\rho_0}{\rho} \right)^{n-1} \left( \frac{v_0}{v} \right)^{2n-1}$$

The flow coefficients,  $C_i$ , are assumed to be determined under standard conditions (20°C and 101.3 Pa), and the temperature adjustment factors,  $K_i$ , are used to adjust the computed flows if the actual state of the air is different. For pure viscous flow, the flow rate increases as much as 30 % at -20°C. The viscosity in this case represents about 40 % of the increase.

CBSAIR uses form (3.1) of the flow equation, and AIRNET utilises form (3.2). CONTAM94 employs both forms (3.1) and (3.2) of the flow equation and relates the form (3.2) to the orifice equation ( $Q = C_d A [2 \Delta P / \rho]^{1/2}$ ) such that  $C_b = 2^{1/2} A C_d$ , relating the flow coefficient to physical quantities.

Form (3.1) can be converted to form (3.2) in one of the following manners:

$$C_b = C_a \sqrt{\rho} \quad (3.4)$$

$$A = \frac{C_a}{C_d} \sqrt{\left(\frac{\rho}{2}\right)} \quad (3.5)$$

by assuming a value for  $C_d$  (e.g. 0.6), or:

$$C_d = \frac{C_a}{A} \sqrt{\left(\frac{\rho}{2}\right)} \quad (3.6)$$

by assuming a value for  $A$  (e.g.  $C_a$ ).

Version 1.3 of COMIS which uses form (3.3) of the flow equation and CONTAM94 are used in this paper. In COMIS, the density is calculated at the air leakage temperature in the crack as a function of different parameters [Feustel, 1990]

In CONTAM94, AIRNET, and CBSAIR, the density is that of the fluid flowing through the flow path. Therefore, in all programs the density depends on the flow direction in a non-isothermal case.

In Table 3.9, the simulated mass link flow rates, zone pressures and link pressure differences for COMIS, AIRNET, CONTAM94 (3.2) and CBSAIR are given. As shown, there is good agreement between the results obtained from these models. The pressure values are within a 5% agreement of each other, for both the zones and the links; except for link 6 where the difference is about 23%. For example, in the COMIS model (version 1.3), the stack pressure between links 6 and 7 is an interpolation between the stack pressure when the flow is positive and when it is negative. This interpolation is necessary to prevent convergence problems. The air flow rates for the links are in agreement by roughly 11%..

Table 3.9 - Results for paper building

Zone	PRESSURE (Pa)				FLOW RATE (kg/s)			
	COMIS	AIRNET	CONTAM	CBSAIR	COMIS	AIRNET	CONTAM	CBSAIR
1	-36.72	-37.27	-37.3	-37.12	0.0260	0.0263	0.0262	0.0266
2	-38.80	-39.41	-39.4	-39.33	0.0313	0.0320	0.0319	0.0322
3	-2.09	-1.99	-2.0	-1.80	0.0270	0.0276	0.0275	0.0279
4	-4.08	-4.07	-4.1	-3.96	0.0254	0.0260	0.0260	0.0265
<b>Link</b>								
1	8.64	8.31	8.31	8.31	0.0244	0.0247	0.0247	0.0252
2	4.91	4.78	4.78	4.78	0.0270	0.0276	0.0276	0.0279
3	-7.58	-7.84	-7.84	-7.85	-0.0313	-0.0320	-0.0320	0.0322
4	-2.59	-2.64	-2.63	-2.63	-0.0200	-0.0203	-0.0203	0.0209
5	2.08	2.14	2.14	2.14	0.0260	0.0263	0.0263	0.0266
6	0.0044	0.0043	0.0043	0.0043	0.0016	0.0016	0.0016	0.0014
7	0.0499	0.0568	0.0568	0.057	0.0054	0.0057	0.0057	0.0056
8	1.99	2.09	2.09	2.08	0.0254	0.0026	0.0026	0.0265

The CONTAM94 model was then used to investigate the impact of the flow equation form on the model's predictions of mass link flow rate and pressure difference. Table 3.10 gives the values of the simulated mass link flow rates and pressure differences for PLR (refers to form (3.2), PLR(T) (form (3.2) with temperature adjustment), PLC (refers to form (3.1) and PLC(T) (form (3.1) with temperature adjustment):

The major causes for the differences observed in Table 3.9 and Table 3.10 are the form of the mass flow equation used or the numerical manipulation used to avoid convergence problems. The AIRNET and PLR results are in excellent agreement since they use the same model. The temperature adjusted calculations agree almost exactly - as they should. The PLC model is better than the PLR model if no temperature adjustment is made. Temperature adjustment is faster with the PLR model since it is not needed when  $n = \frac{1}{2}$ . This is not a difficult test for the non-linear equation solver. The problems occur when the flow coefficients for the different paths differ by several orders of magnitude. This test has been useful in confirming that the flow equations have been correctly used in the programs. The test is not a difficult challenge from the point of view of execution time - the solution is computed in less than the 0.05 seconds resolution of the timing algorithm.

Table 3.10 - Impact of the flow equation form on the model's predictions

Zone	PRESSURE (Pa)				FLOW RATE (kg/s)			
	PLR	PLC	PLR (T)	PLC (T)	PLR	PLC	PLR (T)	PLC (T)
1	-37.27	-37.08	-37.12	-37.13	0.0263	0.0266	0.0266	0.0266
2	-39.41	-39.29	-39.31	-39.31	0.0320	0.0322	0.0321	0.0321
3	-1.99	-1.79	-1.84	-1.84	0.0276	0.0278	0.0278	0.0278
4	-4.07	-3.95	-3.98	-3.98	0.0260	0.0265	0.0263	0.0263
Link	PRESSURE (Pa)				FLOW RATE (kg/s)			
1	8.31	8.12	8.17	8.17	0.0247	0.0252	0.0251	0.0251
2	4.78	4.59	4.64	4.64	0.0276	0.0278	0.0278	0.0278
3	-7.85	-7.97	-7.95	-7.95	-0.0320	-0.0322	-0.0321	-0.0321
4	-2.63	-2.75	-2.73	-2.73	-0.0203	-0.0209	-0.0208	-0.0208
5	2.14	2.21	2.18	2.18	0.0263	0.0266	0.0266	0.0266
6	0.0043	0.0033	0.0037	0.0037	0.0016	0.0014	0.0015	-0.0015
7	0.0568	0.0541	0.0539	0.0539	0.0057	0.0056	0.0056	-0.0056
8	2.09	2.16	2.13	2.13	0.0260	0.0027	0.0026	0.0263

### Conclusion

This test compares the air flow rates and pressures predicted by COMIS with those predicted by CBSAIR, AIRNET and CONTAM94. The pressure values are in agreement within 5% of each other (except for one link, having very small pressure differential and air flow, where the difference is about 23%); the air flow rates are in agreement within 11%. The major causes for the differences observed are the form of the mass flow equation used or the numerical manipulation used to avoid convergence problems.

### 3.3.5 Test of sensitivity to input errors

A comparison was made between the level of the inaccuracy of output data in relation to the uncertainty of the input data. All the concepts used for this study are explained in Chapter 1 and have been used for the calculation of confidence intervals in Chapter 4. Some results are given here which compare the sensitivity of COMVEN with other simpler models, in particular AIDA, the LBL model, BREVENT and TURBUL (cf. 3.2). A detailed presentation of the sensitivity of each model can be found in [Fürbringer, 1994].

The aim of this study is to find an answer to the question of whether the confidence intervals of detailed models are greater or smaller than those of the simple models if the inaccuracy of the input parameters is taken into account.

To answer this question, a building of 6 zones, corresponding to the Italian test building (cf. § 4.12) has been chosen. The plan is presented in Figure 3.9. It corresponds to a typical one family home on one floor. This structure is a good platform for comparing both detailed and simple models.

In the first instance, the inaccuracy ratios are compared. These are defined as the ratio between the inaccuracy of the observed output and the global inaccuracy of the input parameters. A part of these data are presented in Figure 3.12.

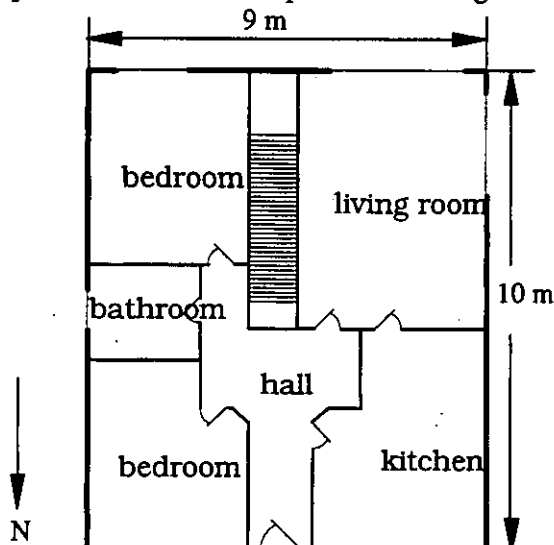


Figure 3.9: Plan of the building

Table 3.11: volumes of the zones

Zone	Volume
1 south bedroom	70 [m <sup>3</sup> ]
2 bath room	30 [m <sup>3</sup> ]
3 north bedroom	70 [m <sup>3</sup> ]
4 entrance hall	70 [m <sup>3</sup> ]
5 kitchen	50 [m <sup>3</sup> ]
6 living room	80 [m <sup>3</sup> ]
	120 [m <sup>3</sup> ]

The results are obtained from different factorial designs for the 4 simple models and COMVEN. For the simple models, the given results correspond to the average for variation ranges of 1% 5% 10% and 20%, except for the LBL model whose result corresponds to a range of 20%. For COMVEN, the results correspond to a range of 1%.

Table 3.12: Air tightness coefficients and exponents

Air tightness	[kg s <sup>-1</sup> Pa <sup>-n</sup> ]	S(C)/C	Exponents	[-]	S(n)/n
C <sub>1</sub>	0.018	24%	n <sub>1</sub>	0.65	8%
C <sub>2</sub>	0.0276	23%	n <sub>2</sub>	0.39	13%
C <sub>3</sub>	0.0048	24%	n <sub>3</sub>	0.86	6%
C <sub>4</sub>	0.0784	23%	n <sub>4</sub>	0.54	10%
C <sub>5</sub>	0.0252	23%	n <sub>5</sub>	0.60	9%
C <sub>6</sub> +C <sub>7</sub>	0.0288	23%	n <sub>6</sub> = n <sub>7</sub>	0.50	10%
C <sub>int</sub>	0.0784	23%	n <sub>int</sub>	0.54	10%

It must be observed here that the answer to the former question is not straightforward. Effectively, for the mean age of air, the simple models have inaccuracy ratios between 1.8 and 3.8, while Comven has inaccuracy ratios distributed between 2 and 10 depending on the wind direction and varying from zone to zone. The following consequences emerge:

- For uniform inaccuracy ranges and for all the input parameters, the inaccuracy ratios of the simple and detailed models are of the same order of magnitude.

- For the simple models, the confidence intervals of the models having a nodal conception (AIDA and TURBUL) are almost half the confidence interval of the model of empirical conception (LBL, BREVENT).
- For detailed models, it can be a considerable difference in sensitivity from one zone to another and for different wind directions. There are critical wind directions and situations for which the level of detail of modelling is not adapted to the precision of measurements because the inaccuracy amplification between input and output data is about an order of magnitude. Except for these critical situations, the inaccuracy ratio is between 2 and 3.

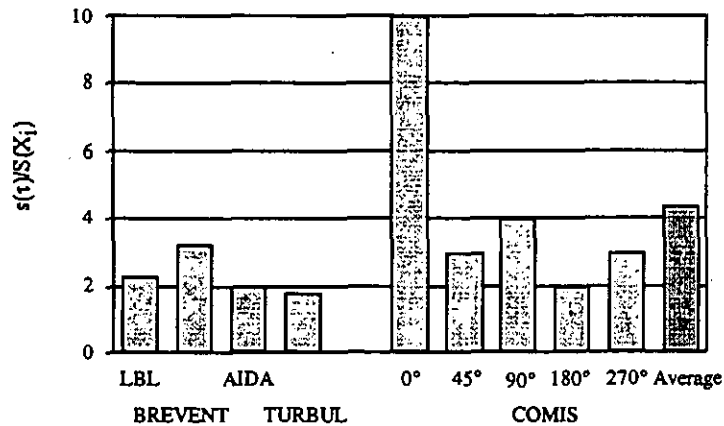


Figure 3.10 - Ratio between the standard deviation of the room mean age of air and the standard deviation of the input parameters.

After observing these comments, it is necessary to advance one more step and focus the discussion on the mean age of air obtained when the experimental inaccuracies for the input data are used. Simulations were then completed by additional runs for each model. For these additional simulations, the variation ranges have been chosen, not uniformly as previously, but in accordance with their respective experimental accuracy. Table 3.13 and Table 3.15 present for each model and each input parameter the considered inaccuracy as well as the final inaccuracy obtained by the simulation. The inaccuracy of the pressure coefficients has been fixed taking into account the variation of data proposed for the different wind exposure in 'Air Infiltration Calculation Technique' [Liddament, 1986].

The calculations have been performed for 3 different wind speeds. These situations correspond to different ratios between wind and stack forces as shown explicitly in Table 3.14. In this table, the Achimedes number is defined by:

$$Ar = \frac{\Delta T g h}{T_i v^2} \quad (3.7)$$

with  $\Delta T$  indoor-outdoor temperature difference, [K]  
 $g$  gravity acceleration, [m/s<sup>2</sup>]  
 $h$  warm zone height, [m]  
 $T_i$  indoor temperature, [K]  
 $v$  wind speed, [m/s]

Table 3.13- Level of inaccuracy for each type of parameters and each model.

Parameters	COMIS	BREVENT	LBL	AIDA	TURBUL
air tightness	±24%	±5 %	±20%	±24%	±24%
exponents	±10%	±8%	±8%	±10%	±10%
volumes	±10%	±10%	±10%	±10%	±10%
temperatures	±0.5[°C]	±0.5[°C]	±0.5[°C]	±0.5[°C]	±0.5[°C]
atmospheric pressure	±0.5%	-	-	-	-
pressure coefficients	±50%	-	-	±50%	±50%
wind speed	±5%	±5%	±5%	±5%	±5%
heights	±1%	±5%	±5%	±1%	±1%
terrain	-	±1	-	-	-
wind exposure	-	±1	-	-	-

Table 3.14 - Simulated climatic situations and corresponding Archimedes number.

	Wind speed	Archimedes	Comment	$Ar = \frac{\Delta Tgh}{T_i v^2}$
1	0.3 [m s <sup>-1</sup> ]	11	stack dominance	
2	1 [m s <sup>-1</sup> ]	1	equilibrium	
3	3 [m s <sup>-1</sup> ]	0.1	wind dominance	

Table 3.15 - Uncertainty of the mean age of air for detailed and simple models when experimental inaccuracy is taken into account. for COMIS, the result for global mean age with south wind

Wind speed	COMIS	BREVENT	LBL	AIDA	TURBUL
0.3[m s <sup>-1</sup> ]	51%	34%	26%	16%	15%
1[m s <sup>-1</sup> ]	38%	22%	29%	24%	19%
3[m s <sup>-1</sup> ]	32%	24%	37%	24%	24%

The conclusions of these simulations are as follows:

- The uncertainty shown by the detailed model is larger than the uncertainty shown by simple models. It is stressed here, however, that this discussion is about the uncertainty coming from the input data, which is in turn propagated by the model, and is not concerned with the exactitude from the physical point of view, as this will be determined during the validation. This distinction is of great importance. For example, the simplest model resulting in an air change rate equal to 0.5 h<sup>-1</sup> will in any case be very insensitive to input errors. It is not more accurate however, than other model.
- As already noticed, the change of uncertainty of the simple model, as a function of the wind speed, is very different from one model to another.
- The nodal models (AIDA, TURBUL) have their uncertainty increasing with the wind speed.
- The LBL model has a maximum uncertainty for a wind speed of 3 [m/s], when the wind effect dominates stack effects. BREVENT has the opposite behaviour, presenting the least uncertainty at equilibrium. This is the consequence of two indices (wind exposure and terrain) whose minimum inaccuracy (+/-1) each results in a 10% inaccuracy in the output.
- A trend of convergence of the output uncertainty can be observed when the wind increases, indicating a larger homogeneity between models in wind dominated situations.

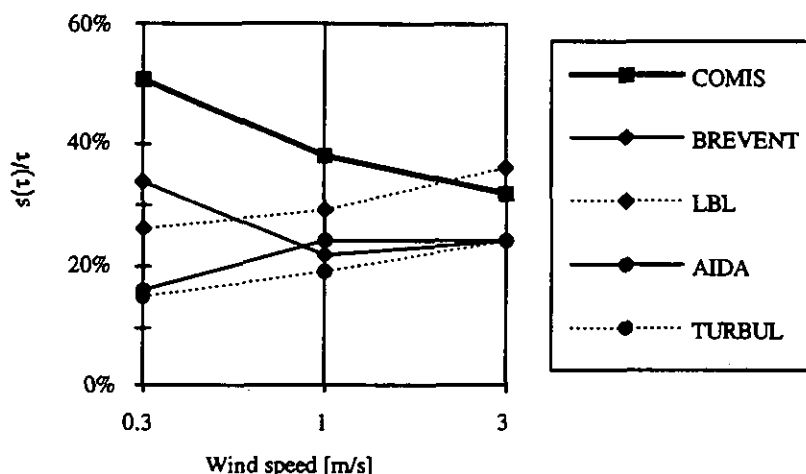


Figure 3.11 - Comparison of the variation of uncertainty of mean age of air  $\tau$  as a function of the wind speed for the considered models.

### Conclusion

The purpose of the test was to compare the sensitivity to the uncertainty in input of different models; the observed output parameter is the mean age of the air and a six zone building was used to perform the test. The same order of magnitude was found for the inaccuracy ratio of the simple models and the detailed model when a uniform inaccuracy range for all the input parameters is used.

When the variation ranges have been chosen not uniformly but in accordance with their respective experimental accuracy, the uncertainty shown by the detailed model is larger than the uncertainty shown by the simple models. A trend of convergence of the output uncertainty is found when the wind increases; This convergence indicates a larger homogeneity in the uncertainty between models in wind dominated situations.

### 3.3.6 Test for smoke control

This work exposes a comparison of the results obtained with two computer programs ASCOS and COMIS that respectively simulate the smoke and the air flows in multizone buildings; both of them represent the building with a unidirectional fluid network and they simulate steady state conditions.

The purpose of the work is to check the possibility of using COMIS, initially studied only for the air movement, for smoke propagation as well and to understand its limit in the applicability. The comparison between the COMIS and ASCOS models was proposed because the same principles are used to simulate the movement of air and smoke in a network (cf. 3.5).

#### Methodological approach for the comparison

The similarities between COMIS and ASCOS have been found by testing four significant cases in order to understand which are the main variables influencing and causing the flow and how the programs treat them. For every case these variables are:

the thermal gradient;

the wind influence: with differences in the velocity and in the wind exponent.

The selection regarding the test cases was made by first considering simple cases using analytical solutions to check the results (see 2.2.3). In this way, the correct use of the two programs was controlled first and more complex cases were considered afterwards. Two different evaluations have been made for every case:

1. change of the thermal gradient between outside and inside without wind;
2. change of wind velocity (from 1 to 9 m/s) and of wind exponent (from 0.16 to 0.40) without thermal gradient.

For the first evaluation the temperature difference,  $\Delta T$ , for a building with  $N$  zones, each of volume  $V_i$  and a *SHAFT*, is calculated with the following method:

$$T_{mean,zones} = \frac{\sum T_{int,i} \cdot V_i}{\sum V_i}; \quad i \neq \text{SHAFT}$$

$$T_{mean,SHAFT} = \frac{T_{top,shaft} + T_{bottom,shaft}}{2}$$

$$T_{mean,SHAFT} = T_{mean,zones}$$

$$\Delta T = \frac{T_{est} + T_{mean,zones}}{2}$$

The total mass flow exchanged between inside and outside,  $G$ , calculated with the two programs is compared. For each case, the relative difference:

$$\delta = \frac{G_{COMIS} - G_{ASCOS}}{G_{ASCOS}} \cdot 100.$$

estimates the difference in percent between the results.

### Test cases and results

The test cases were chosen, starting with simple ones, to have really clear phenomena and then increasingly complex ones to get closer to reality.

#### CASE A: single zone

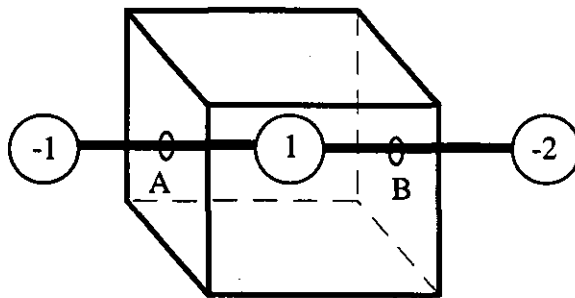


Figure 3.12 - COMIS network for case A

CASE AI) in this sub-set of test cases the thermal gradient between outside and inside was changed and no wind was considered. The test was passed and no mass flow was found.

The files referring to these test can be found in AIS in the directory: ANALYTIC.EVA\POLITEC\COMASCOS\CASE\_A

The structure of the name of the files is: 1AC-NTTT.EXT. Where  $N$  is the name of the program (C for COMIS and A for ASCOS),  $TTT$  is

the temperature difference between inside and outside and  $EXT$  is equal to CIF, COF, DAT or OUT respectively for COMIS input, COMIS output and ASCOS input, ASCOS output files.

CASE AII) in this sub-set of test cases the change of wind velocity (from 1 to 9 m/s) and wind exponent (from 0.16 to 0.40) was taken into account and no thermal gradient was considered. The main data used in this sub-set are the same used for the analytical evaluation and illustrated in Table 2.3; the results are shown in Table 3.16. The files referring to these tests can be found in AIS in the directory: ANALYTIC.EVA\POLITEC\COMASCOS\CASE\_A

The structure of the name of the files is: 1AC-NVEE.EXT. Where  $N$  is the name of the program (C for COMIS and A for ASCOS),  $VEE$  is: V the wind velocity (if there is 0, then all the velocities are considered) and  $EE$  represents the wind exponent at the Meteo Station;  $EXT$  is

equal to CIF, COF or OUT respectively for COMIS input, COMIS output and ASCOS input, ASCOS output files.

Table 3.16 - Results for test All

Wind Velocity	$\delta$ [%]				
	Wind exponent 0.16	Wind exponent 0.22	Wind exponent 0.28	Wind exponent 0.34	Wind exponent 0.40
1	-0.28	-0.26	-0.29	-0.29	-0.29
3	-0.28	-0.28	-0.28	-0.27	-0.25
5	-0.28	-0.29	-0.27	-0.27	-0.28
7	-0.28	-0.27	-0.28	-0.27	-0.28
9	-0.29	-0.28	-0.27	-0.28	-0.27

CASE B: two connected zones on different levels to consider the stack-effect

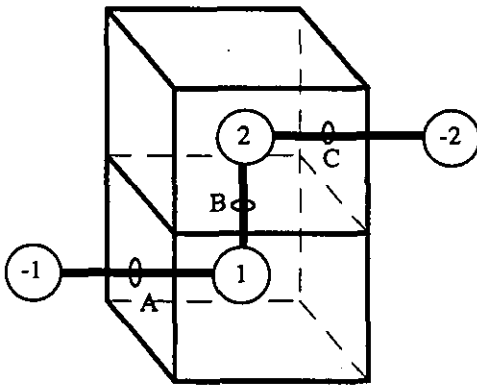


Figure 3.13 - COMIS network for case B

Table 3.17 - Results for test BI

DT	$\delta$
	%
10	-0.72
50	-0.32
80	-0.26
100	-0.25
130	-0.21
160	-0.20
200	-0.17

CASE BI) in this sub-set of test cases the thermal gradient between outside and inside was changed and no wind was considered. The main data used in this sub-set are the same used for the analytical evaluation and illustrated in Table 2.5; the results are shown in Table 3.17.

The files referring to these tests can be found in AIS in the directory: ANALYTIC.EVA\POLITEC\COMASCOS\CASE\_B. The structure of the name of the files is: 2AC-NTTT.EXT (see case AI)

CASE BII) in this sub-set of test cases, wind velocity (from 1 to 9 m/s) and wind exponent (from 0.16 to 0.40) were changed and no thermal gradient was considered. The main data used in this sub-set are the same used for the analytical evaluation and illustrated in Table 2.7; the results are shown in Table 2.7; the files referring to these tests can be found in AIS in the directory: ANALYTIC.EVA\POLITEC\COMASCOS\CASE\_B. The structure of the name of the files is: 2AC-NVEE.EXT.(see case AII)

Table 3.18.

The files referring to these tests can be found in AIS in the directory: ANALYTIC.EVA\POLITEC\COMASCOS\CASE\_B. The structure of the name of the files is: 2AC-NVEE.EXT.(see case AII)

Table 3.18 - Results for test B11

Wind Velocity	$\delta$ [%]				
	Wind exponent 0.16	Wind exponent 0.22	Wind exponent 0.28	Wind exponent 0.34	Wind exponent 0.40
1	0.66	0.92	1.11	1.38	1.68
3	-0.15	-0.11	-0.10	-0.06	-0.02
5	-0.23	-0.22	-0.21	-0.21	-0.19
7	-0.25	-0.25	-0.25	-0.23	-0.23
9	-0.24	-0.26	-0.25	-0.25	-0.25

CASE C: two zones on different levels connected with the shaft

CASE CI) in this sub-set of test cases the thermal gradient between outside and inside was changed and no wind was considered. The main data used in this sub-set are illustrated in Table 3.19; the results are shown in Figure 3.18.

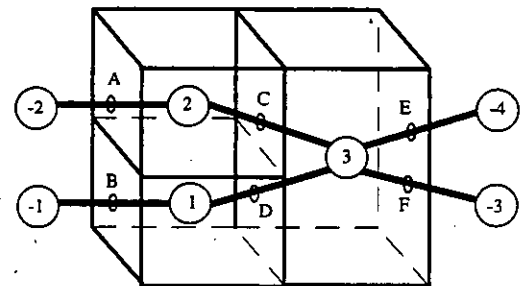


Figure 3.14 - COMIS network for case C

Table 3.19 - Main data used for tests CI

network	node 1: $T_{1int} = 41 - 61 - 91 - 131 - 161 - 211 - 231^{\circ}\text{C}$ ; volume = $45 \text{ m}^3$ node 2: $T_{2int} = 21 - 41 - 71 - 111 - 141 - 191 - 211^{\circ}\text{C}$ ; volume = $45 \text{ m}^3$ node 3: $T_{3int} = 31 - 51 - 81 - 121 - 151 - 201 - 221^{\circ}\text{C}$ ; volume = $90 \text{ m}^3$ link A, B, C, D, E and F: $C_s = 0.0072062 \text{ kg/s}@1\text{Pa}$ ; $n = 0.5$ ; length = 1 m; height link A = height link C = height link E = 4.5 m; height link B = height link D = height link F = 1.5 m; wall properties: thickness = 0.1 m and $U$ -value = $5.174 \text{ W/m}^2 \text{ K}$ ;
external data	Test = $21^{\circ}\text{C}$ ; Rel. humidity = 0 %
$C_p$ value: (reference height = 10 m)	$C_p$ link A = $C_p$ link B = 0.7; $C_p$ link E = $C_p$ link F = -0.7; ( $C_p$ value is calculated with the formula in Table 3.30.)
wind vel. at ref. height:	0 m/s at 10 m
wind direction:	0 deg.
altitude meteo station:	0 m
barometer abs. pressure:	101325 Pa.

The files referring to these tests can be found in AIS in the directory: ANALYTIC.EVA\POLITEC\COMASCOS\CASE\_C. The structure of the name of the files is: 3AC-NTTT.EXT.(see case AI).

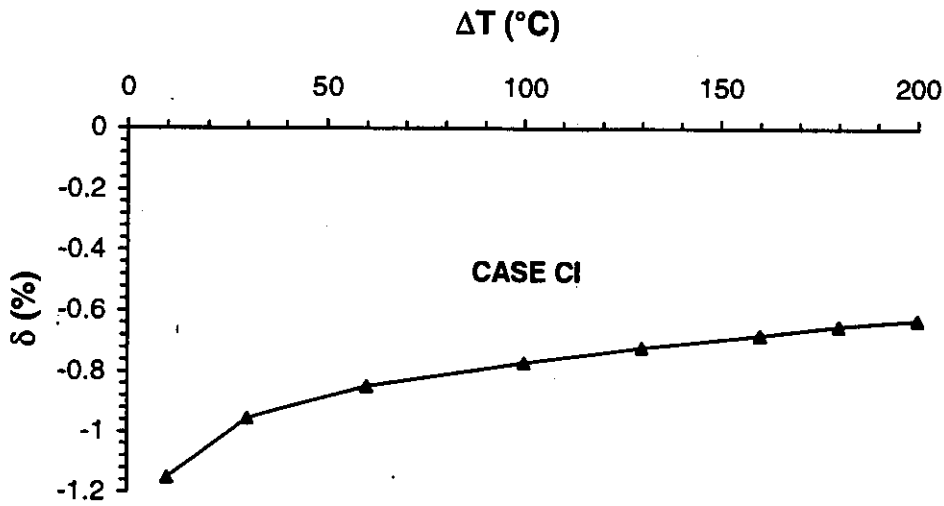


Figure 3.15 - Results for test CI

**CASE CII**) in this sub-set of test cases the change of the wind velocity (from 1 to 9 m/s) and of the wind exponent (from 0.16 to 0.40) was taken into account and no thermal gradient was considered. The main data used in this sub-set are illustrated in Table 3.20; the results are shown in Table 3.21. The files referring to these tests can be found in AIS in the directory: ANALYTIC.EVA\POLITEC\COMASCOS\CASE\_C. The structure of the name of the files is: 3AC-NVEE.EXT. (see case AII)

Table 3.20 - Main data used for tests CII

network	node 1: $T_{1int} = 21\text{ }^{\circ}\text{C}$ ; volume = $45\text{ m}^3$ ; node 2: $T_{2int} = 21\text{ }^{\circ}\text{C}$ ; volume = $45\text{ m}^3$ ; node 3: $T_{3int} = 21\text{ }^{\circ}\text{C}$ ; volume = $90\text{ m}^3$ ; link A, B, C, D, E and F: $C_s = 0.0072062\text{ kg/s@1Pa}$ ; $n = 0.5$ ; length = 1 m; height link A = height link C = height link E = 4.5 m; height link B = height link D = height link F = 1.5 m; wall properties: thickness = 0.1 m and $U$ -value = $5.174\text{ W/m}^2\text{ K}$ ;
external data	$T_{test} = 21\text{ }^{\circ}\text{C}$ ; Rel. humidity = 0 %
$C_p$ value (reference height = 10 m)	$C_p$ link A = $C_p$ link B = 0.7; $C_p$ link E = $C_p$ link F = -0.7; ( $C_p$ value is calculated with the formula in Table 3.30)
wind vel. at ref. height:	1 - 3 - 5 - 7 - 9 m/s at 10 m
wind profile exp. at Meteo Station	0.16 - 0.22 - 0.28 - 0.34 - 0.40
wind velocity profile exp.	0.16 - 0.22 - 0.28 - 0.34 - 0.40
wind direction	0 deg.
altitude meteo station	0 m
barometer abs. pressure	101325 Pa

Table 3.21 - Results for test CII

Wind Velocity	$\delta$ [%]				
	Wind exponent 0.16	Wind exponent 0.22	Wind exponent 0.28	Wind exponent 0.34	Wind exponent 0.40
1	-0.25	-0.22	-0.24	-0.18	-0.16
3	-0.27	-0.26	-0.27	-0.27	-0.27
5	-0.28	-0.27	-0.28	-0.27	-0.26
7	-0.28	-0.28	-0.27	-0.27	-0.27
9	-0.26	-0.25	-0.25	-0.28	-0.27

CASE D: fifteen zones on different levels connected with the shaft

CASE DI) in this sub-set of test cases the thermal gradient between outside and inside was changed and no wind was considered. The main data used in this sub-set are illustrated in Table 3.22; the results are shown in Figure 3.17

The files referring to these tests can be found in AIS in the directory: ANALYTIC.EVA\POLITEC\COMASCOS\CASE\_D. The structure of the name of the files is: 4AC-NTTT.EXT. (see case AI)

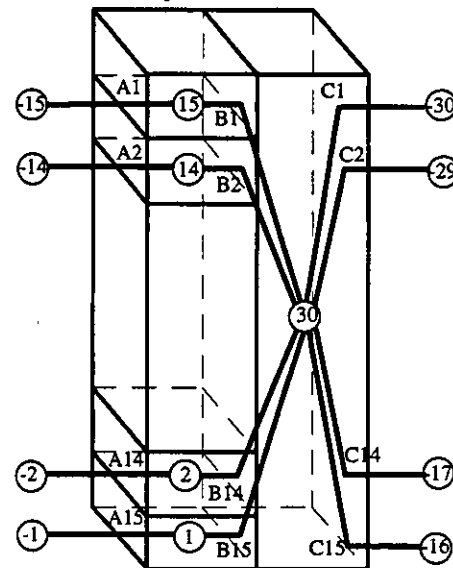


Figure 3.16 - COMIS network for case D

Table 3.22 - Main data used for tests DI

network	node 1: $T_{1int} = 80 - 100 - 120 - 140 - 160 - 156 - 176 - 196$ °C; node 2: $T_{2int} = 50 - 62.5 - 75 - 87.5 - 100 - 127 - 144.5 - 162$ °C; node 3: $T_{3int} = 20 - 25 - 30 - 35 - 40 - 98 - 113 - 128$ °C; node 4: $T_{4int} = 20 - 20 - 20 - 20 - 20 - 69 - 81.5 - 94$ °C; node 5: $T_{5int} = 20 - 20 - 20 - 20 - 20 - 40 - 50 - 60$ °C; node 6: $T_{6int} = 20 - 20 - 20 - 20 - 20 - 20 - 20 - 20$ °C; the volume of all internal nodes from 1 to 15 is $45 \text{ m}^3$ ; internal nodes 6 to 15 are at $20^\circ\text{C}$ ); node 30 (shaft) mean value: $T_{30int} = 26 - 28.5 - 31 - 33.5 - 36 - 46 - 51 - 56^\circ\text{C}$ ; volume = $675 \text{ m}^3$ ; (the top temperature for the shaft is always $20^\circ\text{C}$ ); link Ax, Bx and Cx (with: $1 \leq x \leq 15$ ): $C_s = 0.0072062 \text{ kg/s@1Pa}$ ; $n = 0.5$ ; length = 1 m; height link Ax = height link Bx = height link Cx = $43.5 - [3 \cdot (x-1)]$ m; wall properties: thickness = 0.1 m and $U$ -value = $5.174 \text{ W/m}^2 \text{ K}$ ;
external data	$Test = 21^\circ\text{C}$ ; Rel. humidity = 0 %, no wind, 101325 Pa.
$C_p$ value: ref. Height = 10 m	$C_p$ link Ax = 0.7; $C_p$ link Cx = -0.7; ( $C_p$ value is calculated with the formula in Table 3.30)

**CASE DII** in this sub-set of test cases, the wind velocity (from 1 to 9 m/s) and wind exponent (from 0.16 to 0.40) were changed and no thermal gradient was considered. The main data used in this sub-set are illustrated in Table 3.23; the results are shown in Table 3.24 and in Figure 3.18.

The files referring to these tests can be found in AIS in the directory: ANALYTIC.EVA\POLITEC\COMASCOS\CASE\_D. The structure of the name of the files is: 4AC-WVEE.EXT. (see case AII)

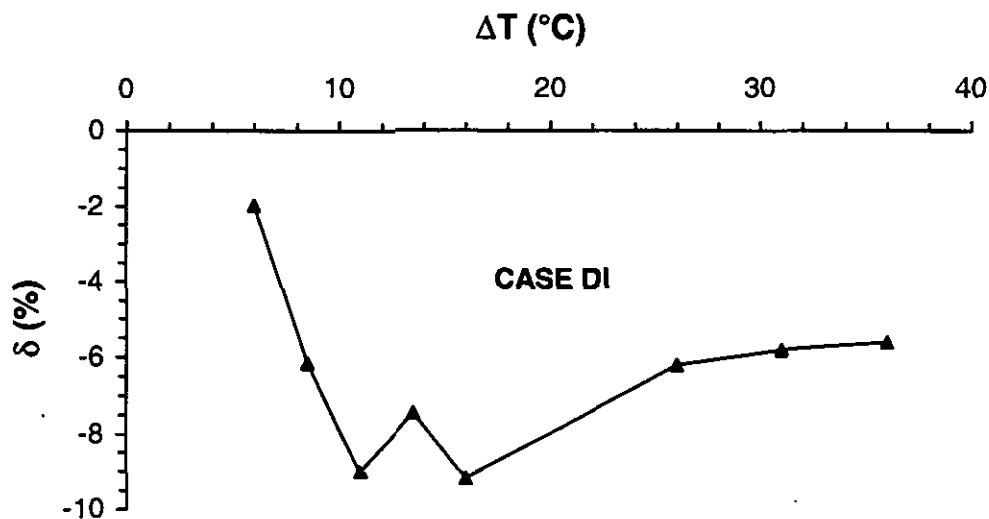


Figure 3.17 - Results for test D1

Table 3.23 - Main data used for tests DII

network	for all the internal nodes: $T_{int} = 21$ °C; volume of all internal nodes from 1 to 15 = $45$ m <sup>3</sup> ; node 30 volume = $675$ m <sup>3</sup> ; link Ax, Bx and Cx (with: $1 \leq x \leq 15$ ): $C_s = 0.0072062$ kg/s@1Pa; $n = 0.5$ ; length = 1 m; height link Ax = height link Bx = height link Cx = $43.5 - [3 \cdot (x-1)]$ ; wall properties: thickness = 0.1 m and $U$ -value = $5.174$ W/m <sup>2</sup> K;
external data	$T_{test} = 21$ °C; Rel. humidity = 0 %
$C_p$ value	$C_p$ link Ax = 0.7; $C_p$ link Cx = -0.7; ( $C_p$ value is calculated with the formula in Table 3.30.)
ref. height for $C_p$ :	10 m
wind vel. at ref. height:	1 - 3 - 5 - 7 - 9 m/s
ref. height for wind speed	10 m
wind profile exp. at meteo station	0.16 - 0.22 - 0.28 - 0.34 - 0.40
wind velocity profile exp.	0.16 - 0.22 - 0.28 - 0.34 - 0.40
wind direction	0 deg.
altitude meteo station	0 m
barometer abs. pressure	101325 Pa

Table 3.24 - Results for test DII

Wind Velocity	$\delta$ [%]				
	Wind exponent 0.16	Wind exponent 0.22	Wind exponent 0.28	Wind exponent 0.34	Wind exponent 0.40
1	0.08	0.71	1.86	2.72	3.35
3	-0.25	-0.20	1.50	2.39	2.88
5	-0.28	-0.29	1.44	2.38	2.81
7	-0.27	-0.27	1.47	2.33	2.85
9	-0.27	-0.27	1.44	2.34	2.83

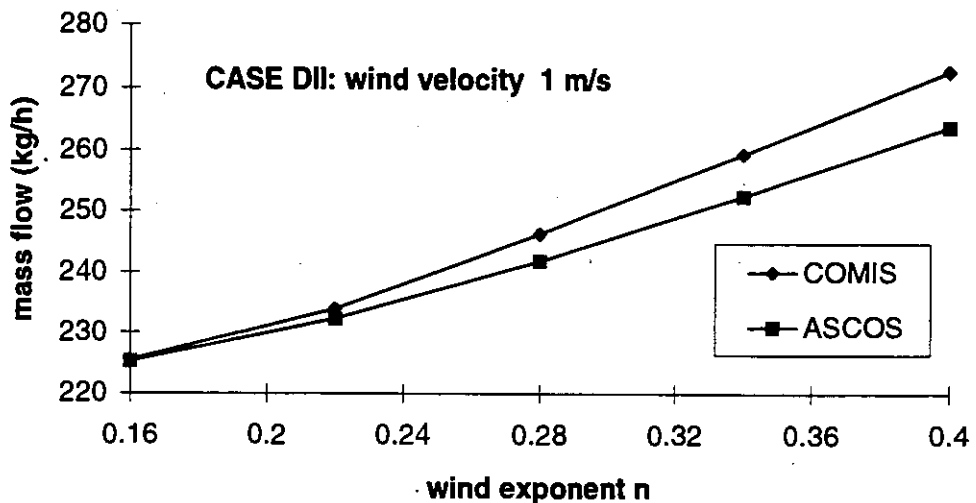


Figure 3.18 - Results for case DII, wind velocity equal to 1 m/s

### Conclusion

The focus of this comparison was to examine the possibility of a further application of the COMIS program: the ability of COMIS to predict smoke spreading in case of fire in a building. Wind speed, thermal gradients from outside and inside and building size with and without elevator and stairs shafts are the main parameters whose values were changed during this comparison.

The relative differences found between the total flow calculated by ASCOS and COMIS are always below 10%. Therefore, it is possible to stress that COMIS can be used for the smoke movement prediction as well as ASCOS, which is a code made especially for that purpose. Since ASCOS does not predict smoke concentration, comparisons on that parameter was not possible.

### 3.4 Conclusion from the inter-model comparison

In this chapter a lot of tests about inter-model comparison, prepared and documented in the frame of the evaluation task of Annex 23, have been illustrated; Table 3.25 summarises the models used for the comparison of each topic tested.

As the tests were conceived for testing defined topics, more interesting information can be obtained by separately analysing the results obtained for each topic (see the conclusion in each paragraph).

The overall analysis of the results given in this chapter show that a good agreement is found between COMIS results and the results of the other models; that is COMIS is able to predict the air flow behaviour as well or as badly as other models which are often developed for defined topics (e.g. smoke control).

Table 3.25 - Summary of the models used in the inter-model comparison

Model	Result Comparison (Aivc)	Large opening (Athens University)	User test 1 (BBRi)	Mass flow equation (Concordia University)	Sensitivity to uncertainty in input data (Leso)	Smoke propagation (Politecnico di Torino)
AIDA					X	
AIRNET		X		X		
ASCOS						X
BREEZE	X	X				
BREVENT					X	
CBSAIR				X		
CONTAM93/94	X			X		
ESP		X	X			
LBL model					X	
MZAP	X					
NORMA		X				
PASSPORT		X				
TURBUL					X	
VENCON			X			

The results detailed in the paragraphs entitled "Comparison of the results using the same sets of input data", "User Test 1" and "Mass flow Equations", show that no differences are found among the results of the models if the same data are correctly applied to each model.

The prediction of the flow for a large vertical opening, in the single side natural ventilation case, has been performed using six different air flow models and the agreements among the results obtained from these six models is very good; the correlation coefficient are greater than 0.95 except for the results obtained using NORMA.

Two special investigations were also performed; the first examined sensitivity to the uncertainty of the input data and it was shown that an increase in the complexity of the input data corresponded to an increase in the uncertainty range in the results; secondly, an investigation devoted to the understanding of smoke control in a building revealed that COMIS is suited to this purpose equally as well as ASCOS, which is a computer program especially developed especially for the smoke control simulation.

### 3.5 Algorithms for some of the air flow models used in 3.2

#### AIDA

This model is based on the conservation of the mass of air in the indoor zone:

$$Q_{tot} = \sum_j C_j (\Delta p_j)^{n_j} = 0 \quad (3.8)$$

with:

$Q_{tot}$	:	total infiltration rate, [ $\text{m}^3 \text{s}^{-1}$ ]
$C_j$	:	air tightness coefficient of crack $j$ , [ $\text{m}^3 \text{s}^{-1} \text{Pa}^{-n}$ ]
$n_j$	:	exponent of crack $j$ , [-]
$\Delta p_j$	:	pressure difference through crack $j$ , [Pa]

The pressure  $p_w$  induced by the wind on the surfaces and the pressure  $p_s$  induced by the stack are given by the following equations:

$$p_w(j) = \frac{\rho v^2}{2 C_p(j)} \quad (3.9)$$

$$p_s(j) = -\rho_0 \cdot g \cdot 273 \cdot h(j) \cdot \left( \frac{1}{T_{ex}} - \frac{1}{T_{in}} \right) \quad (3.10)$$

with:

$\rho$	:	outdoor air density [ $\text{kg m}^{-3}$ ]
$\rho_0$	:	air density at 273 K [ $\text{kg m}^{-3}$ ]
$C_p(j)$	:	pressure coefficient of crack $j$ , [ $\text{m}^3 \text{s}^{-1}$ ]
$v$	:	wind speed at the roof height, [ $\text{m s}^{-1}$ ]
$h(j)$	:	vertical position of the crack $j$ , [m]
$T_{ex}$	:	outdoor temperature, [K]
$T_{in}$	:	indoor temperature, [K]
$g$	:	gravitation, [ $\text{ms}^{-2}$ ]

The flow balance equation is solved using a combination of 'bi-section' and 'addition'. This algorithm is known for its slow convergence but is programmable on a pocket calculator.

#### BREvent

The model is based on the following basic assumptions [Awbi,1991]:

- Uniform distribution of air tightness on the external surfaces, and identical exponent  $n$  for all the cracks.
- Partition walls and solid floors are assumed to be impermeable.
- If the under floor space is ventilated, its surface pressure is obtained by determining the area-weighted mean of the pressures of the exposed walls.
- The volume of the building for infiltration purposes is represented by a rectangular parallelepiped of height  $h$ .
- The pressure generated by the wind is assumed to be uniform across each face of the building and the pressure coefficients have been chosen according to the British code of practice [BS, 1972].

These assumptions result in three equations giving the total infiltration  $Q_{tot}$ , the wind induced infiltration  $Q_w$  and the stack induced infiltration  $Q_s$ .

$$Q_{tot} = Q_p \left( \rho_{ex} v^2 / \Delta P_p \right)^n F_t(Ar, \theta) \quad (3.11)$$

$$Q_w = Q_p \left( \rho_{ex} v^2 / \Delta P_p \right)^n F_w(\theta) \quad (3.12)$$

$$Q_s = Q_p \left( \Delta T \rho_{ex} g h / \Delta P_p \right)^n F_s \quad (3.13)$$

- with  $Ar$  : Archimedes number ( $= \Delta T g h / (T_{in} v^2)$ ), [-]  
 $F_t(Ar, \theta)$  : total infiltration function of Archimedes number  $Ar$  and wind dir.  $\theta$ , [-]  
 $F_w(\theta)$  : wind induced infiltration function, [-]  
 $F_s$  : stack induced infiltration function, [-]  
 $h$  : height of the ventilated space, [m]  
 $n$  : leakage exponent  
 $Q_{tot}$  : air infiltration rate due to wind and buoyancy effects, [ $m^3 s^{-1}$ ]  
 $Q_p$  : air flow rate obtained during a pressurisation test at an arbitrarily chosen reference pressure  $\Delta P_p$ , [ $m^3 s^{-1}$ ]  
 $Q_s$  : air infiltration rate due to buoyancy effect, [ $m^3 s^{-1}$ ]  
 $Q_w$  : air infiltration rate due to wind effect, [ $m^3 s^{-1}$ ]  
 $T_{in}$  : indoor temperature, [ $^{\circ}K$ ]  
 $v$  : wind speed at roof ridge height, [ $m s^{-1}$ ]  
 $\Delta T$  : internal-external temperature difference, [ $^{\circ}K$ ]  
 $\Delta P_p$  : internal-external pressure difference for pressurisation test, [Pa]  
 $\rho_{ex}$  : density of external air, [ $Kg m^{-3}$ ]  
 $\theta$  : wind direction which determines the pressure distribution over the building surfaces, [deg]  
 $g$  : gravitation,  $9.81 [m s^{-2}]$

The function  $F_t(Ar, q)$  is defined as following:

$$F_t(Ar, \theta) = 1/2 \left\{ 1/2 Ar^{(n+1)} \sum_i \left( Q_{pi} / Q_p (\Delta C_{p(i)})^{(n+1)} - (\Delta C_{p(i)} - 2A_r)^{(n+1)} \right) \right. \\ \left. + Q_{pL} / Q_p (\Delta C_{p(L)})^n + Q_{pU} / Q_p (\Delta C_{p(U)})^n \right\} \quad (3.14)$$

- with  $Q_{pi}$  : air flow for the pressure difference  $_P_p$ , obtained during a pressurisation test for the surface  $i$ , [ $m^3 s^{-1}$ ]  
 $Q_{pL}$  : air flow for the pressure difference  $_P_p$ , obtained during a pressurisation test for the roof, [ $m^3 s^{-1}$ ]  
 $Q_{pU}$  : air flow for the pressure difference  $_P_p$ , obtained during a pressurisation test for the underground [ $m^3 s^{-1}$ ]  
 $\Delta C_{p(i)}$  : difference ( $C_p(i) - C_p(Int)$ ) between outdoor and indoor pressure coefficients, indices  $L$  and  $U$  refers to the roof and the underground respectively, [-]

Functions  $F_w(q)$  and  $F_s$  correspond to no temperature difference and no wind respectively. Warren et Webb [1980] propose some values for detached, semi-detached and centre terrace houses. Moreover, the authors propose for the calculation of the effective air flow either to choose the largest of both air flow  $Q_w$  and  $Q_s$ , or to use the following relation to calculate  $F_t$ :

$$F_t(Ar, \theta) = (F_s \times (Ar)^n)^2 + (F_w)^{2,1/2} \quad (3.15)$$

 Table 3.26 -  $F_w(q)$  and  $F_s$  for different types of buildings [Awbi, 1991]

Building	exponent $n$	$F_s$	$F_w$ wind 0°	$F_w$ wind 90°	$F_w$ wind 270°
Detached	0.5	0.26	0.17	0.20	-
	0.6	0.23	0.15	0.18	-
	0.7	0.20	0.13	0.16	-
Semi de- tached	0.5	0.26	0.16	0.18	0.12
	0.6	0.23	0.15	0.16	0.10
	0.7	0.20	0.14	0.15	0.08
Centre terrace	0.5	0.26	0.20	0.13	-
	0.6	0.23	0.18	0.10	-
	0.7	0.20	0.16	0.08	-

### The LBL model

The relation between the equivalent leakage area and the air tightness coefficients  $C$  and  $n$  is the following [Sherman & Grimsrud, 1980]:

$$A_0 = \frac{C(\Delta P_{ref})^n}{\sqrt{\frac{2\Delta P_{ref}}{\rho}}} \quad (3.16)$$

- with  $A_0$  : equivalent leakage area, [m<sup>2</sup>]  
 $C$  : air tightness coefficient, [m<sup>3</sup> s<sup>-1</sup> Pa<sup>-n</sup>]  
 $n$  : exponent, [-]  
 $\Delta P_{ref}$  : reference pressure area, usually 4 [Pa]  
 $\rho$  : air density, [kg m<sup>-3</sup>]

The expressions for the air flow rate  $Q_w$  induced by the wind and  $Q_s$  induced by the stack are the following:

$$Q_w = A_0 v_{st} f_w \quad (3.17)$$

$$f_w = B_{sh} \sqrt[3]{(1-R) \cdot \frac{\alpha_b \cdot (h_b/10)^{\gamma_b}}{\alpha_{st} (h_{st}/10)^{\gamma_{st}}}} \quad (3.18)$$

$$Q_s = A_0 \sqrt{\Delta T} f_s \quad (3.19)$$

$$f_s = \frac{(2+R)}{6} \left[ 1 - \frac{x^2}{(2-R)^2} \right] \sqrt{\frac{gh_b}{T_{in}}} \quad (3.20)$$

- with  $A_0$  : total equivalent leakage area, [m<sup>2</sup>]  
 $A_L$  : equivalent leakage area of the roof, [m<sup>2</sup>]

$A_U$	: equivalent leakage area for the ground, [m <sup>2</sup> ]
$B_{sh}$	: shielding coefficient (Table 3.28)
$R$	: horizontal area ratio, $(A_L + A_U)/A_o$
$X$	: vertical area ratio, $(A_L - A_U)/A_o$
$h_b$	: building height, [m]
$h_{st}$	: wind reference height, [m]
$\alpha_b, \gamma_b$	: coefficients of the wind profile near the building (Table 3.27)
$\alpha_{st}, \gamma_{st}$	: coefficients of the wind profile near the meteo station (Table 3.27)
$T_{in}$	: indoor temperature, [K]
$\Delta T$	: indoor outdoor temperature difference, [K]
$v_{st}$	: wind speed measured at the nearest meteo station, [ms <sup>-1</sup> ]
$g$	: gravitation, 9.81 [m s <sup>-2</sup> ]

This model takes into account a wind speed correction (coefficients  $\alpha, \gamma$  in Table 3.27) when the wind speed is measured at a separate location from the building. The model also takes into account the wind exposure by mean of the shielding coefficient  $B_{sh}$  (Table 3.28) in accordance with the protection provided by trees and buildings in the surrounding area.

The conjunction of flow rates is calculated through Equation 3.17:

$$Q_{tot} = \sqrt{(Q_s)^2 + (Q_w)^2} \quad (3.21)$$

with  $Q_{tot}$  : total flow rate, [m<sup>3</sup> s<sup>-1</sup>]

Table 3.27 Terrain parameters for the calculation of wind profile [Awbi, 1991].

Class	Description	$\gamma$	$\alpha$
1	Ocean or other body of water with at least 5 km of unrestricted expanse	0.10	1.30
2	Flat terrain with some isolated obstacles, e.g. buildings or trees well separated from each other	0.15	1.00
3	Rural area with low buildings, trees, etc.	0.20	0.85
4	Urban, industrial or forest areas	0.25	0.67
5	Centre of large city	0.35	0.47

Table 3.28 - Generalised shielding coefficients for the LBL model [Awbi, 1991].

Class	Description	$B_{sh}$
I	No obstruction	0.34
II	Light local shielding with few obstructions	0.30
III	Moderate local shielding, some obstructions within two house heights	0.25
IV	Heavy shielding, obstructions around most perimeter	0.19
V	Very heavy shielding, large obstruction surrounding perimeter within two house heights	0.11

**TURBUL**

Inside a permeable zone, the pressure  $p(t)$  can be modelled by the following non-linear differential equation of the first order (the thermodynamic properties of air are modelled by the polytropic equation  $p = \rho^\gamma$ ):

$$\dot{p}(t) = \frac{\gamma}{V} p(t) \sum_i Q_i(\Delta P_i(t)) \quad (3.22)$$

with:

- $p(t)$  : indoor pressure, [Pa]
- $\dot{p}(t)$  : time derivative of the indoor pressure, [Pa s<sup>-1</sup>]
- $\Delta P_i(t)$  : pressure difference through the crack  $i$ , [Pa]
- $V$  : zone volume, [m<sup>3</sup>]
- $\gamma$  : polytropic exponent ( $1 \leq \gamma \leq 1.4$ )

The pressure difference through the crack  $i$  results from wind and thermal buoyancy:

$$\Delta P_i(t) = \frac{1}{2} \rho v^2 C_p(i) + \frac{\Delta T \cdot g \cdot h_i}{T_{in}} - p(t) \quad (3.23)$$

The flow rate through the leak can be modelled either by the power law (eq.3.17), or by the quadratic law (eq.3.17) [Etheridge,1988]:

$$Q_i(t) = C_i (\Delta P_i(t))^{n_i} \quad (3.24)$$

$$Q_i(t) = \frac{\Delta P_i(t)}{|\Delta P_i(t)|} \left( \sqrt{\frac{b_i^2}{4a_i^2} + \frac{|\Delta P_i(t)|}{a_i}} - \frac{b_i}{2a_i} \right) \quad (3.25)$$

with:

- $Q_i(t)$  : flow rate through leak  $i$ , [m<sup>3</sup>]
- $\Delta P_i(t)$  : pressure difference through leak  $i$ , [Pa]
- $C_i, a_i, b_i$ : air tightness coefficients of leak  $i$
- $n_i$  : exponent of leak  $i$

The differential equation is integrated using a forward Euler scheme. It has been shown that this scheme requires a time step  $\Delta t$  smaller than the time constant  $\tau_{RC}$  of the system [Fürbringer,1992]:

$$\Delta t < \tau_{RC} = \frac{V}{\gamma \cdot P_{atm} \cdot C_{tot}} = \frac{V \cdot b_{tot}}{\gamma \cdot P_{atm}} \quad (3.26)$$

- with  $P_{atm}$  : atmospheric pressure, [Pa]
- $C_{tot}$  : power law air tightness coefficient, [m<sup>3</sup> s<sup>-1</sup> Pa<sup>-n</sup>]
- $b_{tot}$  : quadratic air tightness coefficient, [Pa s m<sup>-3</sup>]

The air flow rates are calculated by summing up the entering air flows at each time step.

**Comparison of the equation used by ASCOS and COMIS**

From a comparison of the equations used by the programs that describe the air and smoke movement (mass flow and pressure distribution), it is possible to realise which are the correct relations between the input data (see Table 3.29 and Table 3.30).

*Table 3.29 - Mass flow through cracks equations in COMIS and ASCOS*

Program	Equation: mass flow through cracks	Nomenclature
COMIS	$Q = C_Q \cdot (\Delta P)^n = C_S \cdot K_n \cdot (\Delta P)^n$ $K_n = \left(\frac{\rho_0}{\rho}\right)^{n-1} \cdot \left(\frac{v_0}{v}\right)^{2n-1}$	$n$ : flow exponent (depending on flow regime); $v$ : kinetic viscosity; $\rho$ : density of the smoke in the flow path; $C_S$ : coefficient depending duct's shape; $K_n$ : corrective coefficient for thermal gradient.
ASCOS	$Q = C \cdot A \cdot \sqrt{2 \cdot \rho \cdot \Delta P}$	$C$ : flow coefficient (for smoke analysis is 0,6÷0,7); $A$ : flow area; $\rho$ : density of the smoke in the flow path.
INPUT DATA	$Q = C_Q \cdot \sqrt{\Delta P} = C_S \cdot K_n \cdot \sqrt{\Delta P}$ $C_S = C \cdot A \cdot \sqrt{2 \cdot \rho_0}$ $K_n = \sqrt{\frac{\rho}{\rho_0}}; \quad \rho_0 = \frac{P_0}{R \cdot T_0}$	$n$ : 0.5; $R$ : gas constant; $T_0$ : 293.15 K; $P_0$ : 101325 Pa; $C$ : 0.465; $A$ : 0.01.
NOTES	In COMIS input data, the following data have been used when considering thermal gradients: <ul style="list-style-type: none"> <li>• Crack length = 1 m;</li> <li>• Wall Properties: thickness = 0.1 m and <math>U</math>-Value = 5.174 W/m<sup>2</sup> K.</li> </ul>	

Table 3.30 - Pressure distribution due to wind equations in COMIS and ASCOS

Program	Equation: pressure distribution due to wind	Nomenclature
COMIS	Assuming constant density along a streamline: $P_{stat} + \frac{1}{2} \cdot \rho \cdot \bar{v}^2 = const$ If the wind flow is a function of the roughness of the surface surrounding the building: $\frac{v(z)}{v(z_{ref})} = \left\{ \frac{z}{z_{ref}} \right\}^{\alpha}$ Wind pressure distribution: $Cp_k(z_{ref}, \Phi) = \frac{P_k - P_0(z)}{P_{dyn}(z_{ref})}$ $P_{dyn}(z_{ref}) = \frac{1}{2} \cdot \rho_o \cdot v^2(z_{ref})$	$\rho$ : air density; $\rho_0$ : air density at a reference level; $v$ : wind velocity; $z$ : heights; $\Phi$ : wind direction; $\alpha$ : coefficient depending on the roughness of the solid boundary;
ASCOS	$P_{o(i)} = P_{h(i)} + C_w \cdot P_{w(i)}$ Because the outside temperature is constant: $P_{h(i)} = P_{atm} \cdot e^{\left( \frac{g \cdot h(i)}{R \cdot T_{out}} \right)}$ At height $h$ above the ground level the wind velocity is: $v = v_o \cdot \left( \frac{h}{h_o} \right)^n$ The dynamic pressure at height $h(i)$ is: $P_w = \frac{\rho \cdot v_o^2}{2} \cdot \left( \frac{h(i)}{h_o} \right)^{2n}$	$P_{o(i)}$ : outside gauge pressure at height $h(i)$ above absolute pressure at ground level; $P_{h(i)}$ : hydrostatic pressure difference between $h(i)$ and ground level; $P_{w(i)}$ : dynamic pressure due to the wind at height $h(i)$ ; $C_w$ : pressure coefficient; $P_{atm}$ : absolute barometric pressure at ground level; $T_{out}$ : outside absolute temperature; $v_o$ : wind velocity at height $h_o$ ; $n$ : wind exponent.
INPUT DATA	$P_{o(i)} = P_{h(i)} + C_w \cdot P_{w(i)}$ $P_{h(i)} = P_{atm} \cdot e^{\left( \frac{g \cdot h(i)}{R \cdot T_{ow}} \right)}$ $P_{w(i)} = \frac{\rho \cdot v_o^2}{2} \cdot \left( \frac{h(i)}{h_o} \right)^{2n}; \quad n = \alpha$ $C_w = Cp_{h(i)} \cdot \left( \frac{h_{ref,Cp}}{h(i)} \right)^{2n}$	$P_{o(i)}$ : outside pressure at height $h(i)$ ; $P_{h(i)}$ : hydrostatic pressure difference between $h(i)$ and ground level; $P_{w(i)}$ : dynamic pressure due to the wind at height $h(i)$ ; $C_w$ : pressure coefficient $\pm 0.7$ ; $P_{atm}$ : absolute barometric pressure at ground level = 101325 Pa; $T_{out}$ : outside absolute temperature; $v_o$ : wind velocity at height $h_o$ ; $h_o = h_{ref,meteo} = h_{ref,Cp} = 10$ m; $n = \alpha = \alpha_{meteo}$ : wind exponent.

### 3.6 References

- Awbi H.B.: Ventilation of buildings. *E&FN SPON ed., London, GB, 1991*
- Etheridge D.W., Stanway R.J.: A parametric study of ventilation as a basis for design. *Building and Environment, vol. 23, 1988.*
- Feustel H. et al.: Fundamentals of the Multizone Air flow Model - COMIS. *AIVC TN 29, Coventry, UK, 1990.*
- Fürbringer J.-M., Van Der Maas J.: Suitable algorithms for calculating air renewal rate by pulsating air flow through a single large opening. *Building and Environment, 1995.*
- Fürbringer J.-M.: Sensibilité de modèles et de mesures en aéraulique du bâtiment à l'aide de plans d'expériences, *PhD thesis, EPFL, Lausanne, CH, 1994.*
- Haghighat F., Rao J.: Computer-Aided Building Ventilation System Design - A System theoretic approach, *Energy and Buildings Vol. 1, pp. 147-155, 1991*
- Liddament M.: Air infiltration calculation techniques - an applications guide. *Air Infiltration and Ventilation Centre, Coventry, GB, 1986.*
- Liddament M.: AIDA-an air infiltration development algorithm. *Air infiltration review, vol 11, no1, Dec. 1989.*
- Sherman M., Grimsrud D.T.: Infiltration-pressurisation correlation: simplified physical modelling. *ASHRAE Semi-annual Meeting, Denver, USA, June 1980.*
- Sherman M.: Superposition in infiltration modelling. *Indoor Air, vol 2, 1992.*
- Warren P.R., Webb B.C.: The relationship between tracer gas and pressurisation techniques in dwellings. *Proc 1rst AIVC Conf 'Infiltration Measurement Technique', 1980.*

## 4 EXPERIMENTAL COMPARISON

### 4.1 Introduction

The experimental comparison is the key chapter of Subtask 3. Effectively, following the principle of experimental science, the confrontation with experimental data must certify that COMIS works well, in fact, that it works coherently with what we are able to measure.

As it has already been stated in Chapter 1, the experimental data is not free of errors and their confidence intervals must be considered. The result of a simulation or a measurement is not a single number or a graph but an uncertainty range. Moreover, in the case of significant disagreement between experimental data and corresponding simulated data, different possibilities must be investigated before it can be declared that the numerical model or the measurement is wrong (cf. Table 1.1). For many reasons, data coming from both calculations and measurements contain errors, and the comparison shall take account of these errors. The results will be considered as being in good agreement when their confidence intervals present a large overlap, and in disagreement when their confidence intervals do not overlap. The whole process of comparison, as explained in Chapter 1 and used here, is based on those epistemological principles.

To make things clear at the beginning of this important chapter, it can briefly be said that **the purpose of a comparison between measured data and simulation is to find possible discrepancies and not to show that it works**. Two images of reality are compared (Figure 4.1): an experimental model and a numerical one, and the question being asked is when do they differ and, in this occurrence, why ?

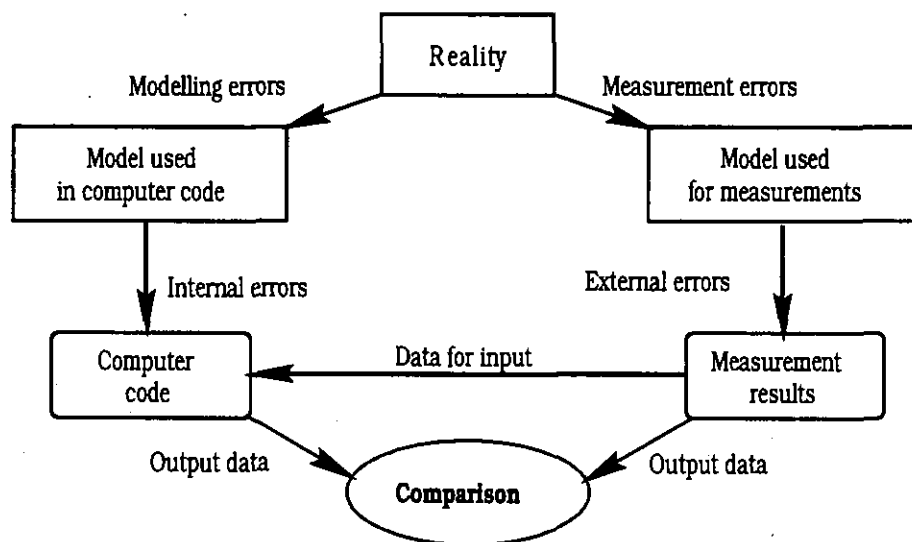
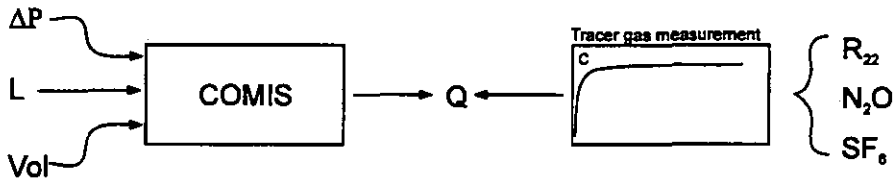


Figure 4.1: Experimental validation is comparing the results of two models of reality.

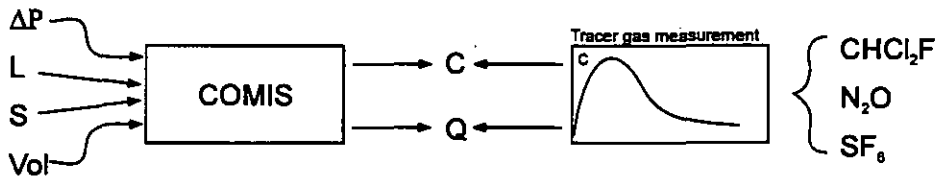
Nine buildings have been investigated in the framework of this annex. Each case is succinctly reported in §4.2 to §4.10 and more extensively in the corresponding appendices A4.2 to A4.10 which are included in the second volume of this report. This choice allows the reader to have a global view of the evaluation of COMIS in this fourth chapter. Those more interested in some particular cases can get more details from the appendix. An introduction to the 9 cases is given below, with a scheme indicating which are the input parameters and the compared data ( $HR$  = humidity,  $L$  = Leakage,  $vol$  = volume,  $S$  = opening, surface,  $C_p$  = pressure coeff.,  $w$  = wind,  $T$  = temperature,  $Q_{fresh}$  = fresh air flow,  $C$  = concentration,  $\Delta P$  = pressure difference)

and Table 4.1 gives their main characteristics and Table 4.2 indicates the features of COMIS used in the test cases.

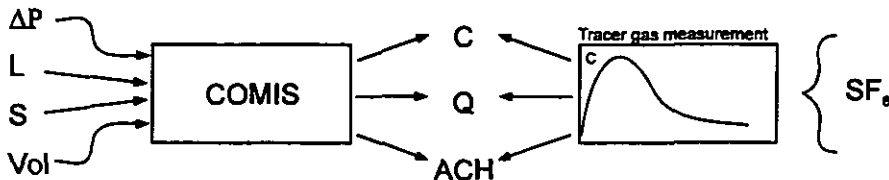
OPTIBAT is an experimental one floor flat, comprising 6 zones. It is built in a large experimental hall at CETHIL of INSA near Lyon. The outdoor environment is controlled: it is not an in situ case. The main interest of the controlled environment is to by-pass the much decried problem of pressure coefficients. Another obviously interesting point is the possibility of imposing the outdoor pressure and temperature conditions. This building is a good candidate for a systematic approach and its situation in a laboratory could allow a 'back and forth' investigation between simulation and measurement. It is also ideally suited for investigating questions concerning multizone ventilation which cannot be answered by in-situ experiments.



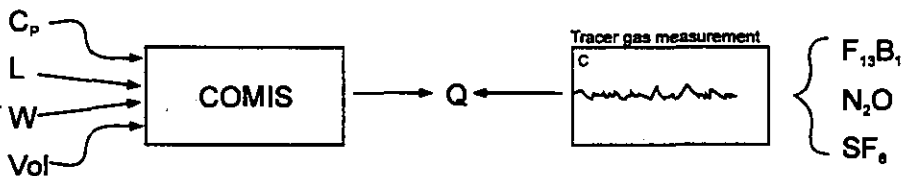
In the Japanese SOLAR HOUSE, the air exchanges between 3 zones on one floor are precisely investigated. The air tightness is well known. The main interest resides in the simplicity of the structure.



The Japanese FAMILY HOUSE has 9 zones distributed over 2 floors. This case represents an important part of the building set. The 2 floors also make it interesting for observing interaction between wind and stack effect. The tracer gas measurement is made by a pulse injection of  $SF_6$  in the living room which is the only room to be heated in this building.

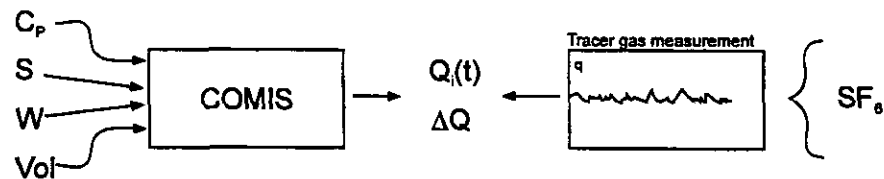


The LESO Building is a 3-storey administrative building. It houses a building physics laboratory and its thermal, as well as its ventilation characteristics, have been investigated for many years. The building is especially well instrumented. The structure of the building is however quite complicated. For the measurements, the 19 rooms are grouped in 11 zones. This case is a good representative of a small office building. Its 3 floors also allow an investigation of the interaction of wind and stack effects. The sensitivity analysis has been especially focused on the problem of the pressure coefficients.

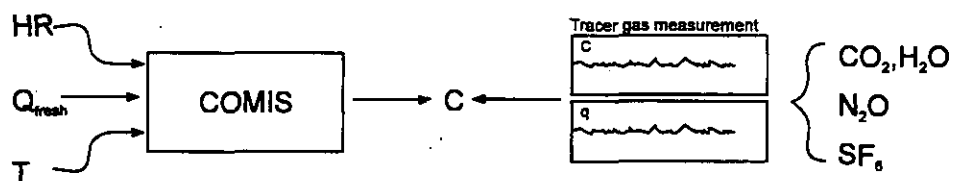


The Belgian and the Greek PASSYS Cells have been investigated by the BBRI and the University of Athens, respectively. The influence of the wind on a large opening was investigated. The experiment is sufficiently simple to be well controlled. The sensitivity analysis has been

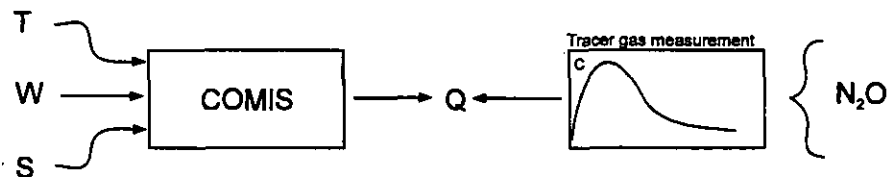
performed very comprehensively including Monte-Carlo technique as well as factorial design for the Belgian case.



The NAMUR FLAT was used for the evaluation of contaminant spreading and also air exchange through large openings. The flat has 7 rooms and is located on the ground floor of a 9-storey building. The sensitivity analysis has also been performed very comprehensively, with the Monte-Carlo technique as well as factorial design. The analysis of the input uncertainty is also exemplary and shows the efficiency of the sophisticated tools developed within this annex.



The so called 'large opening experiment in Greece' case has allowed for an evaluation of the influence of a large opening geometry.



The ITALGAS Building, investigated by the Politecnico di Torino, is a one level family house. Built by a gas company for the investigation of gas heaters, the building is well instrumented. It is a sufficiently simple case to be studied with accuracy, but also sufficiently complex to be representative of real buildings. A large data set was obtained with this facility.

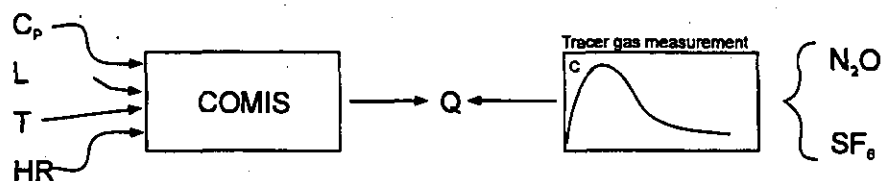


Table 4.1: Main characteristics of the reported cases

Project	OPTIBAT	SOLAR HOUSE	Family house	LESO building
Paragraph	4.2	4.3	4.4	4.5
Appendix	A4.2	A4.3	A4.4	A4.5
Building	flat	little house	Family house	Adm. building
Country	France	Japan	Japan	Switzerland
City	Lyon	Sendai	Sukagawa	Lausanne
Institution	CETHIL, INSA	Tohoku University	Tohoku University	LESO-PB. EPFL
Volume	220 m <sup>3</sup>	83 m <sup>3</sup>	350 m <sup>3</sup>	2165 m <sup>3</sup>
Surface	88 m <sup>2</sup>	40 m <sup>2</sup>	132 m <sup>2</sup>	730 m <sup>2</sup>
Rooms	6	3	8	19
Zones	6	3	9	11
Floors	1	1	2	3
Meteo	-	in situ	in situ	in situ
Season	winter, summer	summer	winter	winter
T <sub>in</sub> -T <sub>out</sub>	21 °C, 0 °C	3 °C : 8 °C	20 °C	16 °C
ΔP	44 Pa : 176 Pa			
Cp	no	no	no	From wind tunnel
Pressure meas.	yes	11 pres. taps	12 press. taps	yes
Wind speed	7 m/s : 20 m/s	.4 m/s : 1.2 m/s	2.3 m/s	0 m/s : 1.5 m/s
n <sub>L50</sub>				
ELA			910 cm <sup>2</sup> @9.8 Pa	
Comparison	8#	15 dt x 3#	180 dt	34 dt x 3#
Time interval		6'	10'	30'
Tracer	IC: N <sub>2</sub> O SF <sub>6</sub> R <sub>22</sub>	CD: N <sub>2</sub> O SF <sub>6</sub> CHCl <sub>2</sub> F	SF <sub>6</sub> pulse in each zone	CC: N <sub>2</sub> O SF <sub>6</sub> F <sub>13</sub> B <sub>1</sub>
Interest	Especially well controlled experiment	Simple network involving 3 interconnected zones	Typical family house	Complex building

Passys cell (B)	Namur flat	Passys cell (G)	Greek L.O. exp.	Italgas building
4.6	4.7	4.8	4.9	4.10
A4.6	A4.7	A4.8	A4.9	A4.10
test cells	flat	test cells	room	family house
Belgium	Belgium	Greece	Greece	Italy
	Namur			Venaria
BBRI	BBRI	Uni. of Athens	Uni. of Athens	Politecnico di Torino
60 m <sup>3</sup>	206 m <sup>3</sup>	66 m <sup>3</sup>	35 m <sup>3</sup>	420 m <sup>3</sup>
m <sup>2</sup>	m <sup>2</sup>	22.5 m <sup>2</sup>	14 m <sup>2</sup>	114 m <sup>2</sup>
2	7	2	1	6
2	7	2	1	1 and 2
1	1	1	1	1
in situ	in situ	in situ	in situ	in situ
summer	spring			winter
-2°C : 12°C				12°C
no	no	no	no	from COMIN
no	no	no	no	no
0 m/s : 2 m/s			1.5m/s:7m/s	0 m/s
0.25 m <sup>2</sup> 0.37 m <sup>2</sup>		2.2 m <sup>2</sup>	2.5 m <sup>2</sup>	
2# (67h, 130h)	2# (2h)		15#	
		30'	30'	15'
CC: R <sub>22</sub> , SF <sub>6</sub>	CC: N <sub>2</sub> O, SF <sub>6</sub> , CO <sub>2</sub> , H <sub>2</sub> O	N <sub>2</sub> O, decay	pulse of N <sub>2</sub> O	CC: N <sub>2</sub> O, SF <sub>6</sub>
Wind influence on single sided ventilation	Contaminant spreading and large opening	Large openings	Large openings	Chimney, typical family house

Table 4.2: features of COMIS used in the reported test cases

	Optibat (F)	Solar house (J)	Family house (J)	LESO (CH)	Passys (B)	Namur flat (B)	Passys (G)	Large Opening (G)	Italgas (I)
<b>Air flow component</b>									
<i>Crack</i>	■	■	■	■		■	■	■	■
<i>Fan</i>						■			
<i>Straight ducts</i>									■
<i>Duct fitting</i>									■
<i>Flow controller</i>									
<i>Large vertical opening</i>					■	■	■	■	
<i>Test data component</i>		■	■						
<b>Zone layer</b>		■	■	■	■	■	■	■	
<b>Pollutant</b>						■			
<b>Schedules</b>									
<i>Links</i>									
<i>Large vertical openings</i>									
<i>Fan</i>						■			
<i>Zone temperature</i>				■	■				■
<i>Zone humidity</i>						■			■
<i>Pollutant source or sink</i>			■			■			
<b>Building orientation, terrain and wind profile data</b>		■	■	■			■	■	■
<b>Pressure coefficients</b>		■	■	■					■
<b>Meteo data</b>	■	■	■	■	■		■	■	■

## 4.2 OPTIBAT facility

### 4.2.1 Presentation of the test facility

OPTIBAT is a real scale experiment consisting of an 88 m<sup>2</sup> four-room dwelling built in the laboratory hall at the INSA in Lyon (Figure 4.2). This dwelling is a replica of an apartment in an existing building located near Lyon. Two facades of this dwelling are submitted to a controlled climate.

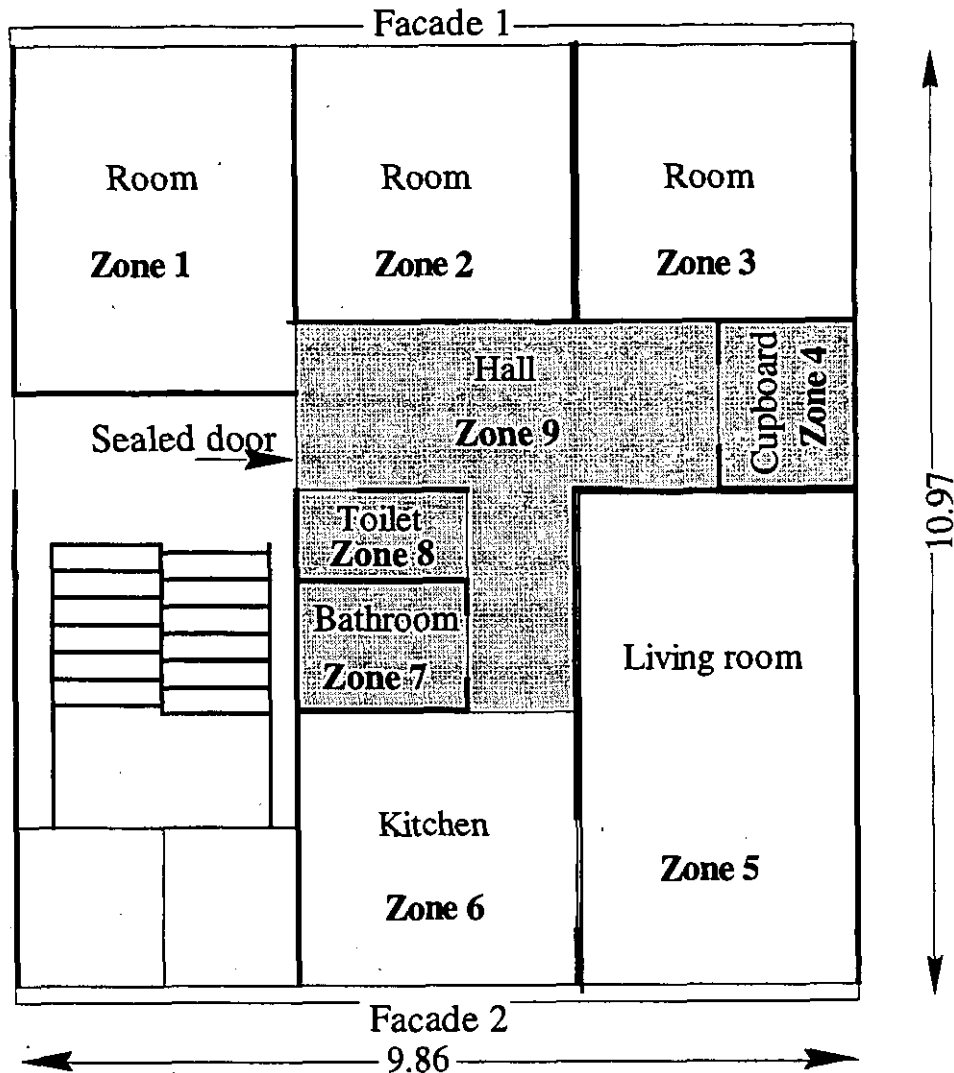


Figure 4.2: The OPTIBAT facility with the nine zones defined for the infiltration measurements.

Climate chambers are added on each face of the experimental cell, in order to control the boundary conditions. The two main facades (top and bottom on Figure 4.2) can be submitted to temperatures between -10 and 30°C, to relative humidity between 30 and 80% and to pressure differentially up to 180 Pa. The other four faces (two walls, floor and ceiling) have thermal and pressure guards, simulating the adjacent apartments.

### 4.2.2 Aim of the comparison

This facility allows measurements of air permeabilities and air flows in a very well controlled environment. Simulations can also be performed with very well controlled boundary condi-

tions. The comparisons between simulations and experiments made with this facility are much more accurate than those performed on real buildings. Since real pressures on facades were directly input for simulations, the possible discrepancies resulting from the use of pressure coefficients are avoided.

### 4.2.3 Elements of comparison

Air permeability characteristics of all inter-zonal links, including links to exterior, were measured using the guarding zone technique [Amara, 1993], [Megri, 1993].

Several climatic conditions, simulating both winter and summer, were imposed by the climate chambers. The wind effect was simulated by pressure differentials at the facades. Air flow rates resulting from these boundary conditions were measured using multi-tracer gas technique and a Bayesian interpretation method. For simulation and measurements, bathroom(zone 7), toilets (zone 8),hall (zone 9) and cupboard (zone 4) were combined in node 4 (open doors).

Simulations were performed with COMIS 1.1, using as input the measured boundary conditions (pressure differentials, temperature and humidity) and the measured air permeability characteristics. Resulting inter-zonal flow rates are compared.

### 4.2.4 Results

Calculations were performed for the various climatic conditions given in Table 4.3

Table 4.3: Climatic conditions adopted for comparisons.  $\Delta P_1$  and  $\Delta P_2$  are pressure differentials on facades 1 and 2 respectively, while  $\Delta P_3$  is the pressure in the staircase.

Scenario	$T_{Out}$ [°C]	$T_{In}$ [°C]	$\Delta P_1$ [Pa]	$\Delta P_2$ [Pa]	$\Delta P_3$ [Pa]
Summer 1	20 ± 0.5	20 ± 0.5	16 ± 1	-81 ± 2	-2.8 ± 0.5
Summer 2	20 ± 0.5	20 ± 0.5	54.1 ± 1.2	-122 ± 3	-13.4 ± 1
Summer 3	20 ± 0.5	20 ± 0.5	25 ± 1	-58.6 ± 2	-6 ± 1
Summer 4	20 ± 0.5	20 ± 0.5	1 ± 1	-43 ± 2	-0 ± 1
Winter 1	-1.3 ± 0.5	20 ± 0.5	15.7 ± 1	-79.6 ± 2	-2.5 ± 1
Winter 2	-1.1 ± 0.5	20 ± 0.5	52 ± 1	-121 ± 3	-12.6 ± 1
Winter 3	-1.7 ± 0.5	20 ± 0.5	21.5 ± 1	-42 ± 2	-4.8 ± 1
Winter 4	-1.5 ± 0.5	20 ± 0.5	1 ± 1	-42 ± 3	-0 ± 1

Global sensitivity analysis was performed using the Monte-Carlo technique: 100 runs were performed, varying all parameters at random before each run. The random changes of the parameters were made following a uniform distribution, with maximum and minimum values as given in Appendix A 4.2. For these calculations, COMVEN 1.3 was used, together with the Misa tool. Comparisons of measured and calculated inter-zonal air flow rates are given in detail in Annex A 4.2.

A summary of these comparisons is shown in Figure 4.3. This Figure represents each flow by a central star surrounded by its confidence rectangle.

It can be seen that very few confidence rectangles touch the 45° line. This means that there are significant differences, as far as confidence intervals are properly estimated. In nearly half of the cases, simulated results are larger than measured air flow rates, while the contrary is true in the other cases.

There are also several air flows which were significantly different from zero when measured, but these were not simulated. These are represented by stars with bars on the vertical axis.

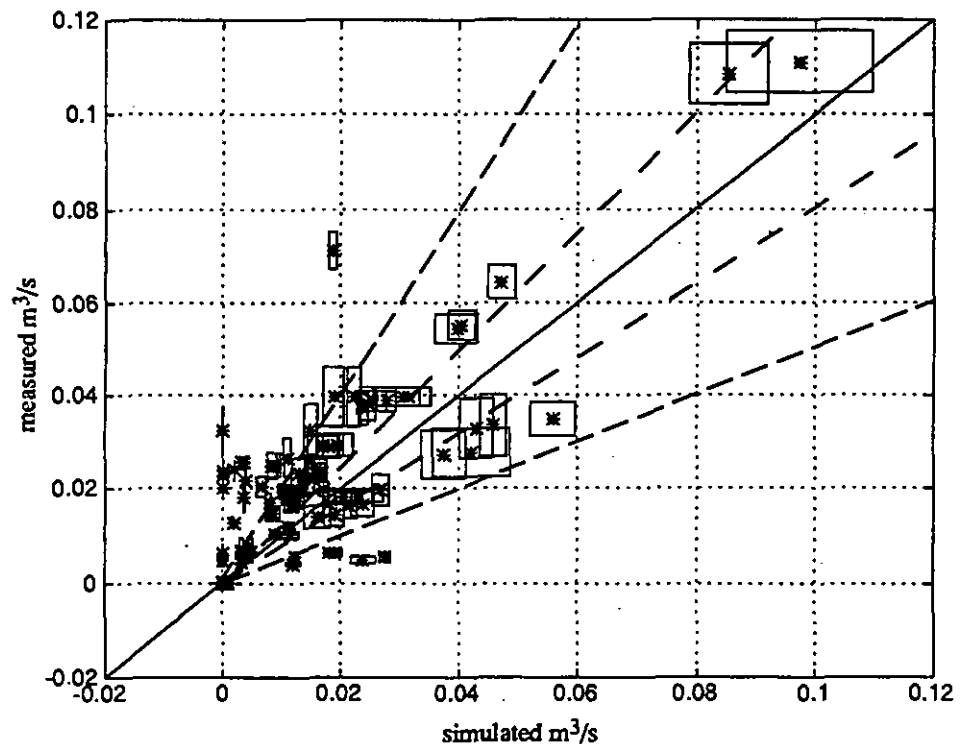


Figure 4.3: Comparison of simulated and measured air flow rates for all zones and all scenarios. Rectangles correspond to confidence intervals.

#### 4.2.5 Conclusions

In most cases, there are significant differences between calculated and measured air flow rates, even for total air flow rates in zones. There could be several reasons for this:

Are there bugs in COMVEN? This does not seem to be the case since inter-model comparisons show results very close to those of other programs [Haghighat & Megri]. The alternative would be that all compared programs present the same bugs.

The way the building is modelled for input in COMIS does not correspond to reality. This is possible, since two modellers have got slightly different results (see Appendix A 4.2).

Confidence intervals on measurements are underestimated: This is also possible, since two different measurement techniques sometimes provide significantly differing results.

It should be said that this comparison is the only one where most of the calculations were performed by a simulating team (LESO) independently from the measuring team (INSA). Up to the time of drafting this report, no close contact had been established between these teams to explain or reduce the discrepancies. Moreover, a closer contact appeared to be impossible, for both time and financial budgets.

## 4.3 Japan Solar House

### 4.3.1 Measured object

A Passive Solar House that was constructed for research on passive solar system performance at the campus of Tohoku University, Sendai, Japan, is used for measurement of air flows. The site plan and elevation are shown in Figure 4.4 (a) and (b), respectively. There are some laboratory buildings on the north and west sides of the house. A semi-underground test house is located on the south of the house. The solar house consists of two rooms of the same size and a corridor between them. The house plan is shown in Figure 4.3.2. The rooms are 2.7 m wide, 5.5 m deep and 2.8 m high.

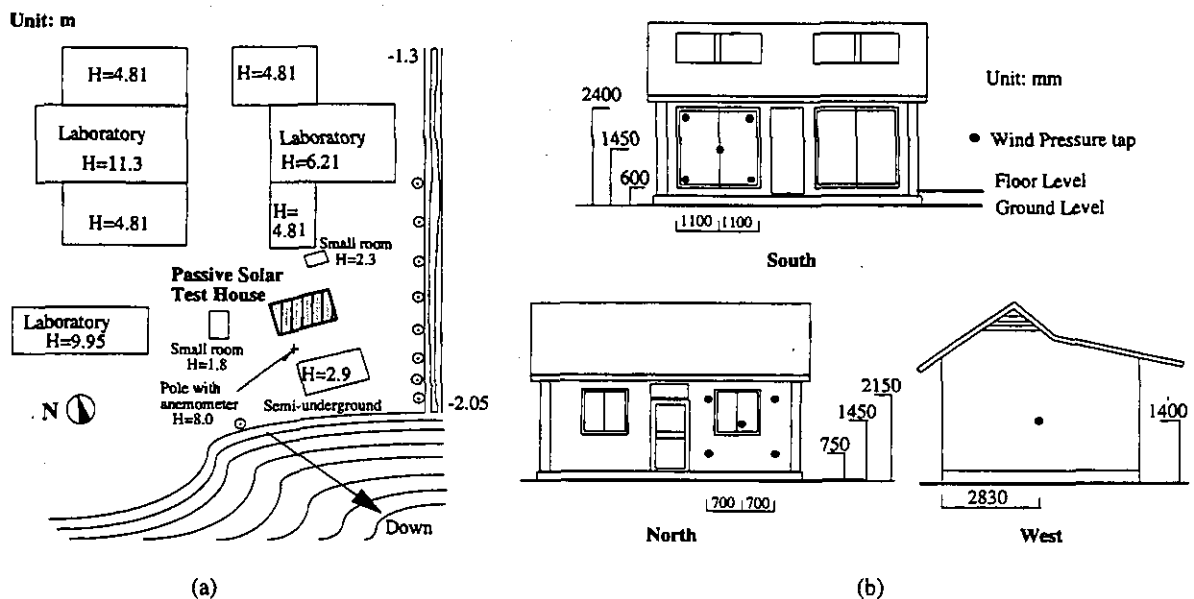


Figure 4.4: Site Plan and Elevation of Passive Solar Test House

For measurement of air flow among three zones, the corridor and Room A which is divided into two zones are used. The house plan of the three zones is shown in Figure 4.5. The doors between two rooms and the corridor, and the partition wall between Room 1 and 2 have a small vertical slit of 1 cm width. The doors between Room A and Room 3 are sealed securely to avoid any air exchange between them.

The 8 m long pole, which is located as shown in Figure 4.4(a), is equipped with a wind direction meter and a wind speed meter at the top. Outdoor temperature is measured at a point close to the north window. Indoor temperatures are measured at the centres of the rooms at a height of 1.4 m above the floor level. Measuring points of tracer gas concentrations are also located at the centre of the rooms and at the same level. Wind pressure taps on the outside walls are situated at the points shown as black circles in Figure 4.4(b). The point of reference pressure is assumed to be at the floor level of room 3. The accuracy of wind speed, temperature and pressure data in measurement is within the limit of (5%).

### 4.3.2 Method and conditions of Measurements

The concentration decay method with tracer gases,  $N_2O$ ,  $SF_6$  and  $CHCl_2F$ , is employed for measurement of air flows among the three rooms. The concentrations of gases are measured every 6 minutes by a Bruel & Kjaer multi-gas monitoring system, which has an uncertainty in gas concentration of  $\pm 3\%$ . The experimental conditions are shown in Table 4.4.

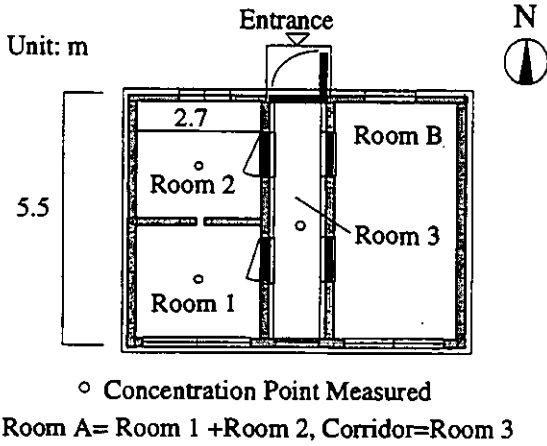


Figure 4.5: Plan and Section of Passive Solar Test House

Table 4.4: Conditions of the measurements for experimental comparison

Case No.	1	2	3	Unit
Wind direction	SE	W	S	
Avg. wind speed	1.06	0.46	1.18	[m/s]
Outdoor temp.	25.3	23.2	23.9	[°C]
Room 1 temp.	33.4	26.0	28.2	[°C]
Room 2 temp.	35.0	26.2	27.6	[°C]
Room 3 temp.	30.0	44.0	29.9	[°C]

### 4.3.3 Comparison of measured and calculated air flows and gas concentrations

The aim of any model validation is to establish the accuracy of the model prediction by comparing the values produced with actual experiments or measurement. Theoretically, the two series of results from measurement and simulation are different and therefore do not have perfect agreement because there are errors and uncertainties of measurement. Initially error analysis is not made as the influence of the respective errors will be estimated by sensitivity analysis and explained in the ensuing section. For now, the comparison is conducted with the average data.

The measured air flows of 3 cases are calculated using the profiles of tracer gas concentration. It was found that the air flow patterns in those cases are different from each other. Figure 4.6 compares the air change rates measured with results calculated using COMIS. As can be seen, the majority of the results of air change rates is within the range of the relative error (25%).

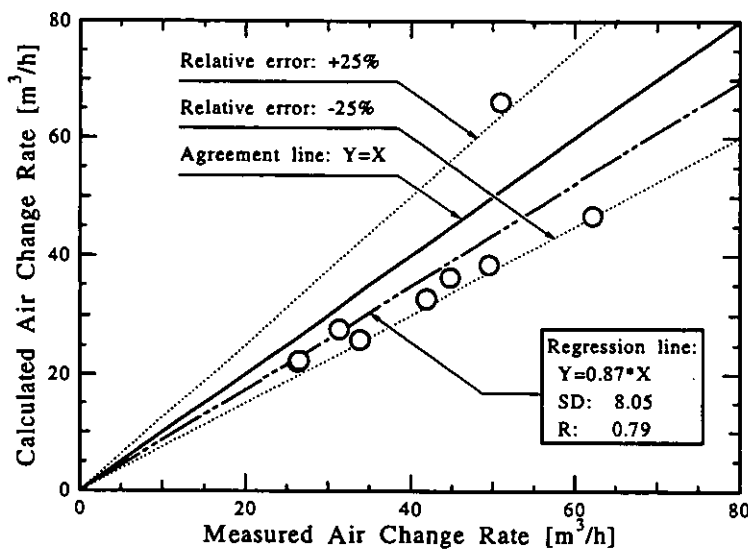


Figure 4.6: Comparison of measured and calculated air change rate

Figure 4.7 is a comparison of gas concentrations calculated with those from measurement of three cases. The results of regression analyses indicate that the measured and calculated gas concentrations have a relatively good agreement, because the standard deviations and correlation coefficients in three cases vary from 2.99 to 4.18 and from 0.97 to 0.99, respectively.

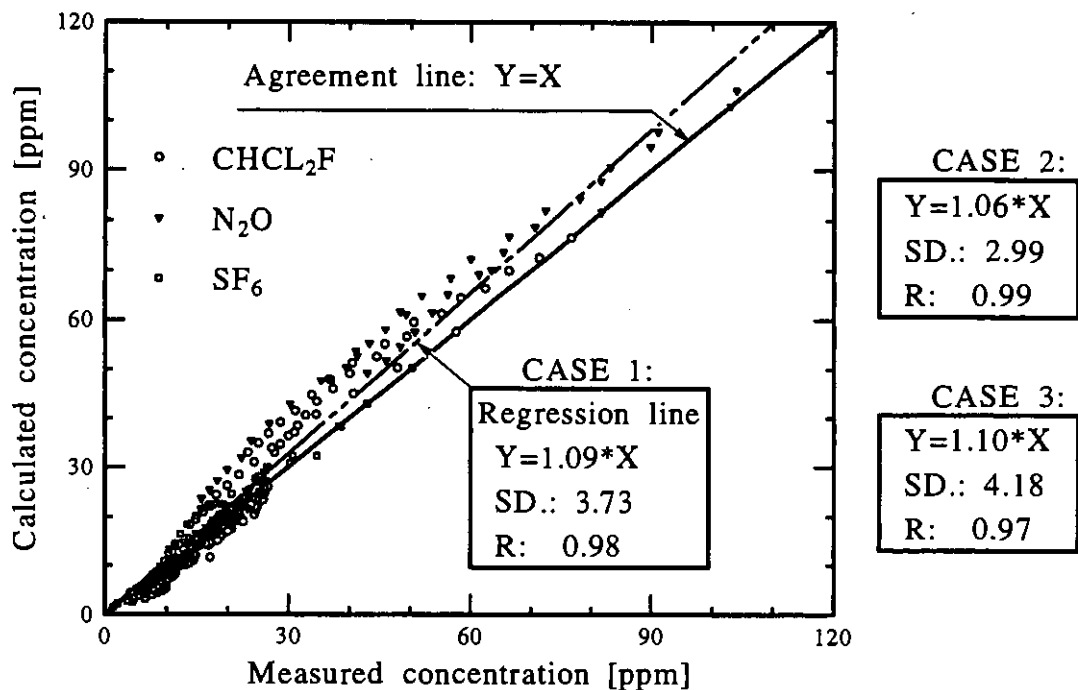


Figure 4.7: Comparison of indoor gas concentrations using regression analysis

For gas concentrations, the average factors from calculated to measured values are from 1.06 to 1.10. The good agreement between measurement and simulation is achieved at certain time steps, but for the other time steps, the agreement is relatively poor. The reason for this may be due to the approximate average input data for simulation, especially wind pressure coefficients, and the differences between measured and calculated air flow rates, and also the "perfect" mixing assumption cannot be satisfied well within every room.

It is a fact that any measured data includes a confidence interval or probable error. Therefore, the comparison between measurement and calculation, using sensitivity analysis, is a necessary task for model validation. In the following section, Case 1 of the passive solar house is used to evaluate COMVEN by a sensitivity analysis method. The input parameters and their uncertainties for sensitivity are related to air tightness, climate data from measurement and default data in simulation. These parameters play an important role in controlling air flow rates in this building.

Air flow results estimated by tracer gas method also include a series of errors. In this study, these errors are assumed so that the accuracy of tracer gases concentrations and temperatures are 3% and 1°C. Figure 4.8 shows the comparison of measured and calculated air flow rates using results of sensitivity analysis. The results take the standard deviations into account. It can be found that the majority of measured and calculated results share a common range.

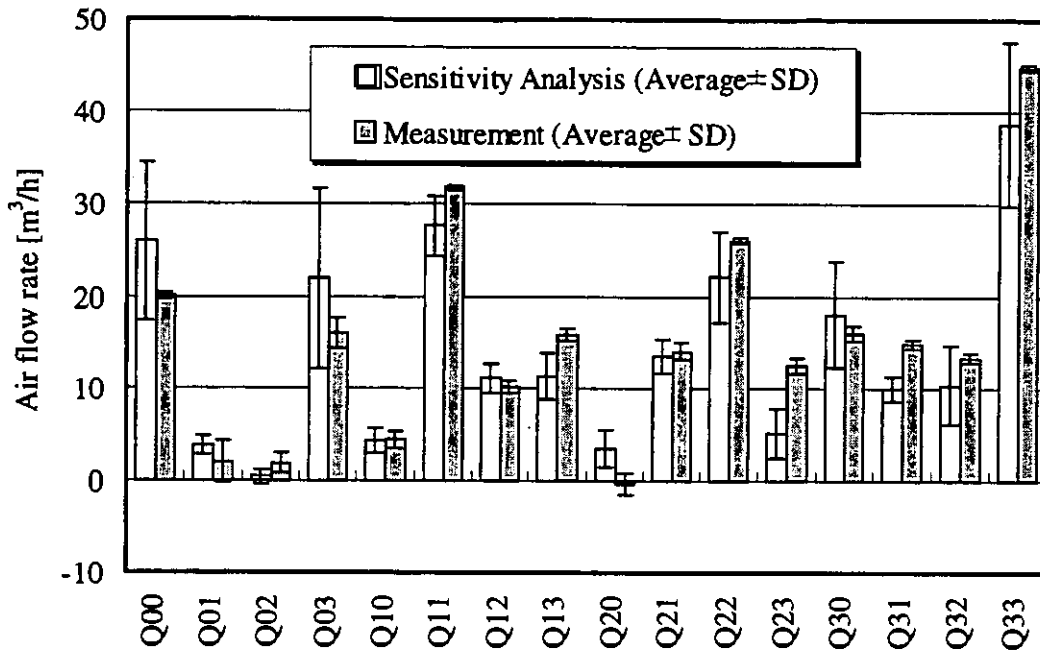


Figure 4.8: Comparison of measured and calculated air flow rates.

#### 4.3.4 Conclusions

By comparing average air flows between measurement and simulation, it can be seen that the relative error of air change rates is mostly within  $\pm 25\%$ . This is both encouraging and reasonable because the drive of natural ventilation is unsteady and is treated by average data. For comparison of tracer gas concentrations, the average factors from calculated to measured values are from 1.06 to 1.10 for three cases. Furthermore, evaluation of the COMIS model is conducted using a sensitivity analysis method in order to assess the effect of uncertainty or error of parameters from measurement. By comparing the air flow range of measurement and simulation, it is found that there are common ranges between the two series of data. So it also can be concluded that the multizone model of COMIS is practicable and available.

## 4.4 Japanese Family House

### 4.4.1 Measured object

The measurements were conducted using a two storey family house in Japan. Figures 4.9 and 4.10 show the elevation and the floor plan of the house. The first and second floors are 0.6 and 3.4 m above the ground level floor, respectively. The width from the east to the west of the house is 10 m and the depth from the north to the south is 8 m. The total floor area of this house is 133 m<sup>2</sup> with an air volume of 350 m<sup>3</sup>. The building height is 7.5 m. The interior of the test house is considered to have nine rooms. The hall on the first and second floors is connected by a void and stairs and is considered to be two zones. The number of zones are shown in Figure 4.10. Zone No. 10 indicates outdoors.

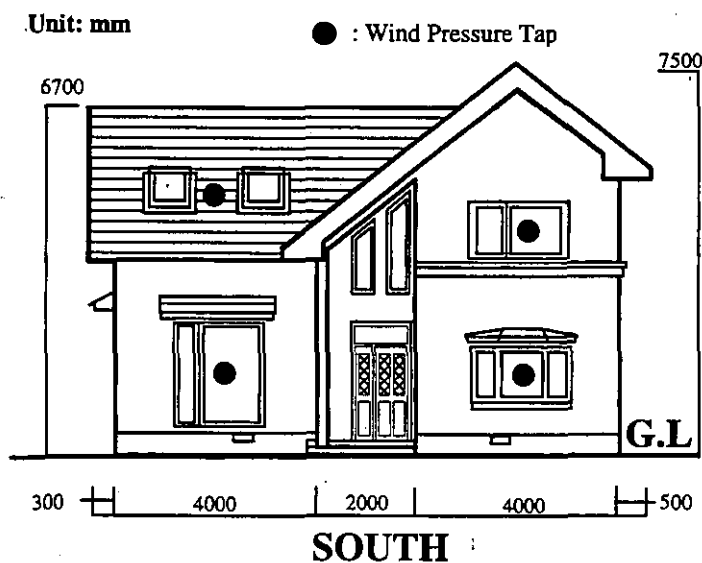


Figure 4.9: Elevation of the Japanese family House

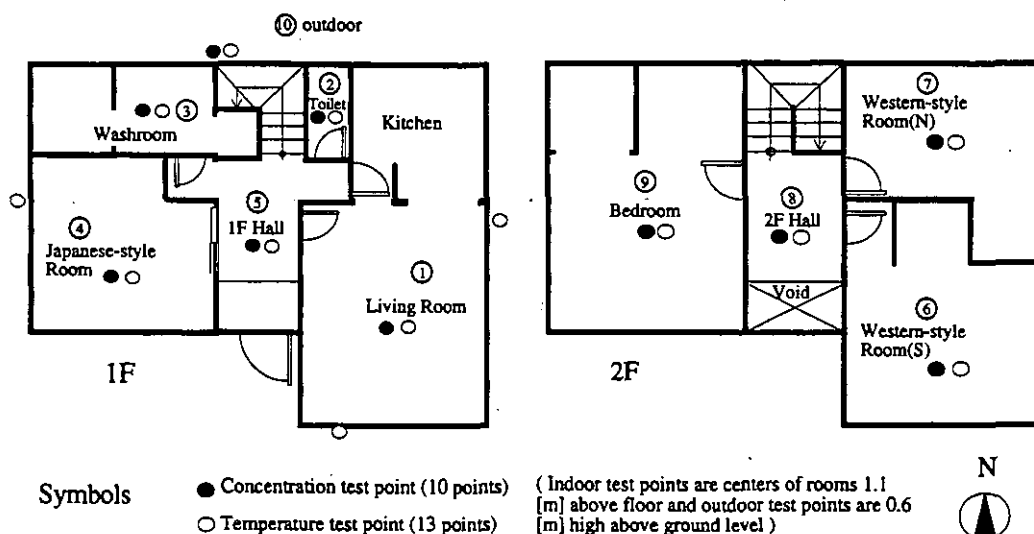


Figure 4.10: Floor plan of the Japanese family house

An 8 m high pole, which is located at the Southwest of the house, is equipped with wind direction and speed meters at the top. Outdoor temperature is measured at the four points around the external walls. Indoor temperatures are measured at the centers of the rooms at a

height of 1.1 m above floor level. Measuring points of tracer gas concentration are also at the same positions. Wind pressure taps on the outside walls are located at the points shown as black circles in Figure 4.9 The point of reference pressure is assumed to be at the ground level below the first floor.

#### 4.4.2 Measurements performed

##### *Method of measurements*

The measurement of air flows is carried out using the system parameter identification method developed by H. Okuyama. Rectangular pulses of SF<sub>6</sub> tracer-gas are injected into each room for identification. The changes of concentration in each zone occur due to the response to the injection. The indoor gas concentration of each room is sampled every ten minutes. Based on these data, one-minute data are calculated by linear interpolation approximation. In each room, fans are used for mixing indoor air with tracer gas. For the evaluation of the multizone indoor pollutant transport model, measurements of indoor gas concentrations are carried out. The system for measuring air contaminant (i.e. tracer gas) concentration is the same as that for air flows. The gas is only injected into the living room for one hour at the beginning of the measurement. The indoor gas concentration of each room is sampled every ten minutes.

##### *Conditions*

Table 4.5: Characterisation of the measurement periods selected for comparison

Measurement	Air flows	Indoor gas concentrations
Date	30 to 31 Jan. 1994	31 Jan. to 1 Feb. 1994
Measurement time	10 hours	16 hours
Time for simulation	3 hours	15 hours
Number of data points	180	900
Time step	10 minutes	10 minutes
Average wind direction	East	East
Average wind speed	2.32 m/s	1.42 m/s
Outdoor mean temperature	-6.86 °C	-4.30 °C
Zone 1 to 9 mean temperature [°C]	33.89, 19.57, 14.63, 11.81, 16.04, 13.60, 13.03, 16.16, 11.24.	33.35, 18.26, 12.54, 15.64, 15.62, 15.94, 13.21, 15.71, 13.20.

For measurements of air flows and indoor gas concentrations, the living room is heated by six heaters with equal power, and the ventilation system is not operated. All internal doors are closed. The average values of wind, and outdoor and indoor temperatures during measurements are shown in Table 4.5.

##### *Air leakage distribution*

Effective leakage areas of the windows, walls, doors and other components are measured by the fan pressurisation method. The equivalent leakage area of external walls and windows is 33.5 cm<sup>2</sup> and 67.0 cm<sup>2</sup>, respectively. The total of the  $\alpha A$  of internal doors is 910 cm<sup>2</sup>. The equivalent leakage area per floor area of the building envelope is 0.8 cm<sup>2</sup>/m<sup>2</sup>.

### 4.4.3 Comparison of measured and calculated data

#### Method

Air flow measurement is done with an airtight test house, and the zone layout of this building is shown in Figure 4.10. Though the hall is treated as two zones for the purpose of measurement, it is considered as one zone for the simulation because of a large opening existing between 1F hall and 2F hall. Therefore, comparison between measurement and simulation does not include air flow between 1F hall and 2F hall.

#### Air flows

Figure 4.11(a) presents a comparison of the measured air change rates and the calculated results. It is clarified that both air change rates are closed in some rooms, but others show a difference between the measurement and calculation result. The correlation coefficient between measurement and calculation is 0.70. On the other hand, Figure 4.11(b) presents a comparison between the measured air flow rates and the calculated results.

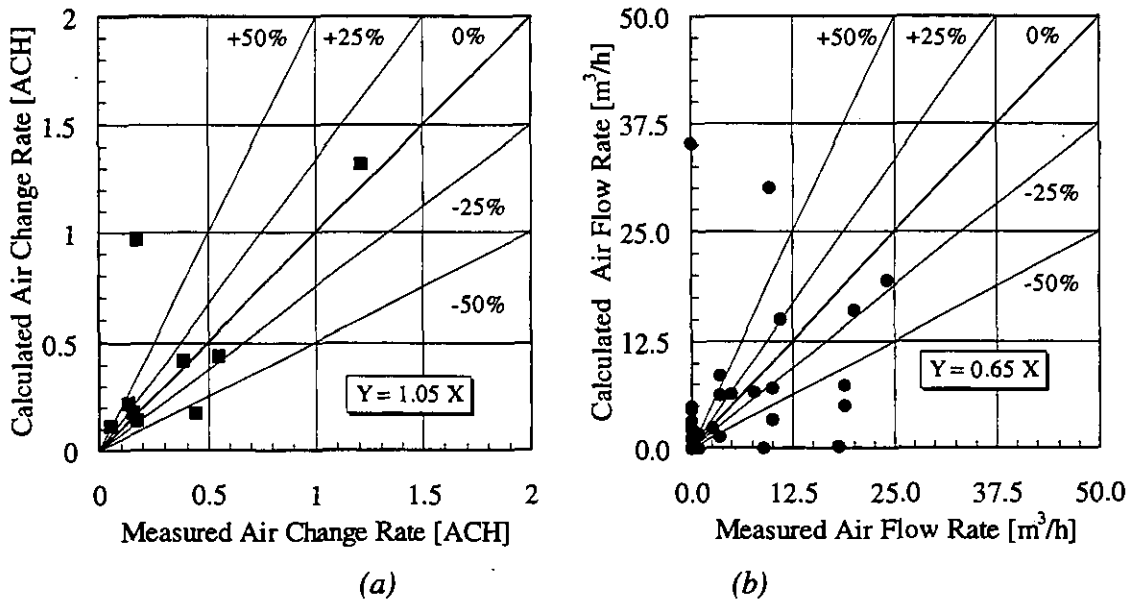


Figure 4.11: Comparison of measured and calculated air flows

It can be found that both air change rates are different for many of the flow paths. The first reason may be due to the fact that the measurement error of the identification method has an accuracy of  $\pm 20\%$ . Secondly the measured results are average values of air flow taken over three hours during which time the climate conditions change and air flow rates are not always stable, whereas simulated results are air flows in a stable condition where the climate data are average values from measurement. Moreover, well-mixing is difficult to achieve because a large fan affects the air flow of a zone and it can not be used for mixing. Overall, the simulation results are considered reasonable because their accuracy is based on the accuracy of the average input data and the measurement technique.

#### Indoor gas concentrations

Figure 4.12 shows the comparison of indoor concentrations measured and simulated in all zones of the building. The results indicate that the measured and calculated gas concentration are not the same but neither are they remarkably different. The good agreement between measurement and simulation is achieved for some rooms, but for the other rooms it is a little worse. The reason may be that air flow rates for pollutant transport calculation have some

differences compared with the actual ones. In addition, it may be the approximate average input data for simulation, especially wind pressure coefficients and distribution of leakage.

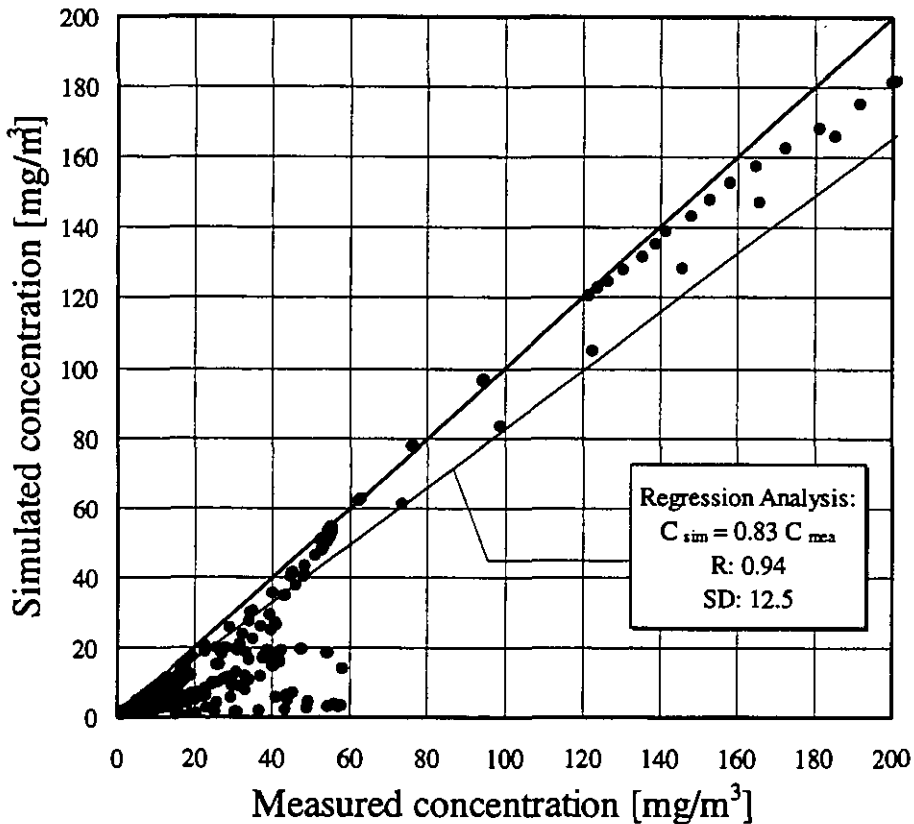


Figure 4.12: Comparison of measured and simulated gas concentrations

#### 4.4.4 Conclusions

For air change rates, the regression coefficient and correlation coefficients between the two sets of air change rates is 0.95 and 0.70. But for air flow rates, the large difference between measurement and simulation exists. For indoor gas concentrations, the regression coefficient and correlation coefficients of two sets of results are 0.83 and 0.94, respectively. The good agreement between measurement and simulation is achieved for some rooms, but for the other rooms it is not so good. The reason may be that air flow rates for pollutant transport calculation have some differences compared with the actual ones, etc. Overall, the simulation results are considered reasonable because their accuracy is based on accuracy of the average input data and the measurement technique. From the results of these case studies here, the conclusion can be drawn that the COMIS model is useful for simulation of multizone, air flow and pollutant transport.

## 4.5 LESO three storey office building

### 4.5.1 Measured object

The LESO building is a medium-sized office building. It consists of nine south oriented cells with passive solar façades, a few differently oriented rooms, and a staircase. To the north, the building is attached to another laboratory building, the LEA building. Figure 4.13 shows the building and its room numbers.

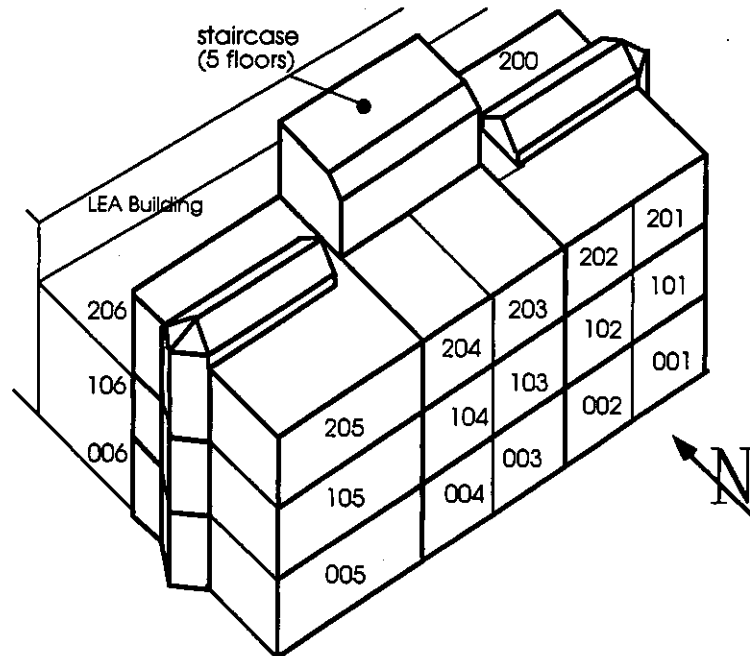


Figure.4.13: The LESO building

### 4.5.2 Measurements

In this building, component leakages have been carefully determined followed by extensive measurements of the boundary conditions as well as the air flows.

Building related measurements, including aeraulic data, have been measured. The data concerning the leakage characteristics and the air flows have been compiled in a set referred to as the "LESO data set" [Fürbringer et al, 1990].

From this data set, three periods with different wind conditions have been selected for the comparison. Measured and calculated air flows have been compared. Air leakage data have been measured using a guarding zone technique with two fans. Air flows have been determined by constant concentration multitracer gas technique [Compagnon, 1991]. For each zone  $i$  the global incoming air flow  $Q_{ai}$  was determined. From the per zone values  $Q_{ai}$ , a global value for the whole building is formed as given below, weighting the  $Q_{ai}$ - values per zone with the respective zone volume  $V_i$ :

$$Q_{a-Building} = \frac{1}{\sum_{i=1,N} V_i} \sum_{i=1,N} Q_{ai} V_i \quad (4.1)$$

In fact, this value does not differ significantly from the simple sum of all  $Q_{ai}$ - values.

### 4.5.3 Modelling and simulations

For the sensitivity analysis as well as for the simulation of the measured periods, the building is represented by a network which consists of 11 zones and a total of 28 air flow links. These air flow links represent the measured leakages and are modelled by the well-known power law model for crack flow. Some measured coefficients have been split up arbitrarily between two or more conductance elements, especially in the staircase zone.

A typical section of such a network is given in Figure 4.14 for the second floor of the building. More detailed information on the modelling of the building may be found in [Dorer, 1992]

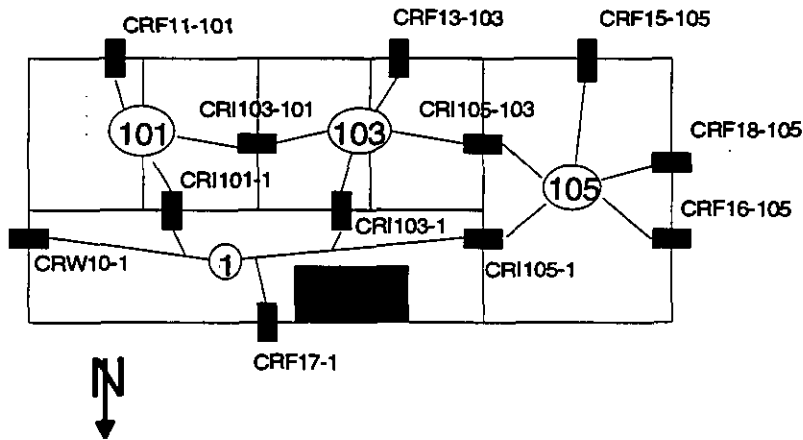


Figure 4.14: Typical section of the flow network ( Floor 2 ).

### 4.5.4 Sensitivity analysis

The sensitivity (to input uncertainties) of the LESO Building simulated with COMIS has been studied using factorial design and Monte-Carlo method [Dorer, Fürbringer et al, 1992].

In that study, a uniform distribution  $U(-1,1)$  has been used to create the design matrix for MISA (cf. §1.3.2). For each time step, 100 simulations were performed.

An additional study was made using Monte-Carlo design to analyse the effect of the pressure coefficient uncertainty which were not included in the confidence interval estimation here above. For that analysis, an arbitrary uncertainty of 50% has been considered. The average of the mean age of air  $t$  in each zone and the corresponding relative standard deviation  $\sigma_t/t$  are shown for the 4 main wind directions  $\theta$  and wind speed  $v$  between 0 m/s to 6 m/s.

Figure 4.15 presents the behaviour of the mean age of air  $\tau(\bar{t}, \theta)$  in the hall. This zone corresponds to the entrance hall which has a very untight door, the stair case through 5 floors (from the basement to the attic) and some additional zones at each floor. The evolution of the mean air age is more or less inversely proportional to the wind speed. Note the stronger ventilation when the wind blows from south. The behaviour of the standard deviation  $\sigma_t/\tau$  (due to the uncertainty of  $C_p$ ) is more complex. When the wind blows from south or north: At low wind speed,  $\sigma_t/\tau$  decreases with the increase of wind since the inverse behaviour is observed at high wind speed. In the situation without wind no error can come from  $C_p$  uncertainty. When the wind blows from west, which corresponds to the most airtight side of this zone, the inaccuracy of the simulation is proportional to the wind speed. When the wind blows from east, the behaviour is different still, showing a quick increase at low wind speed, followed by a cup form. More zones are analysed in Appendix A4.5.

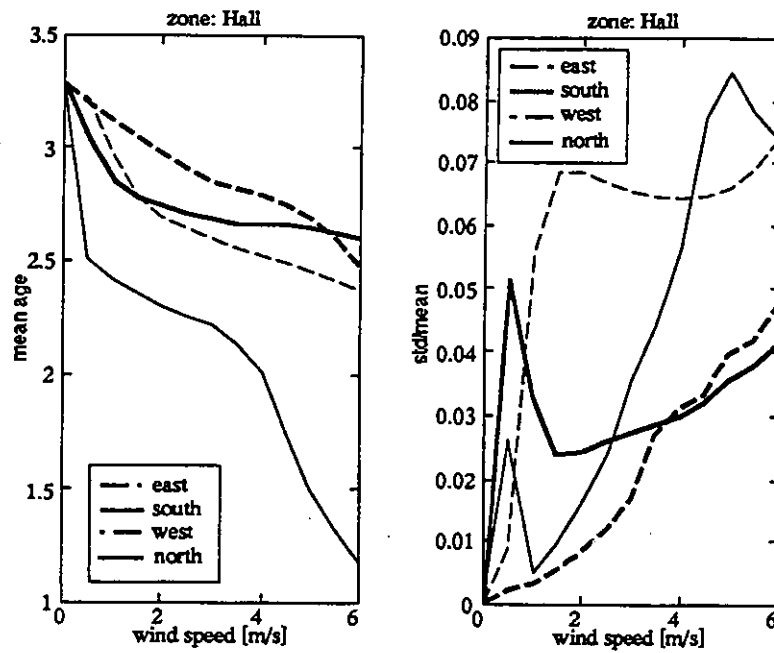


Figure 4.15: Mean age of air and its standard deviation calculated by the Monte-Carlo method for the hall of the LESO Building.

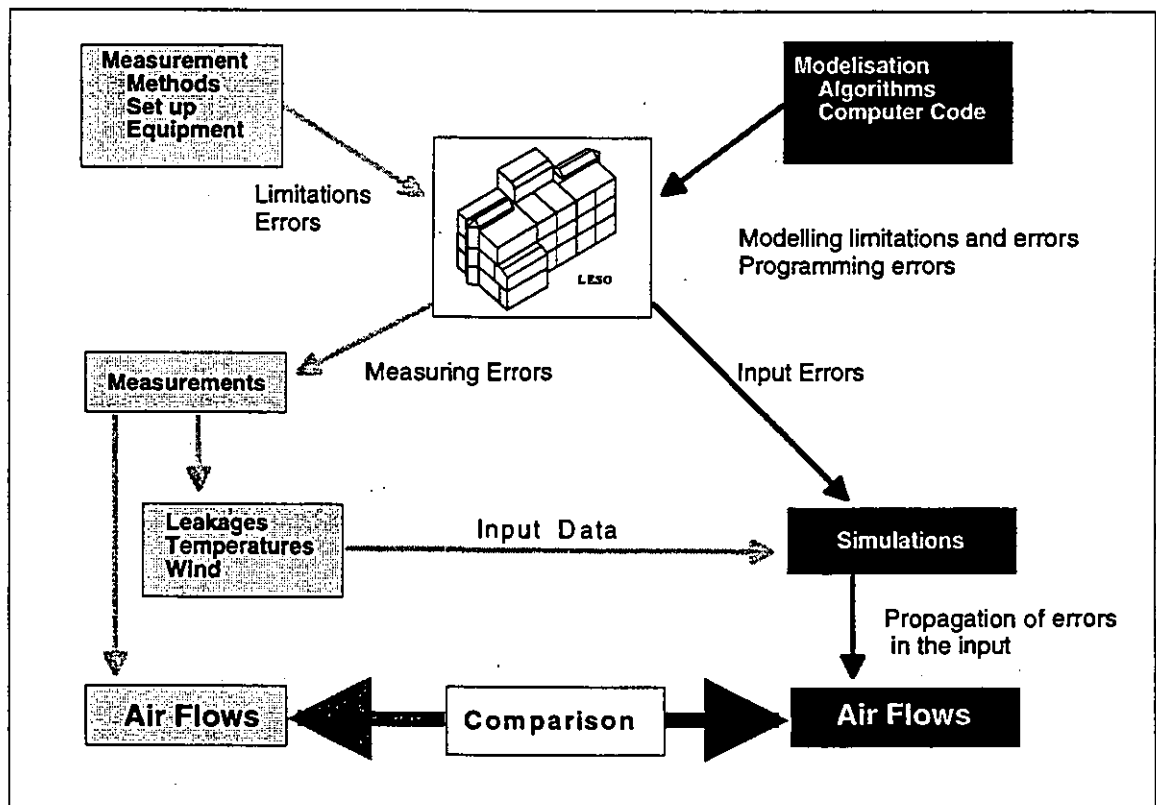


Figure 4.16: Comparison of measured and calculated air flows for the LESO building

The sensitivity to the pressure coefficient uncertainty depends on wind direction and also wind speed. This short study shows once more the necessity of having tools to perform on line sensitivity analysis and parametric study when simulating air flows. This study shows also that pressure coefficients are still critical parameters.

**4.5.5 Comparison of measured and calculated results**

The relation between measured and calculated data and the influence of the respective errors are shown in Figure 4.16 Note that the calculated  $Q_{ai}$  values are not pure simulation results.

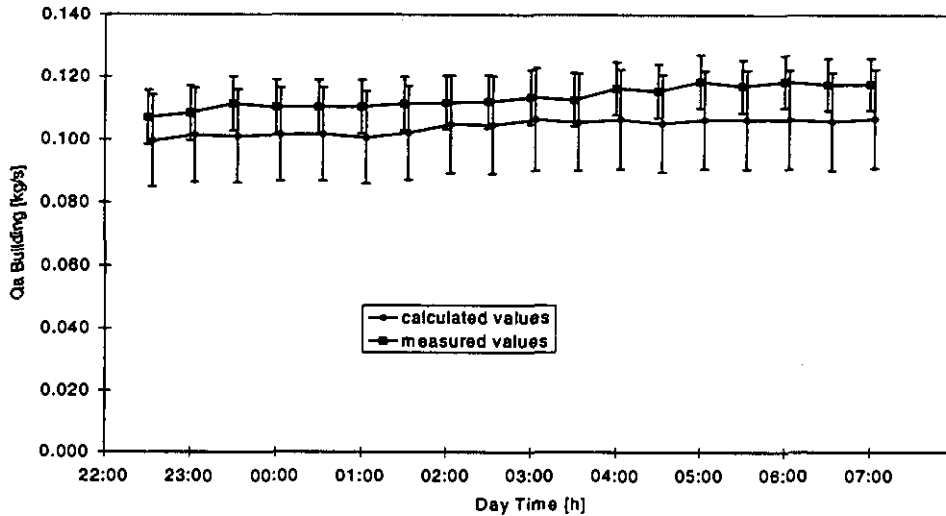


Figure 4.17: Comparison of measured and calculated results, Period 1

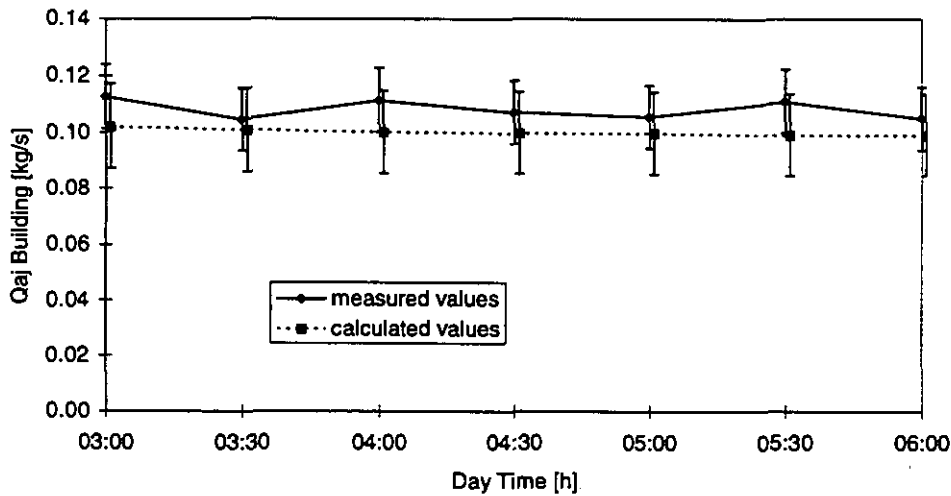


Figure 4.18: Comparison of measured and calculated results, Period 2

The results of the comparison are shown in Figures 4.17 to 4.19 The values for  $Q_a$ -Building from both measurements and simulations are plotted against the time together with the respective confidence intervals. A small time shift has been introduced in the graphics to allow a clear distinction between calculated and measured data.

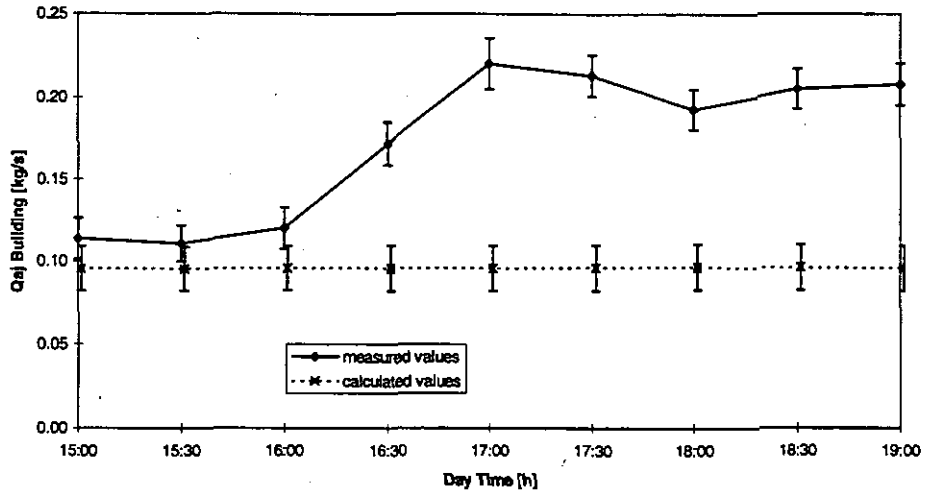


Figure 4.19: Comparison of measured and calculated results, Period 3

Since for the third period, the agreement between measured and calculated data is quite poor, this case has been investigated in more detail (see Appendix)

4.5.6 Conclusions

For a situation without wind (Figure 4.18), the measurements and simulations are in good agreement, that means the respective errors bars overlap. From this it is concluded that the modelling is representing the real building well, especially with respect to the leakage distribution. There is no explanation for the general small underestimation of the air flow.

In period 3 (Figure 4.19) the wind speed decreases from approx. 1m/s to 0.2 m/s at steady wind direction. Surprisingly, the big difference between measured and calculated values appears during the end of the period, where the wind speed is low and one could expect that the agreement should be in the same range as in period 2.

As shown in Figure 4.20 an increase in the flow rate due to lower wind is not unrealistic when being in range A. This effect can be explained by an adversial effect of stack and wind pressures, resulting in a decrease of the overall driving pressure.

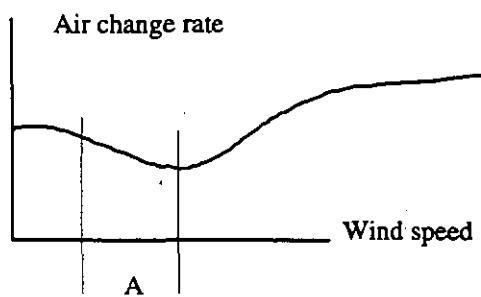


Figure 4.20: Interaction of stack and wind induced air change (qualitative only)

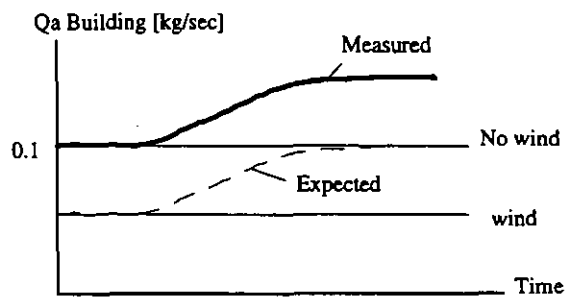


Figure 4.21: Qualitative Measured and expected Qa-Building values (qualitative only).

One could also expect that the values for Qa would coincide rather at the end of the period when the wind is low and that a deviation would more likely occur at the beginning of the period (see Figure. 4.21). Since there was good agreement for Periods 1 and 2, one would

expect that also in this case at least for the low wind time the agreement should be good, which obviously is not the case.

Nevertheless, for the specific building and climatic periods analysed, the wind effects become important only above 1.5 to 2 m/s approximately.

From this one can conclude that the reason for the large difference between measured and calculated values is most probably not related to the modelling itself, but rather to effects of parameters which are not well reflected in the input data. A list of such factors is given below, factors with higher probability are listed first:

Sudden change in the building leakage characteristic (door could be opened)

Wind fluctuations, which have a big effect on ventilation rate, but which are not well represented by the average wind speed input data.

Measurement problems in this specific time interval

Effects of solar radiation changes (quite unlikely because this is low at 16h in the afternoon in December)

## 4.6 Belgian PASSYS cell

### 4.6.1 Presentation of the 'building'

The measurements were performed in an outdoor PASSYS test cell. It consists of 2 rooms: a test room and a service room. The South wall of the test room is exchangeable: during these measurements a wall with a large opening was used. In a first experiment the dimension of the opening was 0.5m x 0.5m, in a second experiment the height was changed to 0.75m. Between the service room and the test room there is a large opening of 1m x 1m.

In this way, single sided ventilation took place in the test room.

### 4.6.2 Measurements performed

The following measurements were done:

- temperatures in the PASSYS cell on different places, in such a way that the vertical gradient can be determined;
- temperature outside;
- wind velocity and wind direction;
- air flow rates through both openings with two tracer gases (R22 injected in the service room and SF6 in the test room).

### 4.6.3 Compared element

The measured air flow rates through both openings are compared with the simulated ones. Much attention is paid to the confidence intervals. The confidence interval of the simulation result is determined by performing a Monte Carlo analysis (in this case it consists of 100 runs): for each simulation run the input parameters get other values depending on the accuracy of the input parameters.

In order to get more variable air flows through the openings (which is advisable if one wants to validate the simulation tool for a wider range of conditions), a heating device is placed in the service room and a cooling device in the test room. A certain sequence of cooling and heating follows and as a consequence the temperature differences over both openings vary significantly with time (and thus also the air flows through both openings).

With a Fractional Factorial analysis the influence of each parameter on the final result is determined. In principle this analysis has to be performed for each time step, because the influence of a parameter will depend on its value. To avoid too much work, one Fractional Factorial analysis will be done during cooling and one during heating.

### 4.6.4 Simulation results and comparison with the measurements

If the confidence intervals of measurement and simulation overlap, one can say that the difference between both is acceptable. It does not mean a priori that one can have total confidence in the tool, but it increases the confidence in the tool for this specific range of input parameters.

In Figure 4.22 the confidence bands of the measured and simulated (with COMIS 1.2) air flow rates through the external opening are given. As one can see the agreement is good for certain periods and bad for other periods. The bad agreement is caused by the fact that the wind effects on large openings cannot be simulated by COMIS 1.2 because there is no algorithm integrated to describe it. In reality the wind has an important effect on the air flow through the large opening.

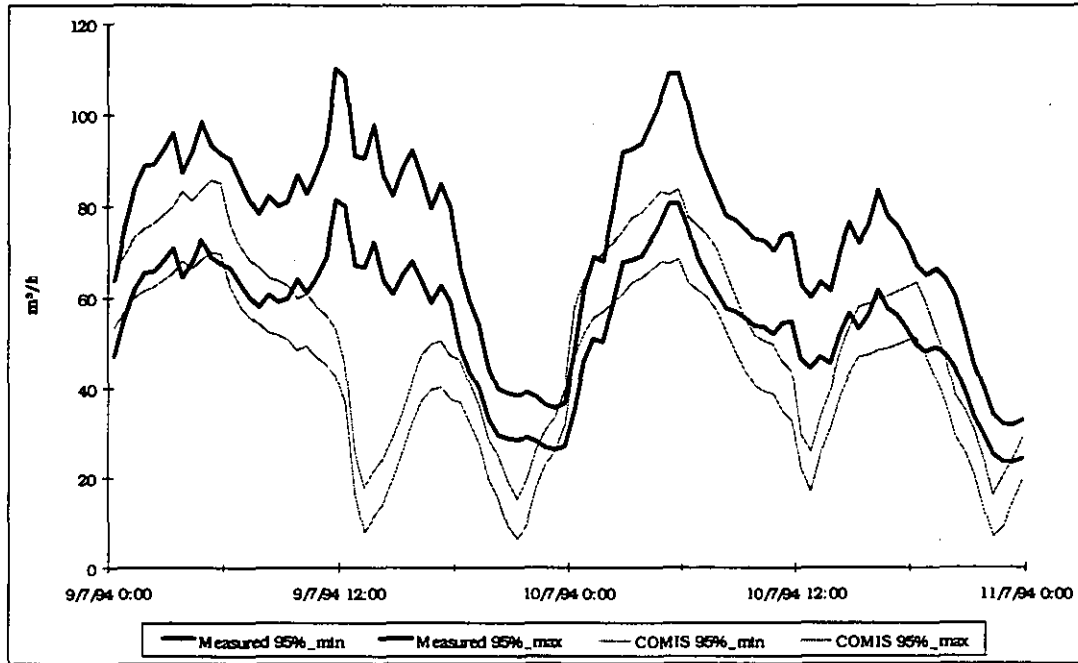


Figure 4.22: Confidence bands of measured and simulated air flow rate through the external opening.

In Figure 4.23 one can see that for the external window there is a strong correlation between the wind speed and the residual of measurement and simulation.

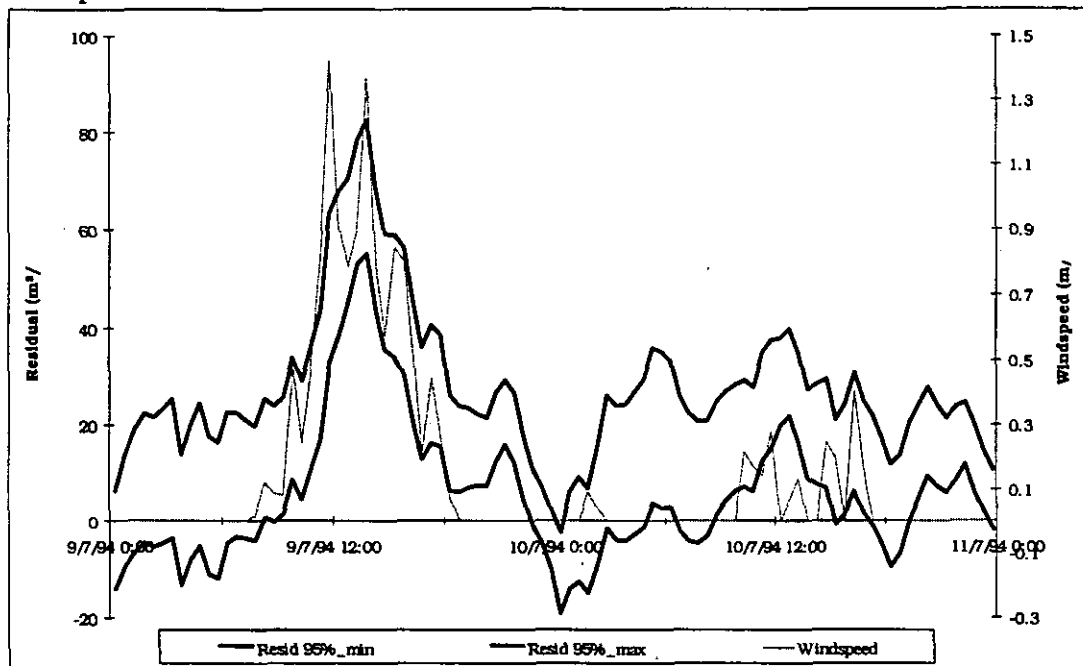


Figure 4.23: Wind speed and confidence band of the residual (= measurement - simulation) of the air flow rate through the external opening.

The above comparisons also clearly show the existence of a so-called turbulence effect. Indeed, one can see that the simulation is nearly always smaller than the measurement (even without wind). This turbulence effect is a constant value which is the minimal air flow through a large opening. Thus, even without any temperature difference and without wind there will still be a certain air flow through a large opening.

In Figure 4.24 one can see that the confidence bands of the measured and simulated air flow rates through the internal opening are not always overlapping. But, in comparison with the external opening, the correlation between the wind speed and the residual doesn't seem to be so good (this can be seen in Figure 4.25).

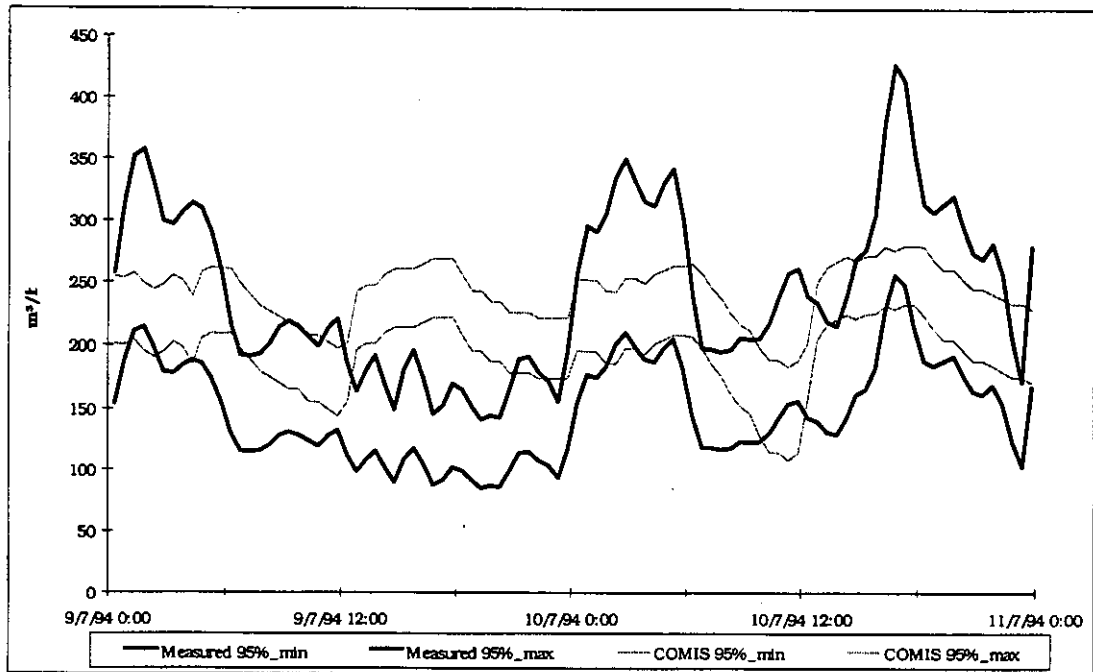


Figure 4.24: Confidence bands of measured and simulated air flow rate through the internal opening

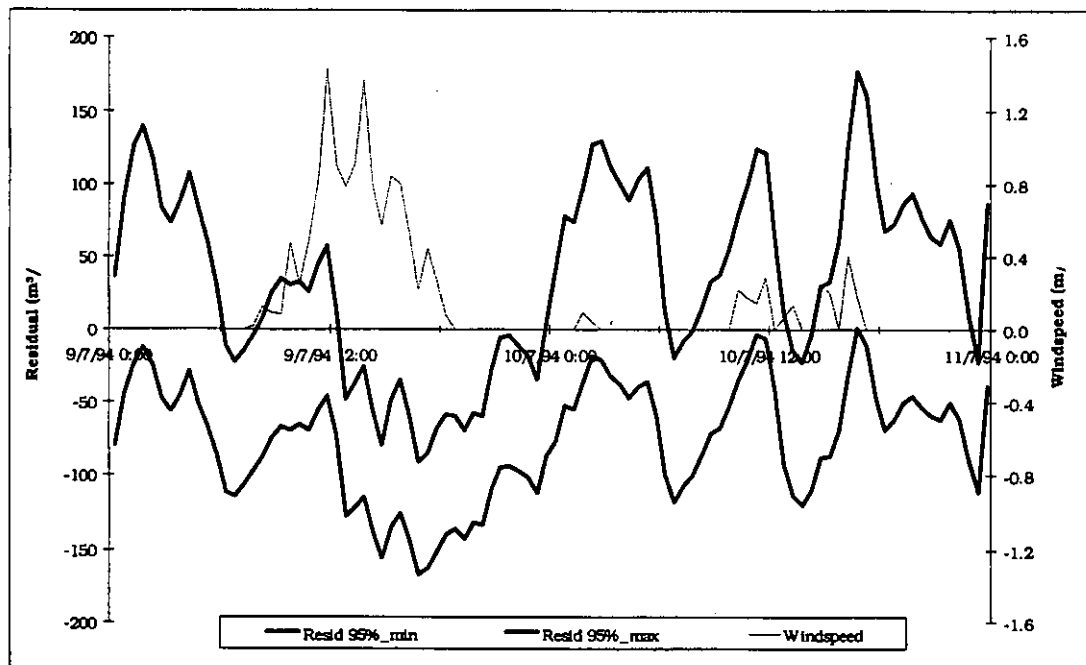


Figure 4.25: Wind speed and confidence band of the residual (= measurement - simulation) of the air flow rate through the internal opening.

Fractional Factorial analysis shows that the discharge coefficient is an important parameter. Besides, the influence of the temperature difference across the opening seems to become more important when its value gets smaller.

#### 4.6.5 Conclusions

In COMIS 1.2,s no algorithm is enclosed to compute the effect of the wind on the air flow rate through large openings. Nevertheless, the wind has an important influence on the air flow through external large openings. For the internal openings, the influence of the wind is not so obvious.

The comparisons also show the existence of a turbulence effect.

It is clear that the integration of models in COMIS to describe the wind effect and the turbulence effect should make it possible to make better predictions of the air flow rates. Unfortunately, such models are not at all evident, because they depend on a whole series of parameters.

## 4.7 Belgian Flat

### 4.7.1 Presentation of the building

The measurements were done in an unoccupied flat in Namur, Belgium. The flat is situated on the ground floor of a building with 9 storeys and is enclosed by two other ones. The air is extracted from the toilet, the bathroom and the kitchen by natural ventilation through common ventilation ducts, by means of a shunt-type connection (that means that the above flats are connected to the same 'main'-duct). A more detailed description is given in Appendix A.4.7).

### 4.7.2 Measurements performed

The following measurements were done:

- air flow rate through the ducts of natural ventilation by means of tracer gas (N<sub>2</sub>O);
- fresh air supply into each room with tracer gas (constant concentration technique with SF<sub>6</sub>);
- contaminant spreading in the different rooms: CO<sub>2</sub> and water vapour were injected in a certain room during specific periods and the concentration was measured continuously in 50 different points all over the flat;
- temperatures:
  - inside the apartment: 50 measurement points;
  - outside.

### 4.7.3 Compared element

The main focus is on the comparison of the spreading of CO<sub>2</sub> in the apartment, starting from given fresh air supplies. The reason why the fresh air supplies are entered as known parameters (and thus not simulated), is that there are big uncertainties on the Cp-values (the pressure differences between inside and outside were not measured), and also the air flow rates through the ducts of natural ventilation are difficult to simulate because different apartments are connected to the same main duct.

The fresh air supplies are simulated by putting a fan in each external wall, which gives the same air flow rate as the measured one; on the other hand the extraction ducts are entered as cracks. The sum of the duct flows is supposed to be the same as the total fresh air supply (assuming that there is no cross ventilation), and it is so because the total measured duct flow was always higher than the measured fresh air supply, which is impossible.

In Figure 4.26 the principle is shown.

To do the comparison between measurement and simulation, much attention is paid to the confidence intervals. The confidence interval of the simulation result is determined by performing a Monte Carlo analysis (in this case it exists of 100 runs): for each simulation run the input parameters are given different values depending on the accuracy of the input parameters.

With a Fractional Factorial analysis the influence of each parameter on the final result is determined.

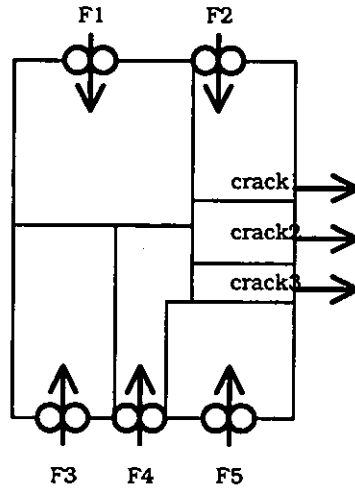


Figure 4.26: Use of fans and cracks to simulate the air flows in the apartment.

Two situations were examined: one with the inside doors open and one with the inside doors closed. In both cases CO<sub>2</sub> and water vapour were injected over 2 hours (from 22h00 to 24h00) in bedroom 2.

#### 4.7.4 Simulation results and comparison with the measurements

##### *Situation with the inside doors open*

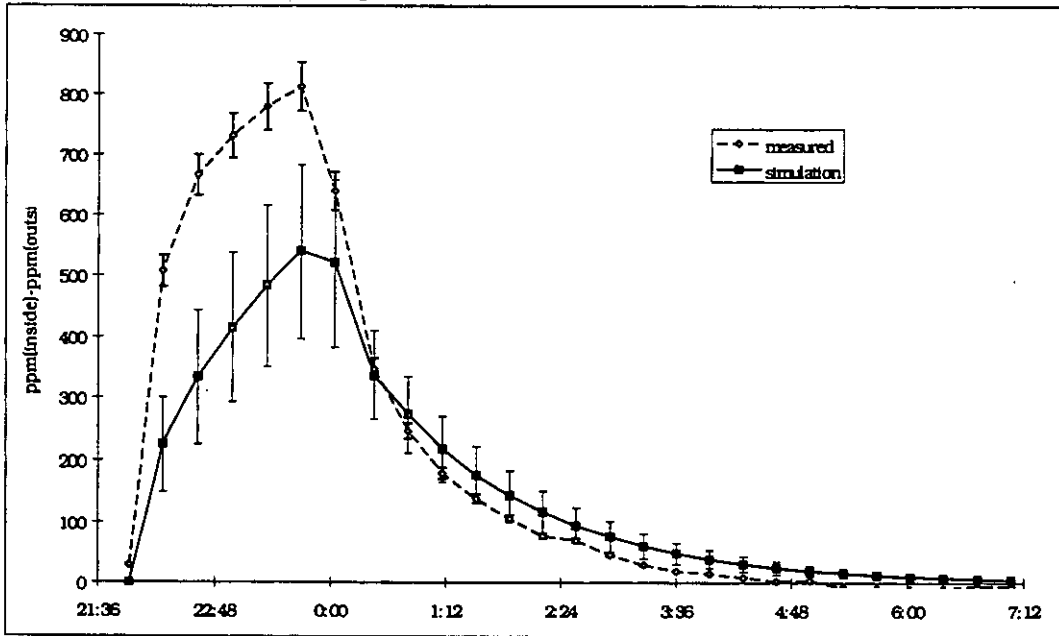


Figure 4.27: Measured and simulated CO<sub>2</sub>-concentration in bedroom 2; doors open.

If the confidence intervals of measurement and simulation overlap, one can say that the difference between both is acceptable. It does not mean a priori that one can have total confidence in the tool, but it increases the confidence in the tool for this specific range of input parameters.

The agreement between measurement and simulation is good for all the rooms (an example is shown in Figure 4.28) except for the injection room (= bedroom 2)(see Figure 4.27). One wonders if the difference for the injection room is an indication of an error in the algorithm or if it is caused by an incorrect value given to a certain input parameter. The following is an

explanation. The distribution of the final results appears to be not normal. This is caused by the value of the temperature difference. Indeed, the concentration in the room is inversely proportional to the square root of the temperature difference. This means that for small temperature differences the air flow rate will be more sensitive to changes of temperature than for higher temperature differences. This is probably the cause of the difference between simulation and measurement: indeed, the runs of the Monte-Carlo analysis with the smallest temperature differences seem to have a good agreement with the measurement.

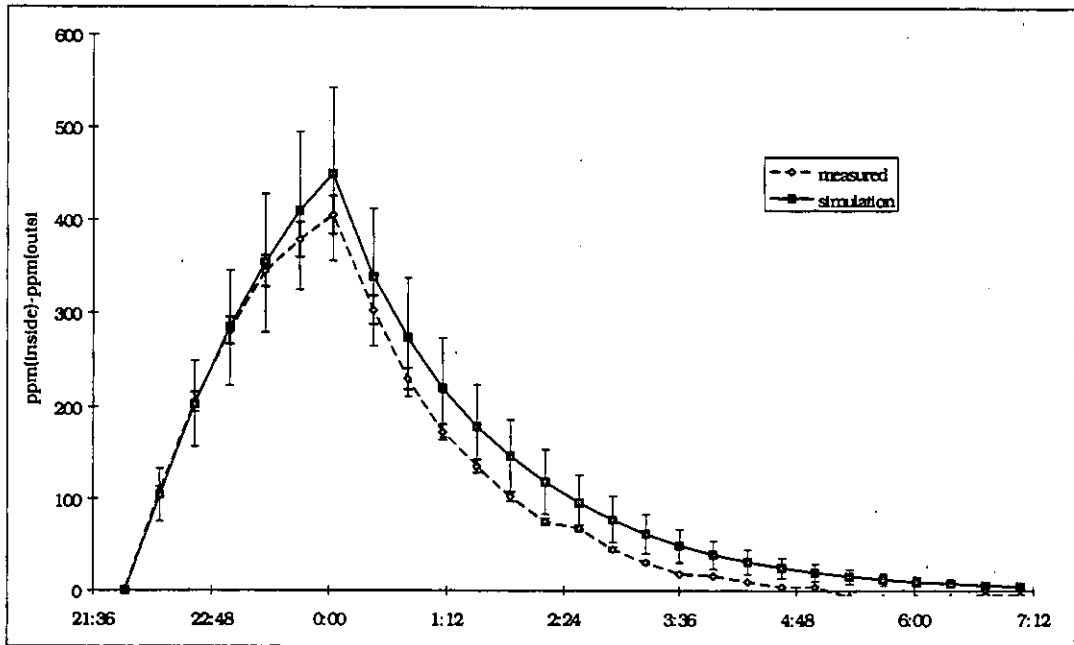


Figure 4.28: Measured and simulated CO<sub>2</sub>-concentration in the toilet; doors open.

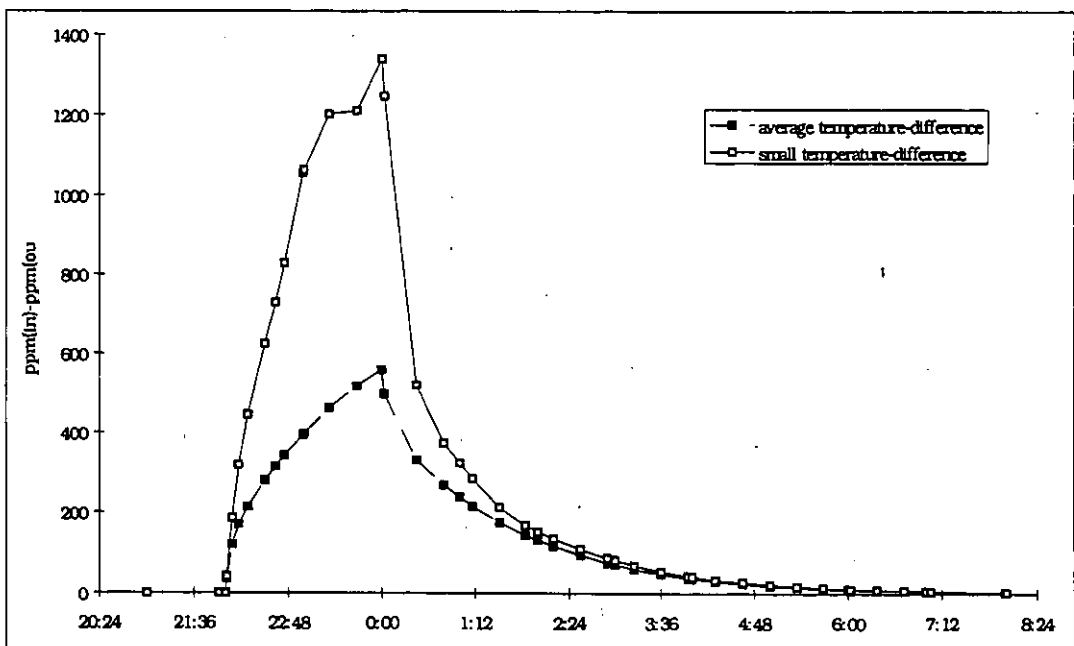


Figure 4.29: CO<sub>2</sub>-concentration in bedroom 2: two COMIS 1.2 -simulations with different temperature difference; doors open.

In Figure 4.29 the importance of a good choice (= good knowledge) of the temperatures in the rooms is shown by doing two simulations: one with a temperature difference of 0.05 K (= small) and one with a temperature difference of 1.8 K: this is the temperature difference calculated with the averages of the room temperatures (in each room the temperature was measured on different places).

The effect of the parameters on the final result changes over a period of time and also from room to room. In Figure 4.30 a result is given of a Fractional Factorial analysis of the injection room. It can be seen that the most important parameters are the injection rate and the temperature difference between both rooms. After injection, the influence of the fresh air flow rates becomes more important.

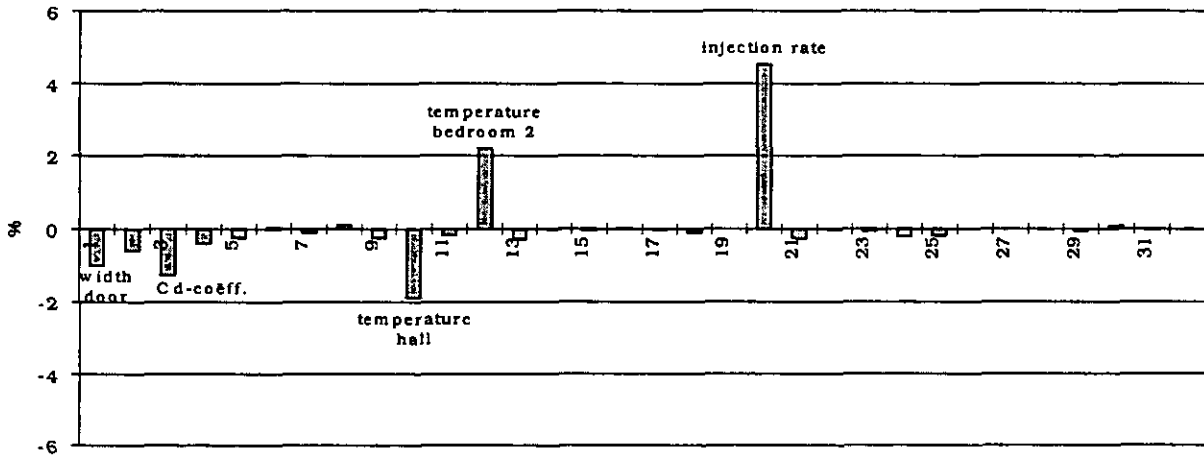


Figure 4.30: Main effects for the CO<sub>2</sub>-concentration in bedroom 2 at 23h00: doors open.

**Situation with the inside doors closed**

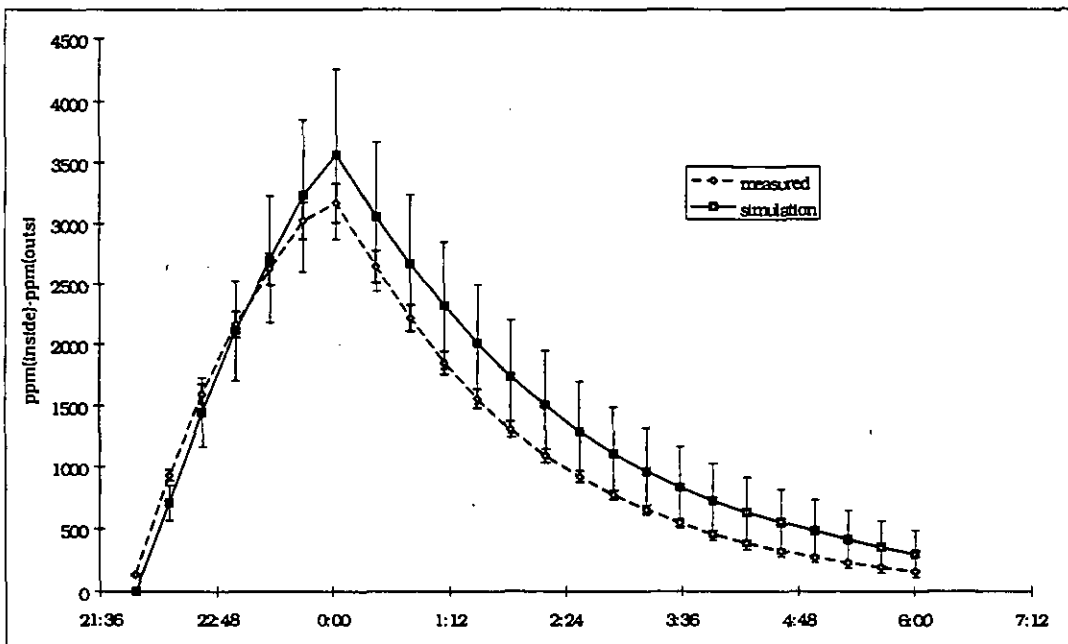


Figure 4.31: Measured and simulated CO<sub>2</sub>-concentration in bedroom 2; doors closed.

There is a rather good similarity between measurement and simulation for the injection room, as one can see in Figure 4.31.

For the other rooms there is no overlap after injection (an example is shown in Figure 4.32). This is probably caused by the fact that cross ventilation occurs, which is not simulated since the fresh air supply is only simulated by one fan per room and all of the fans are supply fans. Simulating the cross ventilation by extra fans is not possible since the cross ventilation was not known (due to measurement problems: total duct flow > total fresh air supply). Due to this cross ventilation a part of the pollutant will leave the flat through the external walls and, as a result, the concentration in certain rooms will decrease faster in reality than in the simulation. It has to be mentioned that cross ventilation is very probable in this case since the internal doors are closed.

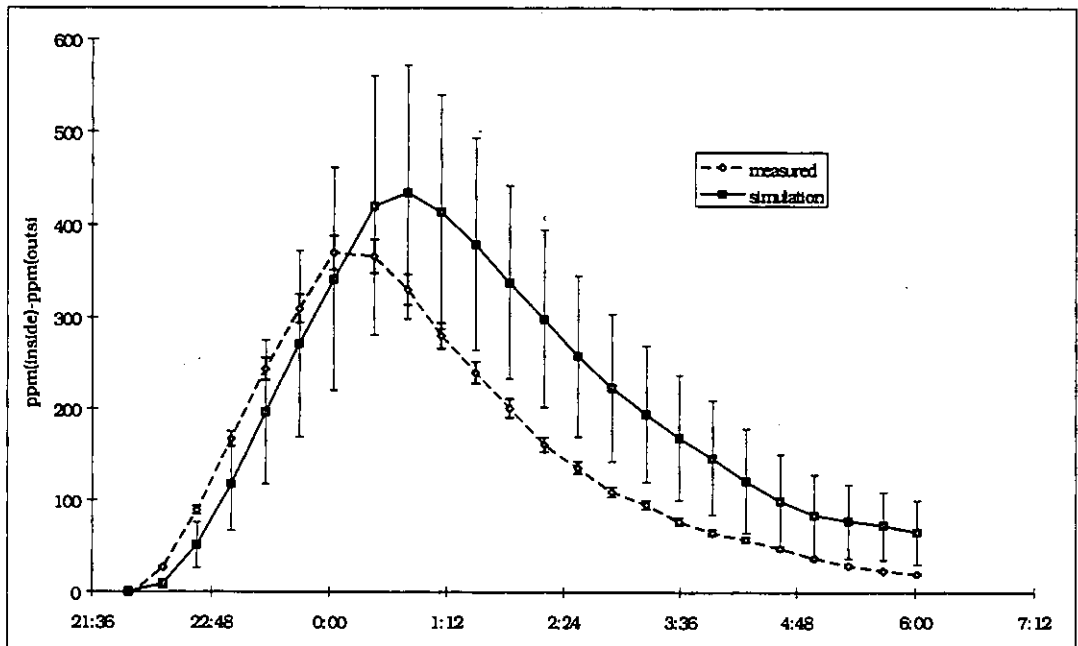


Figure 4.32: Measured and simulated CO<sub>2</sub>-concentration in the bathroom; doors closed.

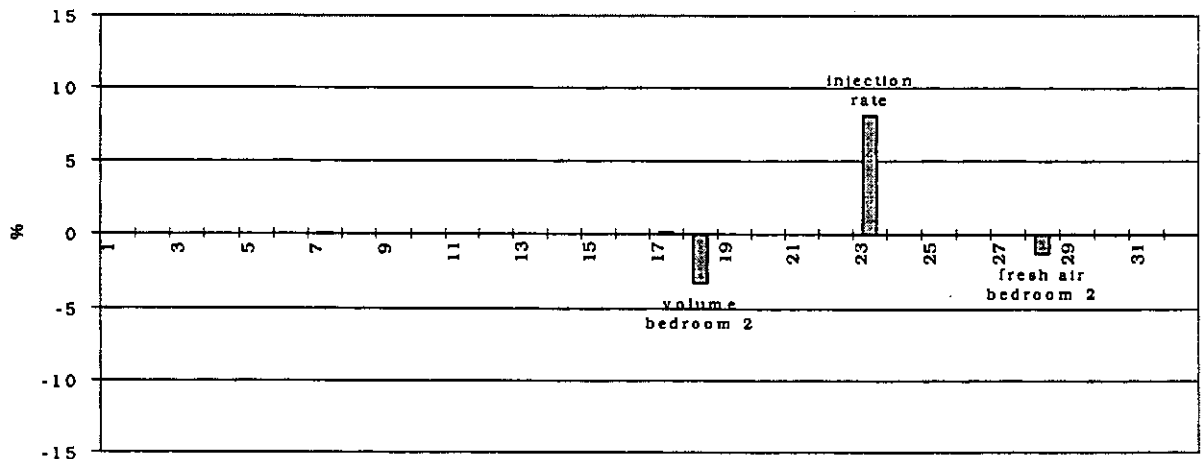


Figure 4.33: Main effects for the CO<sub>2</sub>-concentration in bedroom 2 at 23h00: doors closed.

A Fractional Factorial analysis shows that, for the injection room only, 3 parameters influence the CO<sub>2</sub>-concentration in this room (see Figure 4.33): the injection rate, the volume and the fresh air supply. For the other rooms the characteristics of the doors (= the cracks around the doors) are also important.

Assuming that there is no double flow when the inside doors are closed, it is possible to simulate the air flows in the apartment by a simple model. There seems to be a good agreement between the results of this simple model and the results obtained with COMIS 1.2. This clearly indicates that it is not always necessary to use complex tools to perform a simulation.

#### **4.7.5 Conclusions**

The purpose of these simulations was the evaluation of a part of the simulation tool COMIS 1.2: i.e. the spreading of pollutants.

In a situation with the inside doors open, the temperature difference between the rooms appears to be an important and even critical value. As a consequence, a good knowledge of the temperature distribution in the dwelling is required, as clearly performing a simplified simulation with one temperature for the whole apartment will not give a good prediction of the pollutant spreading if there are temperature differences between the rooms.

In a situation with the inside doors closed the differences between measurement and simulation are caused by not taking into account the cross ventilation. Besides, it is possible to predict the pollutant spreading by using a simple model.

It can be said that COMIS 1.2 can make a good prediction of pollutant distribution assuming that the fresh air supplies are known. The differences between measurement and simulation are mainly caused by measurement problems (temperatures, cross ventilation...).

#### 4.8 PASSYS Cell and large opening experiment in Greece

Single sided natural ventilation experiments were carried out in the Institute of Meteorology and Physics of the Atmospheric Environment of the National Observatory of Athens, Greece. The experiments were held in an office room on the second floor of the building. The room was isolated from the rest of the building. The only exterior opening of the room is a variable-area window, facing north-west. The window is divided into five parts which open separately, thus providing the means to vary the opening surface. The area of each part is :  $A_1 = A_2 = 0.34 \text{ m}^2$ ,  $B_1 = B_2 = 0.60 \text{ m}^2$  and  $C = 0.66 \text{ m}^2$ . A total of 15 different opening configurations were tried.

The same experiment was repeated four times in a PASSYS Test Cell, an outdoor two-zone experimental facility used for thermal monitoring. The cell is divided in two rooms, called the "test room" and the "service room". The test room has a volume of  $38.04 \text{ m}^3$  and a communicating door to the service room. The experiments were carried out in the service room, a zone of a  $28 \text{ m}^3$  volume, with a length of 2.4 m and a floor area of  $8.6 \text{ m}^2$ . The room communicates with the outdoor environment through a  $2.02 \text{ m}^2$  door opening.

Experiments were performed according to the single tracer gas decay technique.  $\text{N}_2\text{O}$  was used as a tracer gas. A BBRI injection-measurement system and an infrared gas analyser were used in order to measure the  $\text{N}_2\text{O}$  concentration in the room. A large number of injection and measurement points were distributed in the investigated zones in order to provide homogeneous mixing of the gas in the room air. The sampling period was 30 s. The thermal behaviour of the rooms where the experiments took place was constantly monitored. Internal and external surface temperatures as well as indoor air temperatures at various heights were measured by PT100 sensors. Two DANTEC sensors were placed at the bottom of the opening in order to measure the air velocity on both sides. During the test cell experiments additional temperature measurements were taken by T-fast sensors placed at various heights inside the service room as well as the opening. The air velocity at the cell entrance was monitored by a vertical array of five triple hot wires and three DANTEC sensors. Climatic data concerning ambient air temperature, wind speed and direction were provided by standard meteorological stations near the test sites.

COMIS was used for a sensitivity analysis in order to study the impact of various parameters (wind, temperature difference, opening geometry and discharge coefficient) on single sided ventilation. The predicted air flow was found to change as a function of the absolute value of the temperature difference as well as a function of the opening height. As in all network models, predictions by COMIS were found to be insensitive to variations in the wind speed.

Analysis of the climatic parameters during the experiments has shown, that experiments were characterised by medium to high wind speeds with unimportant fluctuation on the incidence angle and small indoor-outdoor temperature differences. Use of Warren Plots has proved that the air flow during the experiments was dominated by inertia rather than gravitational forces.

COMIS was used in order to simulate every experiment and predictions were compared to experimental results. A discrepancy was detected between experimentally derived and predicted air flow rates. This inaccuracy is attributed to the fact that COMIS, as well as all other existing network models, fails to consider the impact of inertia forces in the case of single sided ventilation. Based on these experimental data, a new correlation was developed to improve the accuracy of COMIS and network models in general, in predicting the air flow in the case of inertia dominated single sided ventilation.

COMIS was run to predict the air flow for all the single sided ventilation experiments carried out in Greece. For all simulations a discharge coefficient,  $C_d$ , equal to 1 has been attributed to the opening. A correction factor,  $CF$ , defined as:

$$CF = \frac{\text{Mean measured air flow}}{\text{Predicted air flow}}$$

was calculated for each experiment. In an attempt to correlate the correction factor with an index showing the relative importance of wind induced and buoyancy forces, the following methodology was developed.

The  $CF$  values were correlated with the Archimedes number,  $Ar_D$ , defined as:

$$Ar_D = \frac{Gr}{Re_D^2} = \frac{gH^3\Delta T}{TV^2D^2}$$

where  $D$  is the depth of the room, used as a characteristic length,  $L$ , for the Reynolds number:

$$Re_D = \frac{VD}{\nu}$$

The room depth is defined as the distance between the wall, where the opening(s) is(are) and the wall opposite to it in the single sided ventilated zone.

A very satisfactory correlation was found between the correction coefficients,  $CF$ , as calculated for all the experiments and the Archimedes number, as previously defined. Therefore the  $CF$  coefficient can be calculated, for single sided ventilation configurations, from the following expression :

$$CF = 0.08 (Ar_D)^{-0.38}$$

The  $r^2$  of the regression is calculated equal to 0.73. If the correction factor takes values under the limit of 0.6 then  $CF$  is taken equal to 0.6.

The proposed methodology was found to considerably improve the accuracy of COMIS in predicting the air flow rate in the case of single sided ventilation.

The  $CF$  model was based on data from experiments with wind speed ranging from 2 to 10 m/s and temperature differences from 0.5-8 °C. The room depth varied from 3-7 m. The prevailing wind direction during the experiments varied from -60 to 60 degrees from the vertical to the opening.

## 4.9 Italgas House

### 4.9.1 Measured object: Italgas House

An experimental facility has been built in Venaria (Torino) and put into operation in 1990 by the Italian gas utility "Italgas". It consists of two identical single-family buildings. The buildings - which are realistic examples of current building practice in the residential sector in Italy - are very flexible in terms of thermal systems installation, and are fully instrumented for monitoring relevant parameters such as ambient temperatures, meteorological conditions, combustion analyses, etc.

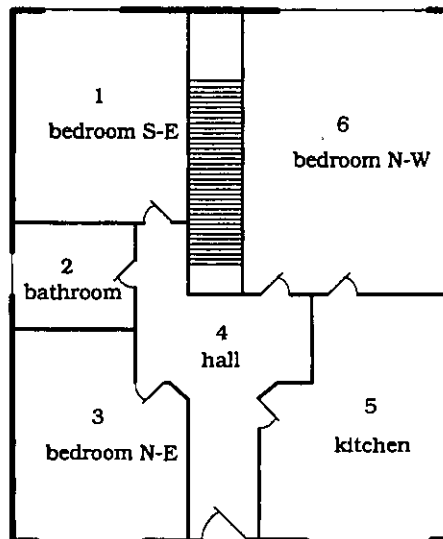


Figure 4.34 - Plant view of one Italgas House

These buildings consist of two storeys: the basement hosts the centralised service equipment and the data acquisition and processing system; the ground floor (in which the tests were performed) has a floor area of 114 m<sup>2</sup>, and includes two bedrooms, a living room, a bathroom and a kitchen. If necessary, the attic space above the ground floor can be heated, so that the test story may also reproduce the thermal condition of an apartment in a multi-storey building. A plan view of the test area is shown in Figure 4.34.

### 4.9.2 Measurements performed and main features examined

The tracer gas measurements, performed for the COMIS evaluation task, have been carried out during two different periods: October 1992 and January 1994. The experimental apparatus developed at Dipartimento di Energetica of the Politecnico di Torino was used. The main features of the measurements are summarised in Table 4.6. During the October 1992 tests, the air change rate in the dwellings which contain individual small gas-fired units for space heating and hot water production, have been measured in order to investigate the influence of purpose-provided ventilation openings (sized according to the national UNI-CIG 7129-72 standard) on air changes and IAQ. In Table 4.6 the values of the air supply area for the purpose-provided opening and the area of the chimney cross section are given for each test.

### 4.9.3 Main results of the comparison

Based on the data collected by the meteorological station at the Italgas Houses and on the results of previously performed pressurisation tests, simulations of the air flow behaviour

during the measurements have been performed using COMIS. The complete sensitivity analysis of the COMIS results for each test have been performed using the Monte-Carlo method with the help of MISA (Multirun Interface for Sensitivity Analysis) [Fürbringer, 1994]. The comparison between the measured and simulated air flows is illustrated by means of diagrams in which the confidence interval for each value, is represented (for 99% probability).

Table 4.6: Summary of experimental measurements in the Italgas Houses

TEST CODE	DATE	PERIOD [s]	N° ZONE	Tracers	NOTES
G3-04	07-10-1992		1	SF6	- air supply area 100%; - chimney cross section 100%
G3-05	07-10-1992		1	SF6	air supply area 100%; -chimney cross section 50%
G3-06	08-10-1992		1	N2O	air supply area 100%; - chimney cross section 25%
G3-07	08-10-1992		1	N2O	air supply area 50%; - chimney cross section 100%
G3-08	08-10-1992		1	N2O	air supply area 50%; - chimney cross section 50%
G3-09	08-10-1992		1	N2O	air supply area 50%; - chimney cross section 25%
G3-10	08-10-1992		1	N2O	air supply area 0%; - chimney cross section 100%
G3-11	08-10-1992		1	N2O	air supply area 0%; - chimney cross section 50%
G3-12	08-10-1992		1	N2O	air supply area 0%; - chimney cross section 25%
G3-15	09-10-1992	3809	2	N2O; SF6	only internal doors of room 5 are closed; the air samples in the rooms 1,2,3,4,6 are mixed before reaching the analyser; N2O is injected in rooms 1,2,3,4,6; SF6 is injected only in room 5; air supply area 50%; chimney cross section 50%
G3-16	09-10-1992	4288	2	N2O SF6	only internal doors of room 5 are closed; the air samples in the rooms 1,2,3,4,6 are mixed before reaching the analyser; N2O is injected in rooms 1,2,3,4,6; SF6 is injected only in room 5; air supply area 0%; chimney cross section 50%
G4-03	14-01-1994	4813	2	N2O SF6	only internal doors of room 5 are closed; the air samples in the rooms 1,2,3,4,6 are mixed before reaching the analyser; N2O is injected in rooms 1,2,3,4,6; SF6 is injected only in room 5
G4-04	14-01-1994	4184	2	N2O SF6	only internal doors of room 6 are closed; the air samples in the rooms 1,2,3,4,5 are mixed before reaching the analyser; N2O is injected in rooms 1,2,3,4,5; SF6 is injected only in room 6

Figure 4.35 refers to the single zone tests (G3-04 ÷ G3-12). The simulated and the measured air flow rate compared in the Figure represents the total (net) flow of Zone 5 which in these tests corresponds to the air flow from outside to zone 5 ( $Q_{05}$ )<sup>3</sup>. In the Figure, the Air Supply Opening (ASO) and the Chimney Cross Section (CCS) are specified for each test, in order to clarify the influence of the purpose-provided ventilation opening and the butterfly valve position on the room ventilation.

The analysis of these results show the strong influence of the chimney stack effect on the room ventilation and therefore special attention should be given to the choice of the single loss coefficient representing the butterfly valves as many different values can be found in literature. There are only two tests in which the error range of the simulated value and the error range of the measured value do not overlap (G3-09 and G3-12); in both tests the chimney cross section is 25%. That corresponds to the maximum value of the single loss coefficient representing the butterfly valve. Probably for such high single loss coefficient values a

<sup>3</sup> Accurate definition of inter-zonal air flows is given in Appendix A 10, Table A4.10.4

greater error range than 25% (here used in the Monte Carlo Analysis) should be used, since when a valve is near to the closed position, a high variation of the single loss coefficient is associated with a small error in the knowledge of the valve position.

The tests of January '94 are chosen in this summary to provide an example of the comparison results for the two zone case. These tests were performed without the gas fired unit and the purpose-provided opening. As the wind velocity was very low or zero, these tests refer to a system in which the air flows are mainly driven by the thermal buoyancy due to temperature difference between inside and outside. For this reason, in Figure 4.36 the temperature difference is plotted together with the measured and simulated total flow rate for tests G4-03 and G4-04.

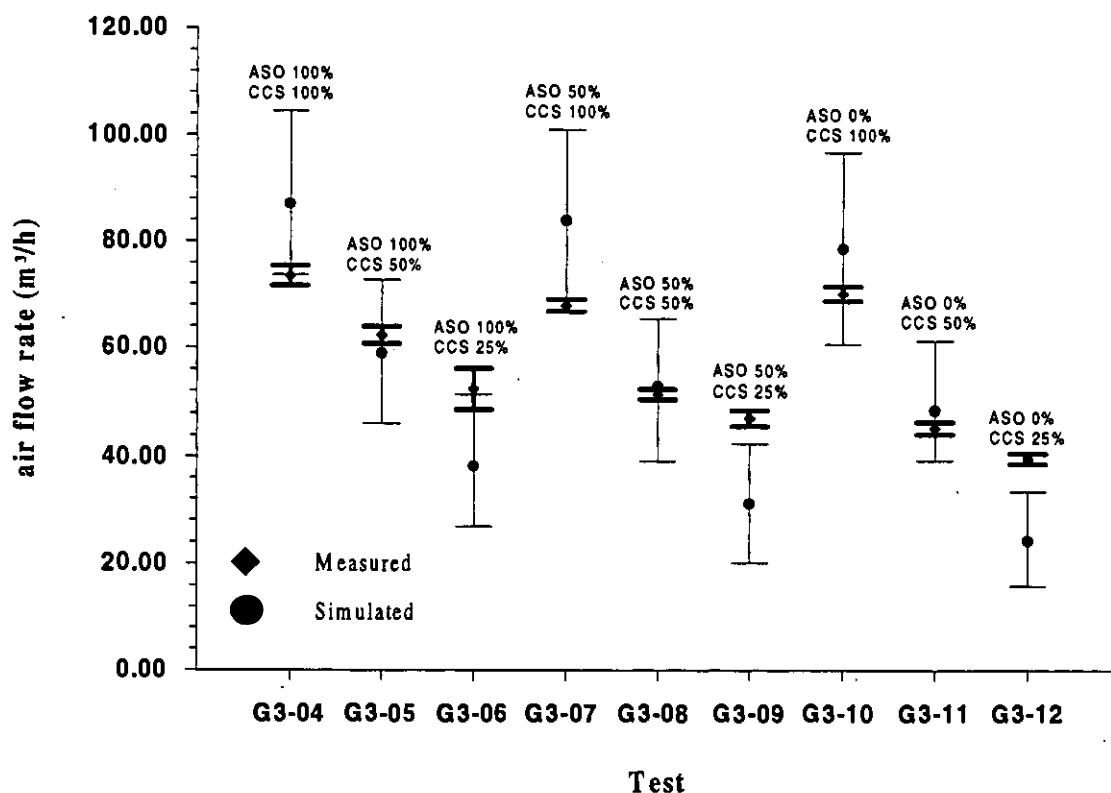


Figure 4.35: Simulated and measured air flow rates for tests G3-04 ÷ G3-12; ASO = Air Supply Opening and CCS = Chimney Cross Section

For test G4-03 a good agreement is found between both the mean value of the simulated and experimental flows and the experimental air flow trend and the temperature difference trend; furthermore in both tests the error ranges of the total air flow rate do overlap.

The largest difference is for flow  $Q_{01}$  (from -10 % to +20%) while in the other flows ( $Q_{05}$ ,  $Q_{51}$  and  $Q_{15}$ ) the discrepancy is smaller. In this test the error range of the simulated flows and the measured flows are always overlapping.

For test G4-04 the simulated flows  $Q_{61}$  and  $Q_{01}$  are very close to the measured flows and the error ranges overlap;  $Q_{06}$  is overestimated by more than 100% but the error range of the simulated values includes the measured value for about half the measurements period. The mean measured value of the measurement period is within the error range of the mean simulated value.

The simulated flow  $Q_{16}$  is about 70% less than the measured value and the error ranges in this case never overlap. There are no evident reasons to explain this complete discrepancy. It is

only possible to suppose that the literature value used to describe the internal door cracks in this case was not close to the actual value as for test G4-03.

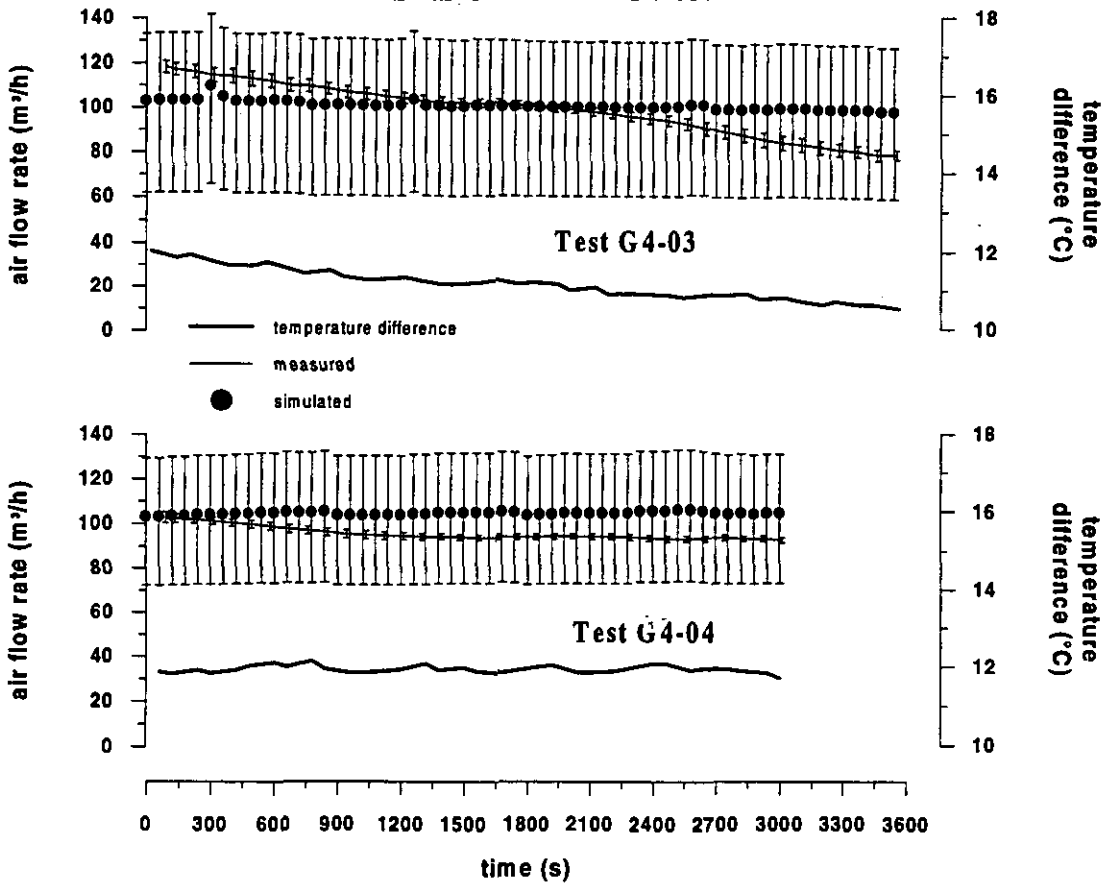


Figure 4.36: Total flow rate for test G4-03 and G4-04

#### 4.9.4 Conclusion

The possibility of simulating devices (i.e. boilers) which are not included in the COMIS data base has been shown in tests G3-04 to G3-12, but special attention has to be paid to the duct description especially as far as the single loss coefficients are concerned.

Furthermore, the sufficient agreement obtained in tests G4-03 and G4-04, allows one to regard COMIS as a useful tool for analysing the air flow inside a detached house when thermal buoyancy is the main force causing the air flows.

Finally, it is important to mention the role of the error range associated with the simulated value in this comparison: most of the values of simulated air flow rates are quite different from the measured values (sometimes more than 100%) and only the overlapping of the error ranges has enabled an agreement to be reached between the measured and the simulated flows. For this reason the use of COMIS in the air flow simulation is strongly related to the knowledge of the associated error range.

## 4.10 Conclusion of the comparison

Here are only the conclusions drawn from comparisons of measurements versus simulations. A general conclusion is proposed in chapter 6.

Comparisons of nine cases have been presented. The level of complexity varies from one case to another as well as the depth of the analysis.

For cases including only cracks as flow components, the following comments can be made:

- a) The OPTIBAT case (§4.2) is the most controlled experiment in this set since this flat is in an artificial environment. In spite of that, when checking concordance at the level of the flow matrix, many flows are found by measurements and not in the simulation, or alternatively, some flows are highly overestimated by the simulation. For many flows, assumed uncertainties do not sufficiently explain the discrepancies: the actual difference between simulated and measured data must be admitted. The explanation for this is still to be found.
- b) For the Japanese solar house (§4.3) the comparison works well. This experiment has the advantage of being simple enough to be well controlled. The fact that it has the same number of zones and gases allows the estimation of all flows. Also, on the experimental side, it gives a comprehensive image of the flow pattern. However, the differences between the measured and the simulated flow matrix, even if covered by experimental uncertainty, are quite large. The appearance of a negative flow in the measured flow matrix seems to suppose that the tracer gas analysis algorithm is not the best one possible, but it should be also considered that the actual boundary conditions are not the same as those in the simulation, because the external flows do not coincide. Furthermore, it should be noted that, even in simple cases, the determination of the flow matrix is not straightforward and the considerable uncertainty is still present.
- c) The case of the Japanese family house (§4.4) is similar to the Optibat case. In Figure 4.11 (b) one can observe the same tendency with measured flows not found in the simulation, and vice versa. Many flows are situated outside of the  $\pm 25\%$  interval. An error analysis would show whether confidence intervals overlap.
- d) The LESO case (§4.5) shows satisfactory agreement for the main flow through the staircase. Unfortunately, the flow matrix was not available experimentally because the zones were too numerous. The sensitivity analysis which focused on pressure coefficient uncertainty shows that the comparison could have been worse. Hopefully, Murphy's law does not work so well for multizone ventilation! In fact, the building is stack dominated and some stability can be observed (cf. Appendix 4.5.). This case also illustrates the difficulty of identifying measurement errors. Another point worth noting is that this particular case is the only one whose tracer gas measurements have been performed using the constant concentration technique.
- e) The ITALGAS case shows some agreement and some discrepancies, between simulated and measured air flows. From this case, it can be observed that the confidence intervals are much larger for the simulation than for the measurement, highlighting the problem of precisely defining a network and its boundary conditions. It seems harder to determine the former than to measure air flows. A higher sensitivity to meteorological parameters ( cf. Figure 4.36) by measurement rather than simulation, has also been observed.

For cases which include large openings, the following comments can be made:

- a) These cases have demonstrated the limits of the large opening algorithm included in COMIS. The wind influence observed in the measurements is not taken into account in the simulation.
- b) Mainly, these cases illustrate the necessity and the advantage that a sensitivity analysis (including factorial design) represents. On that subject, the Namur flat (§4.7) is exemplary.

This series of comparisons illustrates the present state of the art in simulation and measurement of multizone air flow, as well as validation.

Significant differences between the measured image of ventilation and the numerical one exist in some situations which are not yet sufficiently identified even if some clues exist.

The main problem seems to be the description of the actual network and the determination of the boundary conditions. The uncertainty acts as a screen, and hides a part of the comparison which then makes it difficult to see the differences between our two representation of reality.

#### 4.11 References

- Amara, F., Depecker, P., Allard, F.: Air flow patterns study in Optibat cell - Inter-zonal air flows. Personal communication.
- Amara, F.: Contribution a la caractérisation aéraulique des bâtiments. Étude des transferts aérauliques dans les locaux multizones. *Phd thesis at INSA de Lyon, April 1993*
- Compagnon, R.; Fürbringer, J.-M. and Jakob, M.: "Mesure d'échange d'air entre les locaux et avec l'extérieur". *Final report project NEFF 339.2, EPFL-LESO, Lausanne, Switzerland 1991.*
- Dorer, V.; Fürbringer, J.-M.; Huck, F. and Roulet, C.-A.: "Evaluation of COMERL with the LESO Data set". *Final Report ERL B4.1, EMPA 175, CH-8600 Dübendorf, Switzerland, Dec 1992.*
- Dorer, V.; Fürbringer J.-M.: "Comparison of Multizone Air Flow Measurements and Simulations of the LESO Building including Sensitivity Analysis, *14th AIVC Conference, 1993*
- Fürbringer J.-M. : Sensibilité de modèles et de mesures en aéraulique du bâtiment à l'aide de plans d'expériences, PhD thesis, EPFL, Lausanne, CH, 1994.
- Fürbringer, J.-M.; Compagnon, R. and Roulet, C.-A.: Projet NEFF 339.1 "Validation de programmes de calcul des échanges d'air à l'aide de mesures expérimentales". *Final report, LESO-PB, EPFL, Lausanne, Switzerland, 1990.*
- Haghighat, F., Megri A.: Inter-program and experimental validation of two air flow models: COMIS and CONTAM. Personal communication.
- Megri, A.: Modélisation des transferts aérauliques dans les bâtiments multizones équipés d'un système de ventilation; prise en compte de la qualité de l'air. *PhD thesis at INSA de Lyon, January 1993*

## 5 USER TESTS

### 5.1 Introduction

The objectives of a user test performed on a computer program are:

- to assess the difficulties experienced by users when applying the data,
- to use the results to improve the specification of data sets and the input routines of multi-zone models, and
- to determine the errors made by users in interpreting multi-zone input data.

Two tests, prepared by the LESO and AIVC are proposed. The first represents a simple benchmark analysis in which a network and input data are provided. No interpretation of building leakage and weather data is necessary. The second is an open test requiring interpretation of the data by the user. The user must devise the network from the general information provided.

In each example, a simple data set is provided which should be used to prepare an input file. The results of the simulations, that is input and output files, were returned along with replies to a short questionnaire concerning the performance of the model.

The **questionnaire** asked the following questions:

1. Program and version used for the test
2. Purpose for which the program is mostly used
3. Data input processing:
  - a) Input processor
  - b) User friendliness(from -5, bad; through 0, OK; to + 5, good)
  - c) Problems encountered
  - d) Proposals for improvement.
  - e) Value of User Guide for input instructions(from -5,bad; through 0, OK; to + 5, good)
4. Data output processing:
  - a) Output processor
  - b) User friendliness(from -5, bad; through 0, OK; to + 5, good)
  - c) Problems encountered
  - d) Proposals for improvement.
  - e) Value of User Guide for output instructions(from -5, bad; through 0, OK; to + 5, good)
5. Other comments

### 5.2 User tests on case 1

#### 5.2.1 Presentation of the case

The USERTEST1 building is presented in Figure 5.1. It comprises a four zone system of 5 external flow openings and 5 internal flow openings. This test network has been devised to test input and output routines for a very simple example and to test the performance of the model in simulating both horizontal and vertical flow, thermal gradients and flow through vastly different sizes of opening. The wind pressure coefficient is given for each of the external openings while the height, leakage coefficient,  $C$  and exponent,  $n$ , are given for all openings. The objective is to evaluate the ventilation rate in each zone and the air flow rate in each path for the following set of conditions:

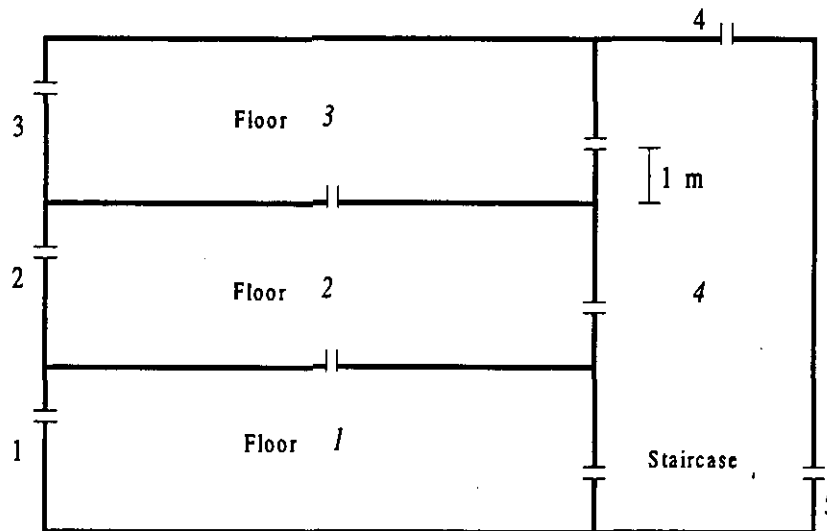


Figure 5.1: The building USERTEST1. Number of zones are in italics, while envelope elements are numerated in normal numbers.

The characteristics are presented in Table 5.1. All the outdoor-indoor conductances have the same air tightness. Between the zones and the stairwell, the conductances modelling the door are less tight especially in the first floor. The leakages through the ceilings are small.

Table 5.1: Characteristics of the zones of building USERTEST1.

Zone	1	2	3	4	
Volume	150	150	150	135	m <sup>3</sup>
Height	3	3	3	9	m
Floor above ground	0	3	6	0	m
Temperature	18	20	23	10-25	°C

Outdoor temperature is 10°C and there is a wind speed of 2 m/s at roof height (9m above ground). There is a uniform upwards temperature gradient of 1.67 K/m in zone 4.

Table 5.2: Characteristics of the envelope elements of building USERTEST1.

Envelope element	1	2	3	4	5	
Height above ground	2	5	8	9	1	m
Leakage coefficient	0.02	0.02	0.02	0.02	0.02	kg/s
Exponent	0.66	0.66	0.66	0.66	0.66	
Pressure coefficient	0.2	0.4	0.5	-0.4	-0.3	

Table 5.3: Characteristics of internal leakage's of building USERTEST1.

Leakage path	1-2	2-3	1-4	2-4	3-4	
Height above ground	3	6	1	4	7	m
Leakage coefficient	0.004	0.004	2	0.04	0.05	kg/s
Exponent	0.66	0.66	0.66	0.66	0.66	

### 5.2.2 Sensitivity analysis

In order to evaluate the effect of the variation of input parameters on responses of the model a sensitivity analysis, using factorial design [Fürbringer, 1992 and 1994], has been performed for this case. The infiltration rate in a building depends a priori on the ratio between the forces induced by the wind and by the thermal buoyancy. For that reason the sensitivity analysis has been performed for different wind speeds between 0.5 [m/s] and 4 [m/s].

A 2(24-16)IV fractional factorial design has been used. It allows, after 256 runs, the determination of 136 coefficients among the 301 corresponding to a linear model of 24 parameters. It is a design in which the main effects  $\alpha_i$  are neither confounded between themselves, nor with first order interaction coefficients, whilst the first order interaction coefficients are aliased between themselves. (cf. §1.2.4 and related literature) The tested parameters are listed in Table 5.4.

Table 5.4: tested parameters

Description	COMVEN parameters
1. elementary indoor - outdoor air tightness	CR_OUT
2. indoor-outdoor exponent	n_OUT
3. air tightness between the floors	CR_FL
4. exponent between the floors	n_FL
5. air tightness between zone 1 and stairwell	CR_ST1
6. exponent between zone 1 and the stairwell	n_ST1
7. air tightness between zone 2 or 3 and the stairwell	CR_ST2
8. exponent between zone 2 or 3 and the stairwell	n_ST2
9. temperature in the 1. floor	T_fl1
10. temperature in the 2. floor	T_fl2
11. temperature in the 3. floor	T_fl3
12. temperature in the stairwell	T_st
13. temperature gradient in the stairwell	grad(T)
14. windward pressure coefficient. in front of zone 1	Cp(1)
15. windward pressure coefficient. in front of zone 2	Cp(2)
16. windward pressure coefficient. in front of zone 3	Cp(3)
17. pressure coefficient. on the roof	Cp(4)
18. leeward pressure coefficient. at back of zone 4	Cp(5)
19. wind profile coefficient	W_profil
20. wind speed	W_speed
21. outdoor temperature	Tex
22. outdoor humidity	Humidity
23. atmospheric pressure	Patm

#### Results from the sensitivity analysis

The third zone is in a critical situation when the stack pressure compensates the wind pressure near 2.1 m/s. The fresh air cannot enter from the window and very little air enters from the stairwell. Consequently there is a very high age of air in this zone. Such situations are critical under the steady state conditions assumed for calculations. In reality, wind speed and direction fluctuate, and thereby smooth out the asymptotic low ventilation zone.

A similar phenomenon occurs for the stairwell when the wind speed is close to 2.2 m/s. The equilibrium between stack and wind pressure at the low opening of this zone results in less

ventilation compared to what occurs when one cause dominates. When the stack effect dominates, fresh air enters but it goes out when the wind is dominant.

The two other zones have monotone behaviour, the mean age of air always decreasing when the wind increases.

The air flows with the corresponding flow matrices are shown in Table 5.5. The elements of the flow matrix are defined as follows [Roulet & Vandaele 1991]:

$Q_{ij}$  = minus the air flow going from zone  $j$  to zone  $i$ :

$$Q_{ii} = \sum_{j=0}^N Q_{ji} (1 - \delta_{ij}) \quad (5.1)$$

In the first line of the matrix are the algebraic sums of respective columns, that is the total infiltration rate of each zone. In the first column of the matrix are the algebraic sums of respective lines, that is the total exfiltration rate of each zone.

Table 5.5: Flows matrices and flows for typical Archimedes number

Wind speed	Ar	Flow matrix	Flow scheme																								
1.3m/s	2.5	$l/s$ <table style="display: inline-table; vertical-align: middle;"> <tr> <td>0</td><td>0</td><td>50</td><td>122</td></tr> <tr> <td>71</td><td>71</td><td>0</td><td>0</td></tr> <tr> <td>38</td><td>-8</td><td>46</td><td>0</td></tr> <tr> <td>0</td><td>0</td><td>-9</td><td>50</td></tr> <tr> <td>63</td><td>-63</td><td>-37</td><td>0</td></tr> <tr> <td></td><td></td><td></td><td>163</td></tr> </table>	0	0	50	122	71	71	0	0	38	-8	46	0	0	0	-9	50	63	-63	-37	0				163	
0	0	50	122																								
71	71	0	0																								
38	-8	46	0																								
0	0	-9	50																								
63	-63	-37	0																								
			163																								
2.2m/s	0.7	$l/s$ <table style="display: inline-table; vertical-align: middle;"> <tr> <td>0</td><td>0</td><td>9</td><td>151</td></tr> <tr> <td>79</td><td>79</td><td>0</td><td>0</td></tr> <tr> <td>60</td><td>-7</td><td>67</td><td>0</td></tr> <tr> <td>0</td><td>0</td><td>-9</td><td>9</td></tr> <tr> <td>21</td><td>-73</td><td>-58</td><td>0</td></tr> <tr> <td></td><td></td><td></td><td>151</td></tr> </table>	0	0	9	151	79	79	0	0	60	-7	67	0	0	0	-9	9	21	-73	-58	0				151	
0	0	9	151																								
79	79	0	0																								
60	-7	67	0																								
0	0	-9	9																								
21	-73	-58	0																								
			151																								
3m/s	0.4	$l/s$ <table style="display: inline-table; vertical-align: middle;"> <tr> <td>0</td><td>0</td><td>0</td><td>256</td></tr> <tr> <td>97</td><td>97</td><td>0</td><td>0</td></tr> <tr> <td>94</td><td>-3</td><td>97</td><td>0</td></tr> <tr> <td>65</td><td>0</td><td>-7</td><td>73</td></tr> <tr> <td>0</td><td>-94</td><td>-89</td><td>-73</td></tr> <tr> <td></td><td></td><td></td><td>256</td></tr> </table>	0	0	0	256	97	97	0	0	94	-3	97	0	65	0	-7	73	0	-94	-89	-73				256	
0	0	0	256																								
97	97	0	0																								
94	-3	97	0																								
65	0	-7	73																								
0	-94	-89	-73																								
			256																								

The Archimedes number  $Ar$  is defined as:

$$Ar = \frac{\Delta T g h}{T_i v^2} \quad (5.2)$$

with  $\Delta T$  indoor-outdoor temperature difference, [K]

$g$  gravity acceleration, [ $\text{m/s}^2$ ]

$h$  warm zone height, [m]

$T_i$  indoor temperature, [K]

$v$  wind speed, [m/s]

This number corresponds to the ratio between stack and wind induced forces. It is lower than the one for a wind dominated situation, but larger than the one for stack induced flows.

Except when near the critical situation described above, close to  $Ar = 1$ , the standard deviation does not vary significantly with the wind speed variation. Figure 5.2 shows the standard deviation for the mean age of air for the 4 zones. During a critical situation, when the flows are very weak, an extreme sensitivity is observed, as seen in other cases.

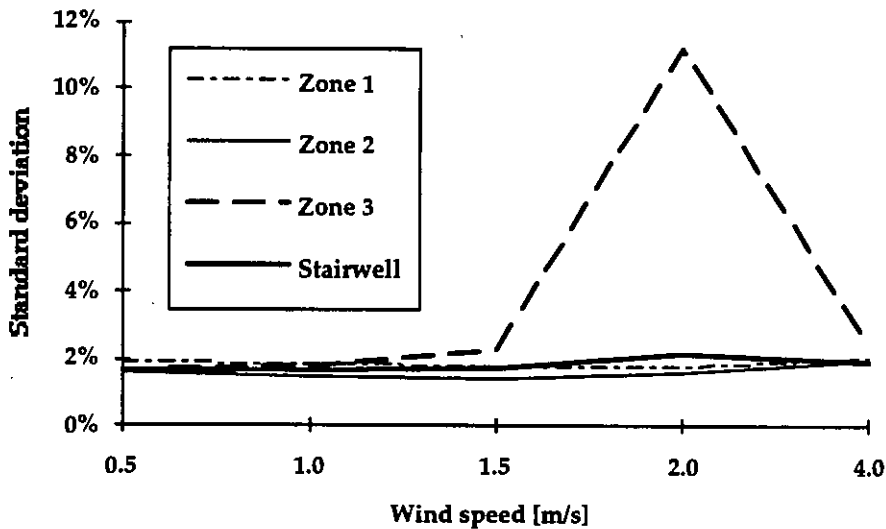


Figure 5.2: Variation of the standard deviation  $\sigma$  for the mean age of air obtained with 256 simulations.

Figure 5.3 presents the evolution of the largest main effects of the global mean age with increasing wind speed. The critical situation appears clearly here also, even hiding the monotone evolution of the effect of the wind speed and the temperatures.

We see that the test case, with a wind speed of 2 m/s, corresponds to the critical situation where small changes in temperatures and wind speed induce large changes in the results.

When comparing a stack dominated situation with a wind dominated one (Figure 5.4), the following remarks can be made:

the wind speed ( $W\_speed$ ) effect increases with the wind speed, but the relation is not linear as expected.

the same can be observed for the pressure coefficients ( $Cp(i)$ )

the inverse is observed for the temperatures ( $T_{ex}$ ,  $T_{fl2}$ ,  $T_{fl3}$ ,  $T_{st}$ ) and the temperature gradient in the stair well ( $Grad(T)$ ) whose effects decrease when the wind speed increases.

the other dominant parameters are the outdoor indoor air tightness ( $CR_{OUT}$ ) and the atmospheric pressure (1% variation in  $Patm$  corresponds to about 300m height or weather change). the effect of the exponent ( $n_{out}$ ) becomes important when the wind dominates.

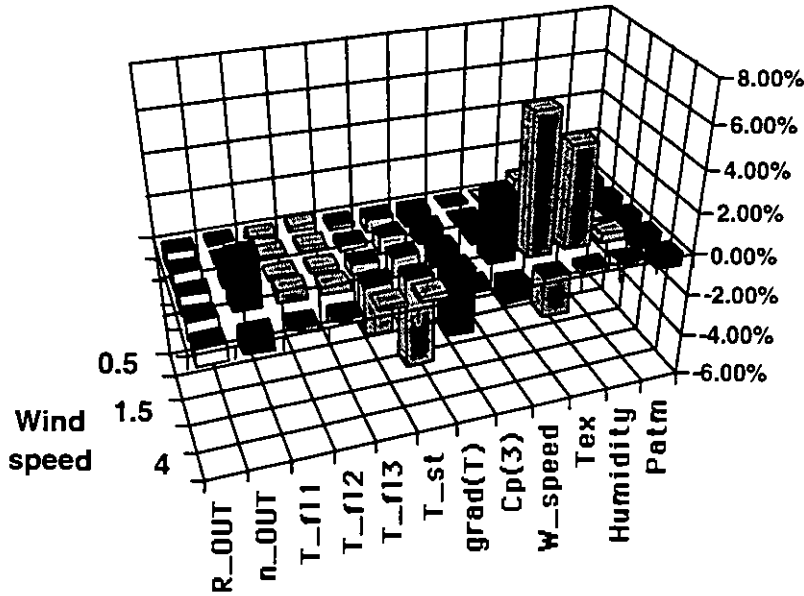
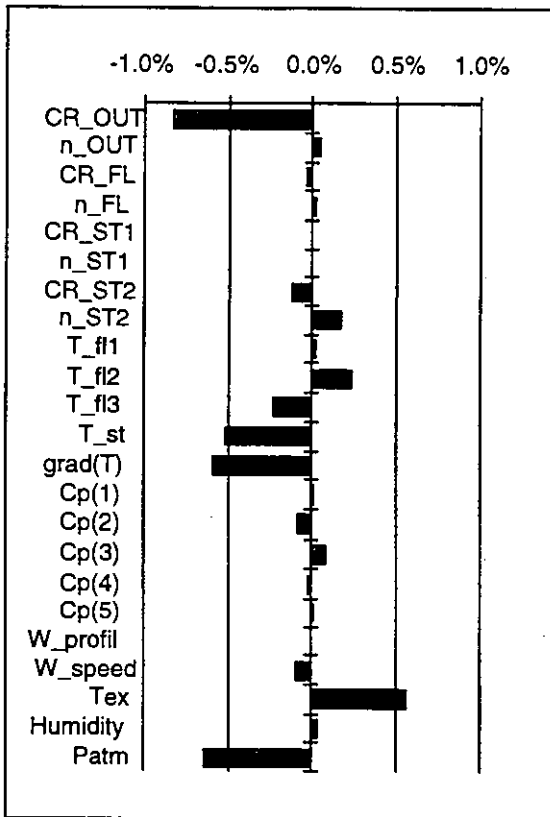


Figure 5.3: Evolution of the largest main effects with the wind speed

**Stack dominated situation**



**Wind dominated situation**

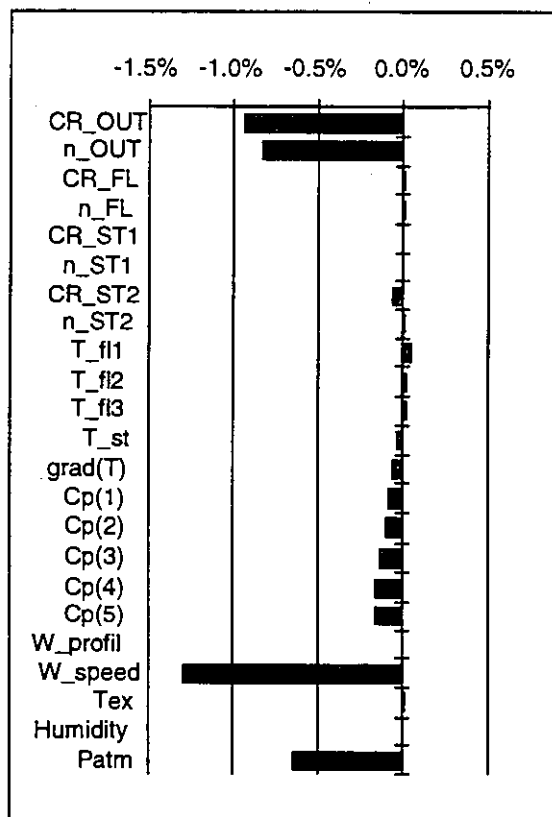


Figure 5.4: Comparison of main effects in a stack dominated situation ( $W_{speed} = 1m/s$ ) and a wind dominated one ( $W_{speed} = 4m/s$ ).

### 5.2.3 Results from first run

Two runs were performed with this building. The first run was initiated in November 1992, and was performed with COMIS 1.1 and the corresponding User Guide. Belgium, Canada, France, Italy, the Netherlands, Switzerland, USA and an anonymous participant replied. Belgium, the Netherlands and USA did not fill in the questionnaire. A summary of results is given in Tables 5.5 to 5.7, and comments, which are the most interesting results from this first run, are replicated below.

Table 5.6: Summary of replies to questionnaires

Program	Can	France	Italy	CH	Anon.
COMIS Version	1.1A	1.0	1.1	1.1	1.0
Input processor	COMIN & DOS editor	Text editor	COMIN	COMIN & text editor	COMIN & PE2
User friendliness	-1	-3	-5	-2	1
User Guide	-3	-1	0	-1	0
Output process.		Text editor		EXCEL	TABOUT
User friendliness		-2		5	3
User Guide		0		5	2

Table 5.7 gives the total pressures in each zone and the total air flow rates going through the four zones. Already severe differences can be seen among the results. As expected, the largest differences occur in zone 3, which is the critical zone: very small pressure differences between zones 3 and 4 may result in large changes in air flow rates.

Table 5.7: Total air flow rates and pressures in zones as calculated by participants

Zone	Total air flows in zones [kg/h]				Pressures in zones [Pa]			
	1	2	3	4	1	2	3	4
BBRI	73.0	59.9	23.3	150.5	-1.276	-37.291	-73.186	-0.977
Canada	16.6	24.6	48.4	95.2	-0.22	-36.404	-72.24	0.08
EMPA	78.4	64.3	18.3	156.4	-1.368	-37.202	-72.955	-1.07
INSA	74.8	64.5	9.9	144.1	-1.232	-37.209	-73.093	-0.933
Japan	74.8	64.5	9.9	144.1	-1.232	-37.218	-73.111	-0.933
LBL	74.8	64.5	9.9	144.1	-1.232	-37.218	-73.111	-0.933
LESO	109.5	36.3	45.5	162.3	-2.01	-37.089	-72.827	-0.712
TNO	74.8	64.5	9.9	144.1	-1.232	-37.218	-73.111	-0.933
Average	72.1	55.4	21.9	142.6	-1.2	-37.1	-73.0	-0.8
St.dev.	23.8	14.8	15.2	19.0	0.5	0.3	0.3	0.3
Minimum	16.6	24.6	9.9	95.2	-2.0	-37.3	-73.2	-1.1
Maximum	109.5	64.5	48.4	162.3	-0.2	-36.4	-72.2	0.1

The differences may be caused by errors in introducing input data and in differences between various versions of COMIS. The causes were not analysed in detail, as it was clear that some differences originated from severe bugs in COMIS 1.1, and that the User Guide clearly needed to be improved. There was also doubt that the same code running on various computers provided different results. A second run for the user test was therefore decided (cf.5.2.4).

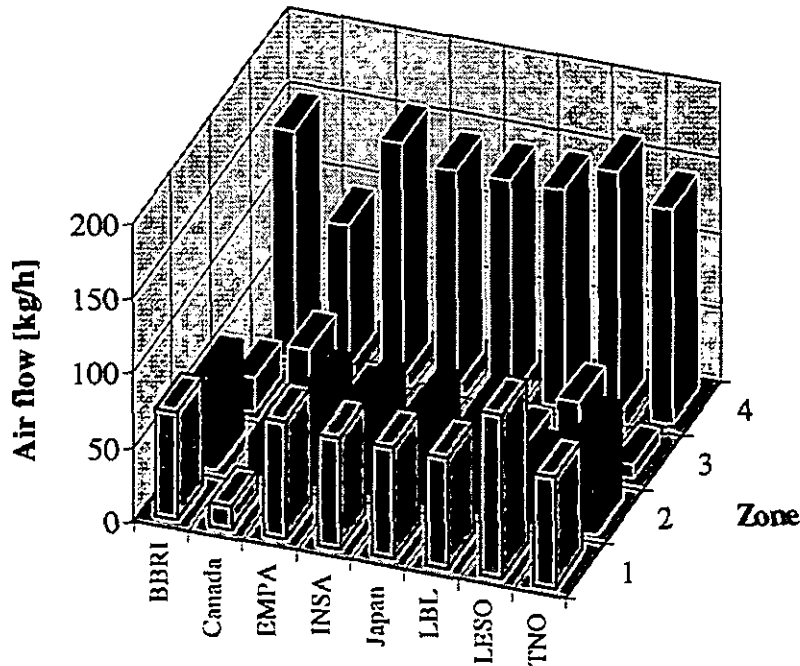


Figure 5.5 Comparison between the zonal air flows obtained by various participants to first run of user test 1

#### **Comments on input processing**

Several comments were made about the User Guide. Users not familiar with this Guide had difficulties understanding some parts. In some cases the User Guide did not correspond to the code. For example, zones were named with letters according to the User Guide, but COMIS 1.1 accepted only numbers.

Bugs in COMIS 1.1 were also revealed by this test. For example, some keywords could not be used, parts of the input file generated by COMIN were lost when saving, optional input parts are in fact mandatory, etc.

#### **Comments on output processing**

Routines for calculating total air change rate, fresh air change rate, inter - zonal and supply air flow for each zone should be provided.

All these comments were forwarded to LBL, who improved both the code and the User Guide, allowing for an easier second run of the user test.

#### **5.2.4 Results from second run**

In order to clearly separate the effects of COMIS versions and users, the second run was performed exclusively with COMIS 1.2, which was version 1.1 corrected for bugs detected by the first run, and which took account of some comments. Eleven institutions participated in this test.

### Comparisons between results

The main results are presented in Figure 5.6, Table 5.8 and Table 5.9. The results of one participant, who made an obvious networking error (see below) is not shown in the tables.

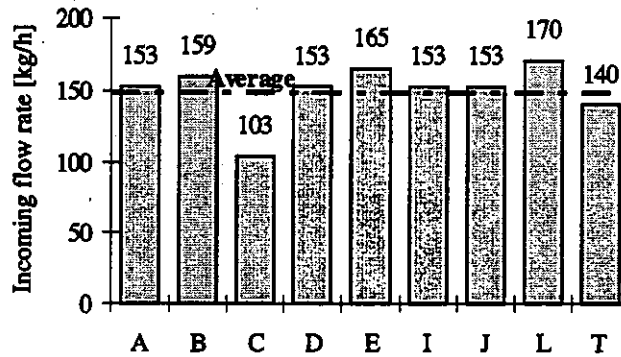


Figure 5.6: Comparison of total air flow rates in the building from second run on user test 1.

Table 5.8: Comparison of pressures in zones [Pa].

	A	B	C	D	E	I	J	L	T	<p>	s
1	-1.23	-1.28	-0.22	-1.23	-1.37	-1.23	-1.23	-2.01	-1.02	-1	0.12
2	-37.22	-37.29	-36.40	-37.22	-37.20	-37.21	-37.22	-37.09	-37.30	-37	0.04
3	-73.11	-73.19	-72.24	-73.11	-72.96	-73.09	-73.11	-72.83	-73.36	-73	0.12
4	-0.93	-0.98	0.08	-0.93	-1.07	-0.93	-0.93	-0.71	-0.72	-1	0.12
p-<p>	A	B	C	D	E	I	J	L	T		
1	-0.04	-0.09	0.97	-0.04	-0.18	-0.04	-0.04	-0.82	0.17		
2	0.04	-0.04	0.85	0.04	0.05	0.05	0.04	0.17	-0.04		
3	0.08	0.01	0.95	0.08	0.24	0.10	0.08	0.37	-0.17		
4	-0.04	-0.09	0.97	-0.04	-0.18	-0.04	-0.04	0.18	0.17		

Table 5.9: Comparison of air flow rates [kg/h]

	A	B	C	D	E	I	J	L	T	$\mu$	$\sigma$
Total in building	153	159	103	153	165	153	153	170	140	150	0.13
Ext. 1 to 1	75	73	17	75	78	75	75	101	59	70	0.32
Ext. 2 to 2	58	53	15	58	57	58	58	36	42	48	0.30
Ext. 3 to 3	-10	-23	-48	-10	-18	-10	-10	-45	-29	-23	-0.68
Ext. 4 to 4	-143	-136	71	-143	-147	-143	-143	-125	-110	-113	-0.62
Ext. 5 to 4	21	34	-55	21	30	21	21	34	38	18	1.57
1 to 2	7	7	9	7	7	7	7	-9	8	6	0.99
2 to 3	9	9	8	9	9	9	9	8	8	9	0.04
4 to 1	-68	-66	-7	-68	-72	-68	-68	-110	-51	-64	-0.41
4 to 2	-56	-51	-17	-56	-55	-56	-56	-19	-42	-45	-0.36
4 to 3	1	14	40	1	9	1	1	37	21	14	1.12
Flow in zone	A	B	C	D	E	I	J	L	T		
Floor 1	75	73	17	75	78	75	75	110	59	71	0.34
Floor 2	65	60	25	65	64	65	65	36	50	55	0.27
Floor 3	10	23	48	10	18	10	10	45	29	23	0.68
Staircase 4	144	151	95	144	156	144	144	162	131	141	0.14

Except for one participant, C, the results are much closer to each other than for the first run.

### Reasons for differences

Apart from two exceptions, the results are obviously closer to each other than in the first run. In order to find the cause of the differences, input files were carefully analysed. The main reason for these differences are input errors and options taken by participants. These options are summarised in Table 5.10.

Table 5.10: Options used by various participants.

	Air moisture [g/kg]		Wind profile exp.		Reference height [m]	
	In	Out	Meteo	Wind	Wind	$C_p$
A	0	0	0.32	0.32	9	9
B	0	0		---	---	9
C1	0	0		---	---	9
C2	---	1		---	---	---
D	---	0	0.18	0.18	9	9
E	8	4		0.17	9	9
I	0	0	---	0.5	9	9
J	0	0		0.32	9	9
L	4	8		0.32	10	10
T	---	10		0.32	9	9
Z	4	---		---	---	10

--- means no input data, default option is used by COMVEN.

The tables and diagrams show one clear outsider, C. The cause is very likely the error in reference height. The next one is L, who took a strange option for moisture (dry inside and wet outside) and 10 m for overall reference height. T is next, probably also because of moisture: he is the only one to have adopted the default values, that is 0 inside and 10 g/kg outside. When comparing his results with the so-called reference file, E, he tried to get the same results, and in fact succeeded after changing moisture, wind coefficient and wind reference altitude, and finally atmospheric pressure.

A, D, I and J have identical results. They all have zero air moisture inside and outside, but have various wind exponents. This exponent does not seem to be so important, at least for this case, in which reference heights are the same for the building and the meteorological station. Differences in wind profile exponent or reference height did not change the results very much. On the contrary, as seen from sensitivity analysis, air moisture has an influence on density, and hence on the stack effect.

Other specific comments resulting from the examination of the input files are listed below.

#### Input errors

Z made wrong links, all rooms being linked to the same  $C_p = 0.5$ . Link height are also wrong. This was warned in the output file, but the user did not notice. These results are not taken into account in the comparisons.

T made a typing error, changing a 4 into - 4 in the links section. Therefore, the second floor was not linked through a door to the staircase but to the facade element. When receiving the reference file, the user noticed the difference and corrected it. The corrected output file is used for comparisons.

C did not refer to his reference height in one zone to define the links levels, and this significantly modified several air flow rates.

*Crack definitions:*

Four participants defined each crack individually, that is the envelope crack five times, the floor crack twice, etc. This is not necessary. The user guide was not clear enough on the way to define facade elements, cracks, links, pressure coefficients, etc.

*Air moisture*

Humidity inside and outside was not defined in the provided input data. The participants have used all possible methods: default values, or defined moisture content both inside and outside, or defined it either inside or outside only. Table 5.10 provides the details. COMIS 1.2 had 10 g/kg: default value for outdoor air moisture content, while this default value is zero inside. This ugly defaulting was improved in version 1.3.

*Wind profile*

The wind profile exponent at &-ENV-WIND given for the meteorological site is added to COMVEN 1.2. In the case that 2 m/s should be fixed at roof level, the same exponent should be given for the building, and the height of the wind speed reference must be made equal to the roof height of the building.

Since nearly nobody was aware of that, only participant A and D did so. The others either put the default values (no input in this optional data section) or put in wind profile exponents in part 2 only. This exponent ranged from 0.17 to 0.32. Table 5.10 provides the details.

Reference height for wind speed and  $C_p$  was put at 9 m in most cases, but some did not provide it for wind speed and one put 10 m for both.

*Other comments*

Most participants used solver 5, but participants C and I used solver 1.

L is the only one to have defined an own height of 2 m for doors between rooms and staircase.

I provided a huge, complete input file, containing all the optional sections. Of course, only the necessary sections were filled up with data. This way of doing has two major disadvantages: it uses disk space and makes the debugging more difficult.

**5.2.5 Comparison between versions and computers***Japanese study*

Four Japanese groups have performed the user test 1 with three different input data, four versions of COMIS and five different computers including a workstation. Computing conditions and results are shown in Table 5.11: Comparison and Figure 5.6.

These results show that:

1. Different input data, such as reference height, etc., give different results (users 1,2 and 5).
2. Different version of COMIS give different results with same input file, but the differences are not significant. Differences are larger between versions 1.1 and 1.2 than between 1.2 and 1.3. The various COMVEN solvers and bugs in 1.1 provide reasons for these differences (users 1, 3, 4, and 6) .
3. The same input data and different version of COMIS give identical output in two cases, (users 1 and 3 with versions 1.1 and 1.1A, users 4 and 6 with versions 1.2 and 1.3).
4. The same input data and the same version of COMVEN give identical output regardless of the different compiler and the hardware. Consistent results can therefore be expected under the same computing environment with the same \*.CIF file.

Table 5.11: Comparison of user test 1 with 6 simulations

Group	1	2	3	4	5	6
<b>Hardware</b>	EPSON NEC compatible 80386SX, 80387SX	NEC not compatible to IBMPC 80486	PC9801		IBM PS55-T04 80386DX, 80387	KUBOTA TITAN 3000 R3000
<b>OS</b>	MS-DOS Japanese version by EPSON	MS-DOS Japanese version by NEC			DOS/V PC-DOS in Japanese	UNIX
<b>COMIS Version</b>	1.1	1.1	1.1A	1.2	1.2	1.3*
<b>Input File</b>	self made	self made	from user 1	from user 1	reference test1 file	from user 1
<b>Results</b>	<b>Total mass flow [kg/h]</b>					
<b>Floor 1</b>	75	93	75	69	77	69
<b>Floor 2</b>	65	52	65	49	61	49
<b>Floor 3</b>	10	60	10	42	26	42
<b>Staircase 4</b>	144	185	144	155	159	155
	<b>Total pressure [Pa]</b>					
<b>Floor 1</b>	1.23	1.64	1.23	1.35	1.39	1.35
<b>Floor 2</b>	37.22	37.67	37.22	37.43	37.25	37.43
<b>Floor 3</b>	73.11	74.01	73.11	73.34	73.00	73.34
<b>Staircase 4</b>	0.93	1.34	0.93	1.05	1.39	1.05

\* Source Code at LBL in January 1994

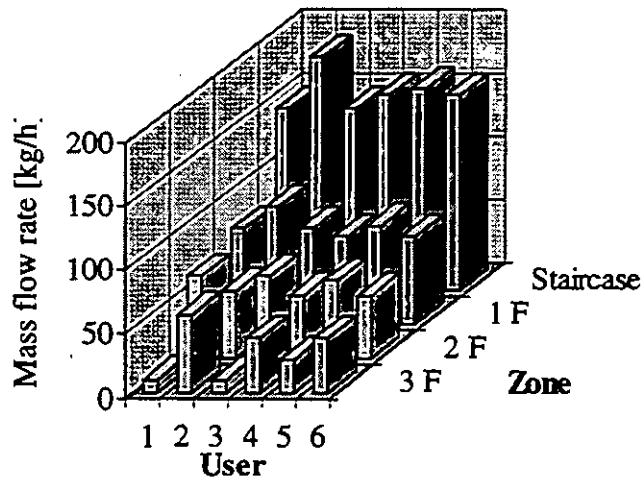


Figure 5.7: Comparison of mass air flow rates from Japanese user tests.

#### Reference test

In order to ensure that the COMIS version 1.2 code does not provide different results on different computers, a reference input file was used by 5 laboratories in different countries. The results were all identical, except for one laboratory. For this laboratory, it appeared that the 1.2 version they had picked-up directly from the LBL was slightly different from the "official" one.

## 5.3 User tests on case 2

### 5.3.1 Presentation of the case

Test case 2 is presented in Figure 5.8. It is based on a building located in mainland Europe comprising a 5th floor apartment situated in the centre of a nine floor apartment block. Ventilation is by natural stack and make up air is provided by natural porosity. Provided data are as follows:

Building:	9 storey + 3 m high ground floor area	
Apartment:	230 m <sup>3</sup> volume, dimensions 9.5 × 9.0 × 2.7 m <sup>3</sup>	
Surroundings:	similar buildings, 40 m spacing, urban.	
Air tightness:	3 air change per hour at 50 Pa, distributed according to Figure 5.8.	
Flow exponent	0.6	
Ventilation	natural duct system	
Ventilation ducts:	Main duct	0.23 × 0.18 m <sup>2</sup>
	WC duct	0.10 × 0.10 m <sup>2</sup> , joining main duct. Inlet at 2.6 m height
	Bathroom duct	0.10 × 0.10 m <sup>2</sup> , joining main duct. Inlet at 2.6 m height
	Kitchen duct	0.23 × 0.10 m <sup>2</sup> , joining main duct. Inlet at 2.6 m height
	Air leakage of main duct	6.9 l/s @ 1 Pa
	Flow exponent of main duct	0.5
Other components	Windows and doors are part of background leakage	
	Internal doors 1 × 2 m <sup>2</sup> , perimeter gap 1 mm	
	Flow exponent of internal doors	0.5

The objective is to calculate the total air change rate of each zone, the air flow in each flow path and the proportion of fresh air into each zone for the following sets of conditions:

Configuration for simulations	External windows and doors closed					
	Internal doors closed except hall to living room					
	Ventilation ducts open					
	Internal temperature	20°C				
	Wind direction:	North	West			
	Wind speed	0	1	2	5	10 [m/s]
	External temp	0	10	20	[°C]	

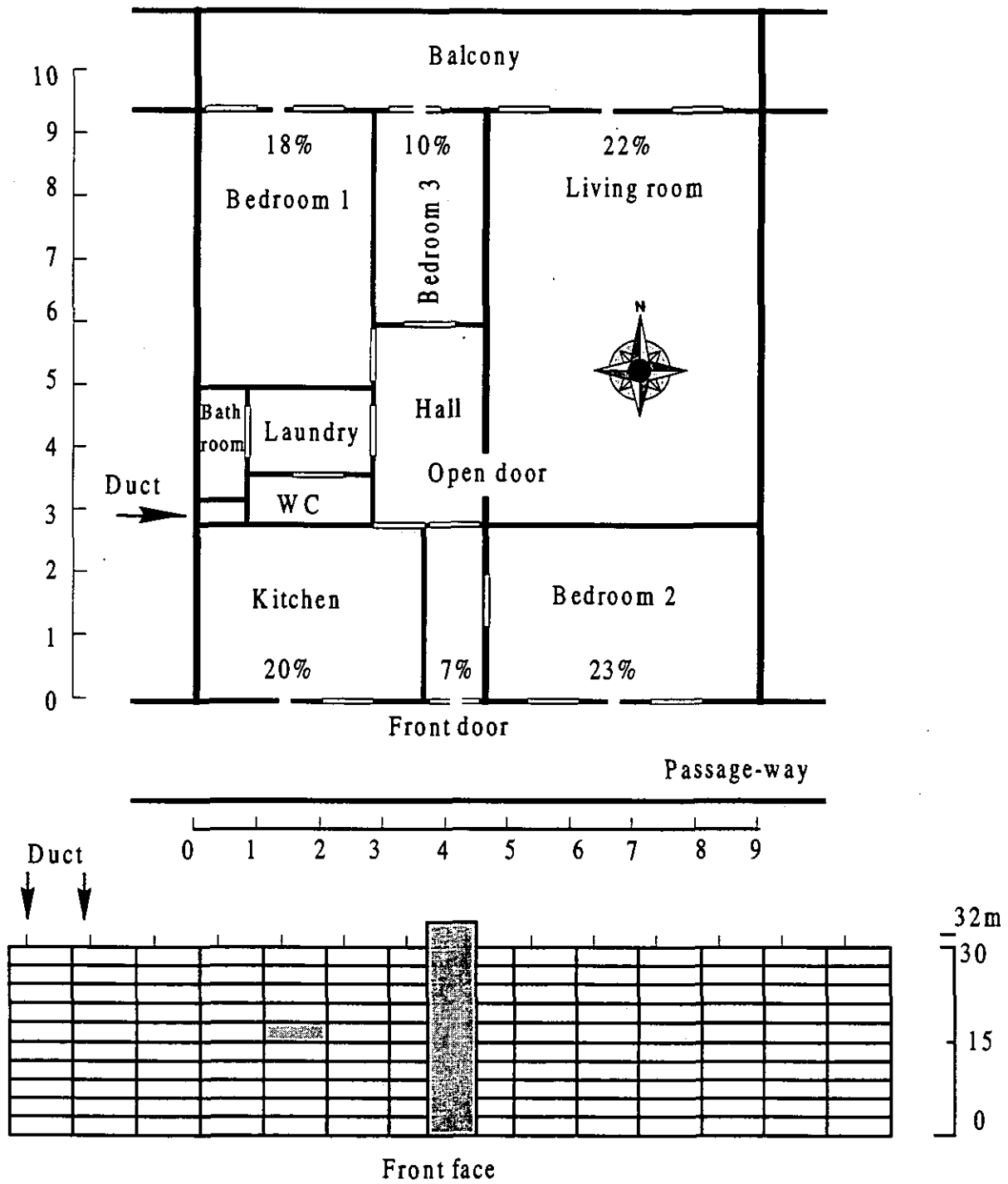


Figure 5.8: User test 2 building.

### 5.3.2 Results

The first results are given in Table 5.12 and Figure 5.9. First of all, large differences in modelling the network for the same flat can be seen: from 10 to 12 nodes, from 17 to 25 links and from 2 to 13 pressure coefficients ( $C_p$ ). Large differences can also be seen in the results.

Table 5.12: Some options taken by participants and total outdoor air flow rate under three conditions:

	COMIS version	Number of network elements			Air flow rate [kg/h] with climate		
		zones	links	$C_p$	cold, no wind	cold and windy	warm, no wind
Athens	1.2	11	25	13	154	347	41
Concordia	1.2	12	19	3	26	123	6
EMPA	1.2	11	19	3	113	263	17
INSA	1.2	11	19	3	80	288	11
Italy	1.01	10	17	2	0	39	0
Japan	1.2	10	18	7	125	261	187
LESO	1.2	11	19	3	128	275	7
WTCB	1.2	11	25	13	154	347	82

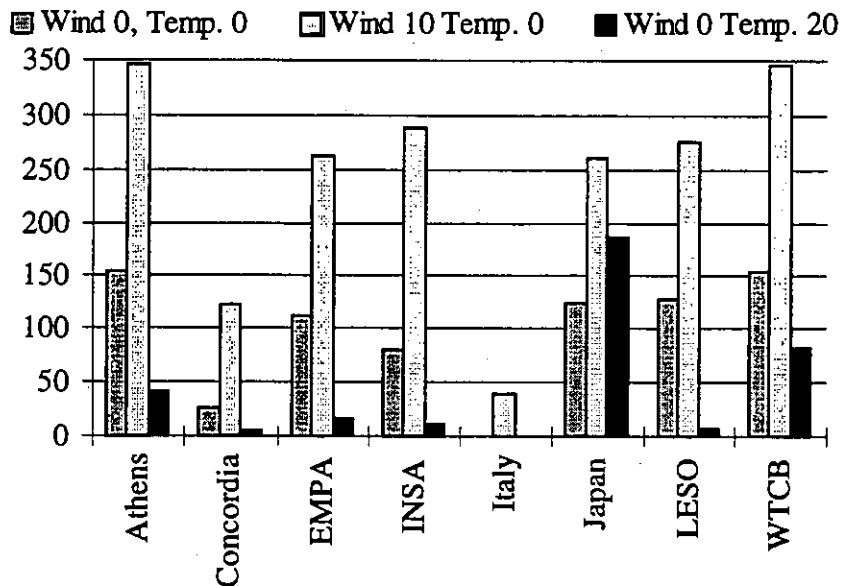


Figure 5.9: Total outdoor air flow rate as calculated by participants for three different conditions.

### 5.3.3 Sensitivity study of input files

In order to eliminate any possible difference resulting from different versions of COMIS, all input files received were run with the same version, COMIS 1.3. A so-called reference input file was also built on the basis of the EMPA file. This file (EMPA2.CIF) was carefully inspected and some minor changes were made (see appendix 5.2). It should be noted that the so-called reference file does not pretend to be the absolute truth.

The main options taken for this reference file are as follows:

- Building reference level and reference level for external elements: 0 m
- Reference level for the internal zones: + 15 m
- 11 internal zones. Open door between hall and living room.
- Level of links between internal zones 1 to 10: 1 m. Exhaust grilles at 2.6 m. Length of main ventilation duct: 14.4 m.
- Leakage exponents of cracks = 0.6. For open door and ducts,  $n = 0.5$
- Wind from North ( $0^\circ$ ) and West ( $270^\circ$ ). Reference height for wind at building and meteorological station is 30 m. Wind exponent is 0.32 at both places.

- Plan area density = 0.144
- Pressure coefficients taken out of the AIVC 'Air Infiltration Calculation Technique' handbook. [Liddament, 1986]
- Location of building: 50° N Latitude; 2° East longitude, 0 m altitude (as for meteorological station), orientation of x half axis: 90°.

An elementary sensitivity study was performed with a star plan, changing only the parameters which were not identical in the various users input files. The result selected for this study is the extract air flow rate, which changes are shown in Table 5.13.

Table 5.13: Effects of some changes on the extract air flow rate for test case 2. These effects are related to the values obtained with the so-called reference file.

Temperature	0	20	0	20	0	20
Wind direction	N/W	N/W	N	N	W	W
Wind speed	0 m/s	0 m/s	10 m/s	10 m/s	10 m/s	10 m/s
Hall and living in one zone	No effect					
Closed door between hall and living.	< 1%					
All internal doors open	No convergence					
Short-circuit bet. N facade and extract.	No convergence					
Short-circuit between N and S facades	No effect	5%	5%	5%	5%	5%
Change in plan area density	No effect					
Changes in internal volume	No effect					
10% change on the roof Cp	No effect	5%	20%	10%	5%	5%
10% change on the N facade Cp	No effect	<1%	10%	<1%	5%	5%
10% change on the S facade Cp	No effect	1%	10%	1%	5%	5%
10% change on the internal doors Cs	2%					
10% change on the infiltration Cs	2%					
10% change on the Cs of main duct	2%					
10% change on the wind exponent	2%					
100 m on altitude of building	1%					
100 m on altitude of meteo station	1%					
Meteo ref. height at 10m instead of 30	No effect	20%	40%	35%	45%	45%
10° change in building orientation	No effect	9%	17%	3%	4%	4%
2 m change in wind reference height	No effect	1%	2%	1%	2%	2%

Large changes come from the meteorological station reference height and building orientation. Any change in pressure coefficient also has a large influence. Such change may come from reference heights, and from Cp values themselves.

Whenever one door between extraction and the facades is closed, the other internal leaks do not have a large influence on global air change. If there is a short circuit between extraction and the facades, no solution can be found.

### 5.3.4 Comparative study of user's files

Differences between each user's file and the so-called reference file are given below. Differences resulting in large discrepancy between the results are in italics.

#### EMPA

- $\zeta = 1.2$  for ducts
- Air water content = 4 g/kg inside and 8 g/kg outside

- *Default wind exponent (0.14) at meteorological station*
- *Default values for building wind height, location and orientation.*
- *Plan area density = 0.25*

### **LESO**

- $\zeta = 1.2$  for ducts
- Air water content = 4 g/kg inside and 8 g/kg outside
- *Default wind exponent (0.14) at meteorological station, reference height 10 m*
- *Default values for building wind height and location.*
- *Plan area density = 0.25*
- *Wind direction 90° for West*

### **Japan**

- Different control parameters
- $\zeta = 1.5$  for ducts. Cylindrical main duct with  $C_s > 0$ . Duct end type 4 (circular)
- *Dry air inside and outside.* Infiltration temperature 20°C
- Link height 1.5 m, and 2.7 m for exhaust grid. *17 m for exhaust duct.*
- *Pressure coefficients from CPCALC, which are different than those from AIVC.*
- Wind exponent = 0.28 at meteorological station and building, reference height 32 m
- Other latitude, longitude and altitude.
- *Plan area density = 0.25*
- *Building turned 180° (North facade towards South)*

### **Athens**

University of Athens provided two identical files with different names.

- Internal doors simulated by closed windows with low  $C_s$  and exponent  $n = 0.5$ .
- $\zeta = 1.5$  for very smooth ducts. Cylindrical main duct with  $C_s > 0$ . Default duct end.
- *Dry air inside and outside.* Reynolds numbers given for transition zones between ducts.
- Two link height (0 and 2.7 m) in facades, each with half the permeability. Internal links at 0 m. *14.4 m for exhaust duct.*
- *Reference height of building + 15 m.*
- *Different pressure coefficients for facades, but identical roof  $C_p$ 's.*
- *Default values for building wind height and location.*

### **Comut2.cif**

File very similar to Japan file

- Different control parameters
- Internal doors with lower  $C_s$ .
- $\zeta = 1.5$  for ducts. Cylindrical main duct with  $C_s > 0$ . Duct end type 4 (circular)
- *Dry air inside and outside.* Infiltration temperature 20°C
- One zone for living room and hall. Link height 1.5 m, and 2.7 m for exhaust grid. *17 m for exhaust duct.*
- *Pressure coefficients from CPCALC, which are different than those from AIVC.*
- Wind exponent = 0.28 at meteorological station and building, reference height 32 m
- Other latitude, longitude and altitude.
- *Building turned 180° (North facade towards South)*

### **Concordia**

- Internal doors with lower  $C_s$ . Open door treated as a link with  $C_s = 2.2$ ,  $n = 0.5$

- $\zeta = 1.5$  for ducts. Cylindrical main duct with  $C_s > 0$ . Duct end type 4 (circular)
- *Dry air inside and outside.*
- *Kitchen, front door and bedroom 2 connected to a supplementary zone "promenade", which is not connected to external node.*
- Wind exponent = 0.22 at meteorological station.
- Plan area density = 0.25
- *Default values for building height, orientation and location.*
- *Wind direction 90° for West*

### INSA

- Different control parameters
- Internal open doors with exponent  $n = 0.7$ .
- $\zeta = 0$  for ducts. Cylindrical smooth main duct 17 m long. Default duct end
- *Dry air inside and outside.* Infiltration temperature 20°C
- Reynolds numbers given for transition zones between ducts.
- Link height 1.35 m in rooms. 17.6 m for exhaust duct.
- *Pressure coefficients defined for 90° but not for 270°. Different  $C_p$  for 0°.*
- *Pressure coefficients from CPCALC, which are different than those from AIVC.*
- *Building height, orientation and location variables all at 0.*
- *Default wind exponent = 0.14 at meteorological station, and 0.5 at building.*
- *Wind direction 90° for West*

### Italy

- Different control parameters
- Internal open doors with lower  $C_s$  and exponent  $n = 0.53$
- $\zeta = 2.5$  for main duct, and 0.5 for other ducts. Default duct end.
- HVAC system defined (code 17) for connection of secondary ducts to main duct. This is not accepted by COMVEN 1.3 Reynolds numbers given for transition zones between ducts.
- *Dry air inside, 10g water per kg dry air outside.*
- *Kitchen, front door and bedroom 2 connected to a supplementary zone "promenade", which is not connected to external node.*
- WC, bathroom and kitchen connected to external node directly through main duct.
- *Link height not defined (default values).*
- *Different pressure coefficients*
- *Default values for building height, orientation and location.*
- *Default wind exponent = 0.14 at meteorological station, which altitude is put at 50 m.*
- *Plan area density = 0.49*

### Comparisons

Since comparisons of files presenting strong differences because of unclear definitions are not easy, input files were corrected and made similar to the reference file for the following variables: reference heights, building orientation, wind direction and wind exponent.

Relative differences in extract air flow rates are related to the reference file:

$$\text{Relative difference} = \frac{\text{Extract flowrate} - \text{Reference extract flowrate}}{\text{Reference extract flowrate}}$$

Table 5.14: Relative difference in extract air flow rate between users results and reference. Calculation made with corrected input files (see text).

Temperature	0	20	0	20	0	20	Main reason for difference (apart reference heights and building orientation)
Wind direction	N/W	N/W	N	N	W	W	
Wind speed	0 m/s	0 m/s	10 m/s	10 m/s	10 m/s	10 m/s	
EMPA	-5%	-7%	-2%	-8%	-1%	-2%	Relative humidity
LESO	-5%	-7%	-2%	-8%	-1%	-2%	Relative humidity
Japan	-1%	-100%	+55%	+181%	+40%	-35%	Cp, dry air
Athens	<+1%	-100%	+50%	+90%	<-1%	<+1%	Cp, dry air
Comut2.cif	-15%	-100%	+50%	+95%	+30%	+40%	Cp, dry air
Concordia	-50%	-100%	-10%	+30%	-70%	-75%	Geometry, dry air
INSA	-20%	-100%	-20%	-20%	+50%	-45%	Cp, dry air
Italy	<-1%	+35%	10%	-7%	-65%	-70%	Cp, geometry, humidity

When there is no density gradient and no wind, COMVEN gives a zero air flow rate, which is correct. Large relative differences in the third column result from slight differences in air density caused by differences in air humidity.

## 5.4 Conclusions

From this user test, it was found that

1. Identical input files give identical results on different computers or with codes issued by different compilers, if the same source version of COMIS is used. The code is not too sensitive to numerical noise.
2. Large differences between results come from modelling errors or input typing errors. Some misunderstandings of the User Guide resulted in large changes in wind velocity at the facade level. The most common misunderstandings occur when defining reference heights of buildings, zones, and the meteorological station; and when defining the building orientation.
3. Slight differences may result from different options chosen by the user.

This test has revealed substantial useful information which can be used for the improvement of both the code and the User Guide.

## 5.5 References

- Fürbringer, J.-M.: Evaluation Procedure Using Sensitivity Analysis of Model and Measurement. *International Symposium on air flow in multizone structures, Budapest Sept. 9 (1992)*.
- Fürbringer, J.-M.: Sensibilité de modèles et de mesures en aéraulique du bâtiment à l'aide de plans d'expériences. *PhD Thesis No 1217, EPFL, Lausanne, (1994)*.
- Liddament M.: Air infiltration Calculation Technique - An application guide, *AIVC, Coventry, GB, (1986)*
- Roulet, C.A. and Vandaele, L.: Air Flow Patterns within Buildings, *Measurement Techniques, AIVC Technical Note 34, Coventry, GB, (1991)*.
- Yoshino H., Zhao Yun, Utsumi Y., Nakamura T., Arai T., Hasegawa K., Ishikawa Y.: IEA Annex 23 User Test 1 - Comparison of the results with 6 simulations. *Internal Annex 23 report, October 1994*.

## 6 SYNTHESIS

### 6.1 General results

The work undertaken with the aim of evaluating COMIS (an air flow multizone model) is reported in this document. The methodology is presented in the first chapter. It consists basically in comparing the image of the reality obtained using COMIS with other images of the reality obtained with analytical solutions, other program outputs and finally with measurement data.

The evaluation was sustained by a continuous reflection resulting in an improvement of the validation techniques, thus overcoming the numerous practical difficulties which make validation quasi-impossible. The main innovation is the sensitivity analysis of simulation outputs. Factorial design has been used to identify the parameters whose uncertainty disqualifies most heavily the output data. The main parameters are not always the same, they change from one case to the other. Monte-Carlo design has been used to calculate the output confidence intervals. It has been shown that this simulation uncertainty is often larger than the corresponding experimental confidence intervals.

The result of this study is also that the sensitivity depends on the studied case. This means that it is not possible to provide accurate validity limits and clear advice on allowable input errors. In that perspective however, an important effort has been made to provide tools to the user: they are MISA (Multirun Interface for Sensitivity Analysis) to help the systematic variation of input files and LiSA (Library for Sensitivity Analysis) which is a Library developed to bring out the sensitivity coefficients and the related information. These tools have ended in the development of a new module of COMIS: SAM (Sensitivity Analysis Module) which should allow the user of COMIS 3.0 to perform a sensitivity analysis on line.

Mostly versions 1.1 to 1.3 of COMVEN were used within this evaluation. However, the benchmarks developed for the analytical comparison were also run with the successive versions of COMIS (2 and 3). It was checked this way that the successive versions are at least as correct as the 1.x versions, and that no additional bugs were introduced when improving COMVEN.

### 6.2 Results from specific evaluation tasks

#### 6.2.1 Analytical comparison

The analytical comparison has shown, in a limited number of cases, that the solutions given by COMIS correspond to what is expected and predicted by completely independent models. The consequences of some choices in modelling (density gradient is an example) have been identified.

#### 6.2.2 Inter-model comparison

The inter-model comparison has allowed the comparison of COMIS with 14 different models on different structures and different topics (large openings, mass flow equation, sensitivity, high temperatures). COMIS is able to predict the air and contaminant flows as well as any of these other models. Reciprocally, these 14 other programs take benefit of the analytical and experimental comparisons.

It has been shown that there is a relation between the number of input parameters and the model sensitivity to input uncertainties. This is logical since the error function of a model is a function of the sum of the square of the parameter variance.

When simulating, the user has to balance between:

- simpler models which end in smaller confidence intervals, which can be inaccurate, and
- more sophisticated models which are generally more sensitive to input inaccuracy but which take more phenomena into account.

An example of a very simple model is the model always giving  $0.3 \text{ h}^{-1}$  for the air change rate. Its sensitivity to input errors is zero, since no input is required and the result will always be the same. Its validity domain is however restricted, and its accuracy in reproducing the reality is little.

More sophisticated models such as COMIS are applicable to a broader range of application and may be more accurate, but they require a large effort in input. Of course, the time for performing the simulation and the risk of misusing a complicated model must be considered.

### 6.2.3 Experimental comparison

The experimental comparison is perhaps the most frustrating work in this annex. It represents a huge amount of work when expressed in man-years (about 9 person-years). Monitoring and comparisons were made on nine buildings, each presenting several cases. The convergence of measurement and calculated global air flows within  $\pm 25\%$  has been verified. However inter-zonal flows often differ, principally because of the difficulty of precisely describing the network and the boundary conditions.

Experimental uncertainties, especially when propagated through the code, are large and act as a screen which hides the actual discrepancies between the numerical model and the experimental data. These uncertainties are at the same time critical and extremely difficult to evaluate numerically. In a few words: it is possible to evaluate roughly the air change rates but it is yet uncertain to say where the air and the pollutants go.

Few evidences have been found to show any internal errors or validity limits. For tested cases, COMIS is usually coherent with the experimental data. Limits concerning the wind influence on the large opening algorithm have been observed (as expected).

In principle, internal errors may be found by systematically studying the function of discrepancy between the numerical and the experimental model. But the parameters of this function are not well known as it becomes obvious from the global sensitivity story. The input parameter domain is not sufficiently known. Its dimension depends obviously on the building but a particular mathematical structure could exist and would allow the emergence of some dimensionless approach (i.e. Euler numbers, modal approach, etc.). Moreover, the study of this discrepancy function between the numerical and the experimental model would need the construction of buildings on purpose, which would be very expensive.

The system approach would be an interesting perspective for investigations within the framework of validation of numerical models because it would allow a systematisation of the sensitivity analysis. For the present, and probably for a long time, it is practically impossible to validate a model, it is only possible to validate cases!

In fact, a limited number of cases were validated and an important question remains: How to relate the case under study by the user with the evaluated cases?

Some ideas are arising which still need to be tested. The work reported here has the merit of having clarified the situation, showing for the first time the magnitude of the uncertainty in simulation and the obstacles to overcome before validation ceases to be an impossible goal, an utopia.

### 6.2.4 The User Test

An other innovative aspect of this work, is the user test. From that part of our study, remember that user introduced uncertainty is as large as the experimental induced uncertainty. This must be taken into account by program developers. It must be a challenge for them to provide models which can not be misused too easily. The user is as unavoidable for them as the inhabitant for the architects even if they complicate everything!

### 6.3 A few hints

To avoid large errors in using COMIS or any similar computer code, the following precautions should be taken:

- Only persons having enough knowledge on the physical phenomena involved in ventilation should use these programs.
- Avoid to simulate a too complex building, or use the simplest nodal model of it. For example, it may be more accurate to merge two rooms connected through an open door in one single zone, than to model this by two zones linked by a large opening.
- Results are a direct image of the input: try to obtain high quality input data. A great problem remains in collecting proper pressure coefficients and meteorological conditions which are valid on the site.
- In any case, perform a sensitivity analysis by varying the input in a smart way, to obtain information on the resulting variation of the output.
- The user may have a large influence. To gain confidence in the result, give the problem to two independent users, and compare the results: if they do not differ too much, they may be right. If the difference is large, look for input errors!

### 6.4 Conclusion

As far as it is possible to draw general conclusions from the few (in fact numerous but not enough!) comparisons performed within this work, it can be said that, when proper input is provided:

- Air and contaminant flows resulting from infiltration through cracks and ventilation systems are properly predicted by COMIS and similar programs.
- Air and contaminant flows through large openings (that is openings presenting two-way flows) can be calculated, but the result may not be close to reality. This is especially true in case of wind, and when the building structure acts as a thermal reservoir. These two phenomena, in fact not well known yet, are not modelled in such programs.
- In general, global air flow rates through the building are better predicted more accurately than inter-zonal flow rates.

The initial purpose of the evaluation task was to find the limits of validity of COMIS. Such limits were not found, but this does not mean that they do not exist, since only a spectra of common cases was explored. The main limits are not in COMIS (or in any other similar code). They are in the user of the program: good input data are not commonly available, and it is difficult to model, by a resistance network, something as complex as a multizone building. Complex computer codes like COMIS, even with a very user-friendly interface, should be used only by experts having good knowledge of the phenomena involved in air flow problems within buildings. It was also shown that a sensitivity analysis performed around the studied case provides essential information to interpret the results and to have some confidence in them.

ecbcs bookshop

ANN 23 1996:1